

**Linear and Cross-linked UCST-Type Polymers:  
Synthesis and Properties**

**Dissertation**

zur Erlangung des akademischen Grades eines

**Doktors der Naturwissenschaften**

**(Dr. rer. nat.)**

im Promotionsprogramm „Polymer Science“

der Bayreuther Graduiertenschule für Mathematik

und Naturwissenschaften der Universität Bayreuth

Vorgelegt von

**Fangyao Liu**

aus Nanchang, China

Bayreuth 2015



Die vorliegende Arbeit wurde in der Zeit von Mai 2012 bis Juli 2012 in Marburg am Lehrstuhl Makromolekulare Chemie, Philipps-Universität Marburg und in der Zeit von August 2012 bis März 2015 in Bayreuth am Lehrstuhl Makromolekulare Chemie II unter der Betreuung von Frau Prof. Dr. Seema Agarwal angefertigt.

Vollständiger Abdruck der von der Bayreuther Graduiertenschule für Mathematik und Naturwissenschaften (BayNAT) der Universität Bayreuth genehmigten Dissertation zur Erlangung des akademischen Grades eines Doktors der Naturwissenschaften (Dr. rer. Nat.).

Dissertation eingereicht am: 17. 03. 2015

Zulassung durch das Leitungsgremium: 24. 03. 2015

Wissenschaftliches Kolloquium: 10. 07. 2015

Amtierender Direktor: Prof. Dr. Franz Xaver Schmid

Prüfungsausschuss: Prof. Dr. Seema Agarwal (Erstgutachterin)

Prof. Dr. Andreas Fery (Zweitgutachter)

Prof. Dr. Mukundan Thelakkat (Vorsitz)

Prof. Dr. Matthias Karg



*Say yes if you know, say no if you do not know, which is the wise behavior.*

*---- Confucius*

*知之为知之，不知为不知，是知也。*

*---- 孔子*



## TABLE OF CONTENTS

### Table of Contents

Summary .....	1
Zusammenfassung.....	4
List of symbols and abbreviations .....	7
1. Introduction.....	11
1.1 Thermoresponsive polymers .....	11
1.2 Aims of the thesis.....	34
1.3 Controlled radical polymerization .....	35
1.4 Gold nanoparticles stabilized with polymeric ligands .....	38
1.5 Literature.....	40
2 Synopsis .....	51
2.1 Controlled radical polymerization of <i>N</i> -acryloylglycinamide and UCST-type phase transition of the polymers .....	53
2.2 Atom transfer radical polymerization as a tool for making poly( <i>N</i> -acryloylglycinamide) with molar mass independent UCST-type transitions in water and electrolytes .....	55
2.3 Thermoresponsive gold nanoparticles with positive UCST-type thermoresponsivity.....	57
2.4 A non-ionic thermophilic hydrogel with positive thermosensitivity in water and electrolyte solution.....	59
2.5 Thermophilic films and fibers from photo cross-linkable UCST-type polymers .....	61
2.6 Individual contributions to joint publications .....	63
3 Reprints of Publications .....	65
Publication 1: Controlled Radical Polymerization of <i>N</i> -Acryloylglycinamide and UCST-Type Phase Transition of the Polymers.....	66
Publication 2: Atom transfer radical polymerization as a tool for making poly( <i>N</i> -acryloylglycinamide) with molar mass independent UCST-type transitions in water and electrolytes .....	76

## TABLE OF CONTENTS

Publication 3: Thermoresponsive gold nanoparticles with positive UCST-type thermoresponsivity.....	86
Publication 4: A non-ionic thermophilic hydrogel with positive thermosensitivity in water and electrolyte solution .....	98
Publication 5: Thermophilic films and fibers from photo cross-linkable UCST-type polymers.....	106
4 Outlook .....	117
5 List of publications .....	118
6 Conference participations .....	119
7 Acknowledgments.....	121



## Summary

Thermoresponsive polymers are well studied and applied in both scientific and industrial areas. Among them, polymers with lower critical solution temperature (LCST)-type thermoresponsivity were extensively investigated. However, in some applications polymers with upper critical solution temperature (UCST)-type thermoresponsivity are required. To have a better understanding of UCST behavior, this dissertation deals with the synthesis of polymers, that show UCST-type thermoresponsivity in water or in electrolytes, with different architectures and their properties. There are four main topics in this thesis:

- (1) the effect of polymer characters such as composition, chain ends and molar mass on the UCST behavior;
- (2) chemistry for grafting polymers with UCST-type thermoresponsivity onto metal nanoparticles;
- (3) UCST-type volume changes of chemically cross-linked hydrogels; and
- (4) photo cross-linkable polymer with UCST-type thermoresponsivity.

In the **Introduction**, thermoresponsive polymers showing both LCST- and UCST-type thermoresponsivity in aqueous solutions were summarized as literature background of this thesis. The aims of the thesis were listed based on the challenges in the UCST field. Additionally, controlled radical polymerization methods were introduced as effective technique for synthesizing polymers with linear structures. Gold nanoparticles protected by thermoresponsive polymers were reviewed.

The **Synopsis** introduces the main results of five publications and the connection between each work. Five publications were attached in the form of a journal article.

**Publication 1** and **Publication 2** comprise the synthesis of poly(*N*-acryloylglycinamide) (PNAGA) with a linear structure, by using two controlled radical polymerization methods, namely: reversible addition fragmentation transfer (RAFT) polymerization and atom transfer radical polymerization (ATRP). Both methods exhibited a good control of the synthesis of PNAGA, by showing a linear increase of the polymer molar mass with conversion, narrow molar mass dispersity and successful chain extension experiments. It was found that a non-ionic chain transfer agent (only for RAFT) and a non-ionic initiator were important to keep the key property of the polymers: the UCST-type thermoresponsivity in aqueous solutions. It was shown in

**Publication 1** that the hydrophobic dodecyl end groups caused an increasing of cloud points of polymers with lower molar mass ( $M_n$  below 10000 g/mol). Thus, in **Publication 2**, as consecutive work, a monomer-like initiator was chosen to synthesize linear polymer with primary amide end-groups. The prepared polymers with hydrophilic end-groups showed cloud points independent from the molar mass. In both works, the influence of molar mass, polymer end-groups and salt (NaCl and Na<sub>2</sub>SO<sub>4</sub>) concentrations on the cloud point was analyzed by means of turbidimetry measurements.

In **Publication 3**, the previously synthesized trithiocarbonate end-functionalized PNAGA, synthesized *via* RAFT polymerization (shown in **Publication 1**), was grafted onto gold nanoparticles (AuNPs) by ligand exchange in phosphate buffered saline (PBS) solutions. The PNAGA functionalized gold nanoparticles (PNAGA@AuNPs) showed positive thermoresponsivity in PBS, additionally the UCST-type phase transition was reversible for at least nine cooling/heating cycles. It was found that the grafting process had no negative effects onto the cloud points, as the PNAGA@AuNPs showed similar phase transition behaviour as that of the free-PNAGA sample used for grafting purpose.

**Publication 4** presents the UCST-type thermosensitivity of chemically cross-linked PNAGA hydrogel with *N,N'*-methylenebis(acrylamide) (MBAAm) as cross-linker synthesized *via* free radical polymerization. The hydrogel showed continuously positive volume transitions in water and in electrolyte solutions, meaning the hydrogel swells at high temperature and shrinks by decreasing the temperature. The degree of hydrogel swelling was controlled by varying the contents of cross-linkers. It was found that with less amount of cross-linker, the swelling/deswelling behaviour of the hydrogel became more similar like the linear polymer in aqueous solution. The volume-change was reversible in pure water as well as in PBS, by showing at least seven cooling/heating cycles in a temperatures range between 4 °C and 40 °C.

In **Publication 5**, a terpolymer system with UCST-type thermoresponsivity based on acrylamide (AAm), acrylonitrile (AN) and UV cross-linkable comonomer was reported. Terpolymers with linear structures synthesized *via* free radical and RAFT polymerization showed UCST-type thermoresponsivity in water and in electrolytes. The terpolymers showed almost no hysteresis during cooling and heating cycles. Furthermore, they are stable against hydrolysis for at least nine cycles. The cloud points of the polymer solution can be tuned by varying the AN contents in polymer.

Chemically cross-linked films and nanofibers were successfully produced from terpolymers by solution casting and electrospinning followed by UV irradiation. The hydrogels showed temperature dependent positive volume-change that was utilized for design of microactuators.

In **Outlook**, the challenges and opportunities for UCST-type polymers were discussed. So far nonionic UCST-type polymers are focusing on polymers containing amide or ureido groups. Other hydrophilic polymers with suitable content of hydrogen bonding units could theoretically display UCST property. This may enlarge the UCST-type polymer family greatly. The non-ionic hydrogel with positive thermoresponsivity could be applied for drug loading and release system. Nevertheless, it is now possible to produce cross-linked polymers from linear polymers by using UV light with different forms as demand for example by lithography.

## Zusammenfassung

Thermoresponsive Polymere werden sowohl in wissenschaftlichen als auch industriellen Bereichen eingesetzt. Polymere mit unterer kritischer Lösungstemperatur (engl. *lower critical solution temperature*, kurz LCST) wurden weitgehend untersucht. Jedoch erfordern einige Anwendungen Polymere mit UCST Eigenschaft. Die vorliegende Dissertation beschäftigt sich mit der Synthese von Polymeren verschiedener Struktur und Eigenschaften, welche eine obere kritische Lösungstemperatur (engl. *upper critical solution temperature*, kurz UCST) in Wasser und Elektrolyt-Lösung besitzen. In dieser Dissertation wurden vier Themen gezeigt:

- (1) der Einfluss der Polymereigenschaften z. B. Polymerzusammensetzung, Kettenende und Molarmass auf des UCST Verhalten;
- (2) die Chemie der Pfropfung der UCST Polymere auf Goldnanopartikel;
- (3) UCST-Verhalten von chemisch vernetztem Hydrogel und
- (4) Fotovernetzbares Polymer mit UCST Eigenschaft.

Die **Einleitung** beginnt mit einer Zusammenfassung von literaturbekannten thermoresponsiven Polymeren, welche entweder eine LCST oder eine UCST in wässriger Lösung besitzen. Die Ziele der Arbeit wurden auf Grund der Herausforderungen im Bereich der Forschung zu UCST ausgewählt. Anschließend wird auf kontrollierte radikalische Polymerisationsmethoden eingegangen und deren Anwendung als effektive Technik für die Synthese von linearen Polymeren erläutert. Die durch thermoresponsive Polymere geschützten Goldnanopartikel (engl. *gold nanoparticles*, kurz AuNPs) wurden als relevantes Konzept diskutiert.

In der **Synopse** werden die Schwerpunkte der fünf Publikationen dargelegt und deren Zusammengehörigkeit erläutert. Die fünf Publikationen wurden in der veröffentlichten Form dieser Dissertation beigefügt.

In der **1. und 2. Publikation** wurden die reversible Additions-Fragmentierungs Kettenübertragungs (engl. *reversible addition fragmentation transfer*, kurz RAFT) - Polymerisation und die radikalische Atomtransfer Polymerisation (engl. *atom transfer radical polymerization*, kurz ATRP) als kontrollierte radikalische Polymerisationsmethoden zur Herstellung von linearem Poly(*N*-acrylglycinamid) (PNAGA) verwendet. In beiden Arbeiten wurde eine gute Kontrolle der Polymerisation erhalten, welche durch die lineare Steigerung des Molekulargewichtes mit steigendem

Umsatz und einer engen Molekulargewichtsverteilung bestätigt wurde. Außerdem konnte in beiden Veröffentlichungen eine erfolgreiche Kettenverlängerung durch zusätzliche Reaktionen durchgeführt werden, in denen die Polymere als Makroinitiatoren verwendet wurden. Es wurde festgestellt, dass nicht-ionische Kettenübertragungsmittel (nur für RAFT) und Initiatoren entscheidende Faktoren waren, um Polymere mit UCST-Eigenschaften in wässriger Lösung zu erhalten. In der **1. Publikation** wurde gezeigt, dass die hydrophoben Dodecyl-Endgruppen des Kettenübertragungsmittels eine Temperaturerhöhung der Trübungspunkte von Polymeren mit niedrigen Molekulargewichten ( $M_n$  weniger als 10000 g/mol) verursacht. Aus diesem Grund wurde in der **2. Publikation** ein dem Monomer in der Struktur ähnlicher Initiator gewählt, um lineare Polymere mit primären Amidendgruppen zu synthetisieren. In beiden Publikationen wurde der Einfluss der Molmasse, der Endgruppen sowie der Salzkonzentration (NaCl und  $\text{Na}_2\text{SO}_4$ ) auf den Trübungspunkt durch Trübungsmessungen analysiert.

In der **3. Publikation** wurde über RAFT-Polymerisation (analog **Publikation 1**) trithiocarbonat-endfunktionalisiertes PNAGA synthetisiert und dieses durch einen Ligandenaustausch in einer Phosphatpufferlösung auf AuNPs gepfropft. Die PNAGA@AuNPs-Hybrid Materialien zeigten die UCST-Eigenschaft in einer Phosphatpufferlösung. Die Phasenübergänge sind stabil und reversibel für mindestens neun Kühl-/Heizzyklen. Es wurde gezeigt, dass die Funktionalisierung der AuNP keine Auswirkung auf die Trübungspunkte von PNAGA hatte.

**Publikation 4** präsentiert das UCST-Verhalten von chemisch vernetztem PNAGA-Hydrogel, welches durch freie radikalische Polymerisation und *N,N'*-Methylenbis(acrylamid) (MBAAm) als Vernetzer synthetisiert wurde. Das Hydrogel zeigte kontinuierliche Volumenänderungen in Wasser und in Elektrolytlösungen. Es quoll bei erhöhter Temperatur und schrumpfte beim Abkühlen. Der Quellgrad des Hydrogels konnte durch den Gehalt des Vernetzer im Polymer beeinflusst werden. Bei geringen Mengen an Vernetzer zeigte sich ein ähnliches Quell- und Schrumpfverhalten des Hydrogels wie beim linearen Polymer in wässriger Lösung. Es konnte durch viele Kühl-/Heizzyklen im Temperaturbereich von 4 bis 40 °C gezeigt werden, dass die Volumenveränderung in reinem Wasser sowie in Phosphatpufferlösungen reversibel ist.

In **Publikation 5** wird ein Terpolymer mit UCST-Eigenschaften bestehend aus Acrylamid (AAM), Acrylnitril (AN) und UV-vernetzbarem Comonomer beschrieben. Das Terpolymer mit linearer Struktur wurde durch freie radikalische und RAFT-Polymerisation synthetisiert und zeigte UCST-Eigenschaften in Wasser und Elektrolytlösungen. Die Terpolymere zeigten fast keine Hysterese bei den Kühl- und Heizzyklen und besaßen eine hohe Stabilität gegenüber Hydrolyse. Selbst nach neun Zyklen war keine Hydrolyse erkennbar. Die Trübungspunkte der Polymerlösungen konnten durch den Acrylnitrilgehalt im Polymer variiert werden. Chemisch vernetzte Filme und Nanofasern der Terpolymere wurden durch Lösungsgießen bzw. Elektrosponnen und anschließende UV-Bestrahlung erfolgreich hergestellt. Die so hergestellten Hydrogele zeigten temperaturabhängige Volumenänderungen, die für die Gestaltung von Mikro-Aktoren verwendet werden können.

Im **Ausblick** wird auf die Herausforderungen und Anwendungen von UCST Polymeren eingegangen. Bisher sind nur nicht-ionische UCST-Polymere, welche Amid- oder Ureido-Gruppen besitzen, bekannt. Theoretisch könnten auch andere hydrophile Polymere, die funktionelle Gruppen enthalten, welche Wasserstoffbrückenbindungen ausbilden können, eine UCST-Eigenschaft aufweisen. Dadurch wären deutlich mehr UCST Polymere zugänglich. Das nicht-ionische Hydrogel mit einer thermoresponsiven Eigenschaft könnte für die Arzneimittelfreisetzung genutzt werden. Es konnte gezeigt werden, dass es nun möglich ist, vernetzte Polymere mit unterschiedlichen Formen aus linearen Polymeren durch die Bestrahlung mit UV-Licht herzustellen.

**List of symbols and abbreviations**

AAc	acrylic acid
AAm	acrylamide
AIBN	azobisisobutyronitrile
AN	acrylonitrile
ATRP	atom transfer radical polymerization
AuNPs	gold nanoparticles
BPA	4-acryloyloxybenzophenone
BPAm	<i>N</i> -(4-benzoylphenyl) acrylamide
CGC	critical gel concentration
CMDT	cyanomethyl dodecyl trithiocarbonate
CRP	controlled radical polymerization
DMSO	dimethyl sulfoxide
DSC	differential scanning calorimetry
eq	equivalents
FRP	free radical polymerization
GPC	gel permeation chromatography
IPNs	interpenetrating polymer networks
LCST	lower critical solution temperature
MBAAm	<i>N,N'</i> -methylenebisacrylamide
m, n	degree of polymerization
$M_n$	number average molar mass
$M_w$	weight average molar mass
NAGA	<i>N</i> -acryloylglycinamide

## LIST OF SYMBOLS AND ABBREVIATIONS

NIPAM	<i>N</i> -isopropylacrylamide
NMP	nitroxide-mediated polymerization
NMR	nuclear magnetic resonance
PAAc	propylacrylic acid (monomer)
PAAc	poly(acrylic acid)
PAU	poly(6-(acryloyloxymethyl)uracil)
PEG	poly(ethyleneglycol)
PEO	poly(ethylene oxide)
PBS	phosphate buffered saline
PDI	polydispersity index
ppm	parts per million
PDMAEMA	poly( <i>N,N</i> -dimethylaminoethyl methacrylate)
PMAAm	polymethacrylamide
PNAGA	poly( <i>N</i> -acryloylglycinamide)
PNIPAM	poly( <i>N</i> -isopropylacrylamide)
PSPP	poly( <i>N,N'</i> -dimethyl(methacrylamido propyl)ammonium propanesulfonate)
PU	poly(allylurea)
PVA	poly(vinyl alcohol)
RAFT	reversible addition fragmentation chain transfer
SEM	scanning electron microscopy
SPR	surface plasmon resonance
St	styrene
T <sub>CP</sub>	cloud point



## LIST OF SYMBOLS AND ABBREVIATIONS

TEMPO	2,2,6,6-tetramethylpiperidinyloxy
UCST	upper critical solution temperature
UV	ultraviolet light
V-70	2,2'-azobis(4-methoxy-2,4-dimethyl valeronitrile)
Vis	visible light
VPTT	volume phase transition temperature



## 1. Introduction

Polymers with thermoresponsive property are attracting more and more attention. In this thesis polymers with upper critical solution temperature (UCST)-type thermoresponsivity were prepared and their properties were studied. In section 1.1 the thermoresponsive behaviors of polymers were reviewed, the synthesis and properties of polymers with UCST-type as well as their applications were emphasized. Open questions in this area lead to the aims of this thesis, which were summarized in section 1.2. To achieve the aims, controlled radical polymerization (CRP) was employed as efficient polymerization method in this work to prepare polymers with well-defined structures. Thus, the fundamentals of CRP were highlighted in section 1.3 including discussion of mechanisms. Furthermore, section 1.4 introduces fundamentals of polymer-stabilized gold nanoparticles (AuNPs) and examples of thermoresponsive polymers applied to protect gold nanoparticles.

### 1.1 Thermoresponsive polymers

Every polymer in solution shows more or less sensitivity to temperature: the solubility of any polymer in a specific solvent is affected by temperature. A thermoresponsive polymer, however, changes its property markedly and reversibly in response to minor changes of temperature. Among different types of smart polymers, polymers with temperature responsivity draw increasingly more attention, because temperature can be easily controlled compared to other environmental factors such as pH, salt concentration, magnetic field etc.. In the past decades, thermoresponsive polymers were widely studied in the fields of analytic technology such as ion exchange chromatography<sup>[1,2]</sup>, biology<sup>[3-6]</sup> and medicine<sup>[7-10]</sup>. Focusing on the biological and biomedical applications, thermoresponsive behaviors of polymer in aqueous solution are of interest and discussed in this thesis.

Thermoresponsive polymers are divided into polymers with lower critical solution temperature (LCST) and upper critical solution temperature (UCST) based on their phase transition behavior. The LCST polymers dissolve in the solvent at low temperature and precipitate out upon heating. In contrast to LCST, the phase separation of UCST-type polymers from solvent occurs upon cooling.

The phase behaviour of the polymer solution was normally displayed by isobaric phase diagrams which shows how the phase separation temperature depends on the

## INTRODUCTION

concentration of polymer solution (Figure 1-1). As shown in Figure 1-1, LCST is the lowest phase separation temperature and UCST the highest one in the binodal curve. Thus, above the UCST and below the LCST, only one phase exists for all compositions.

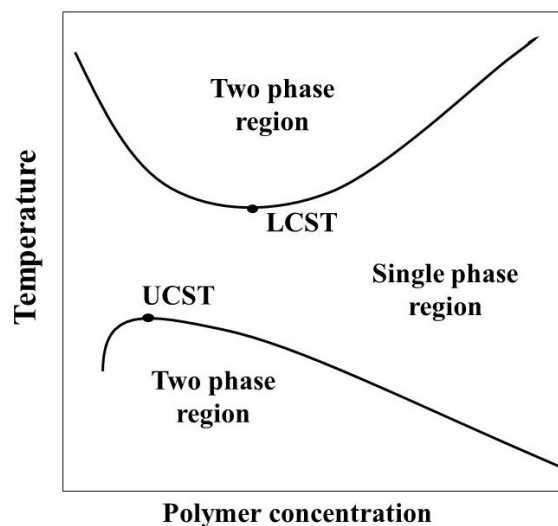


Figure 1-1. Phase diagram for a polymer solution showing lower critical solution temperature (LCST) and upper critical solution temperature (UCST). LCST and UCST are defined as the lowest and highest temperature in the binodal curve, respectively.

The phase transition of a single polymer chain (coil to globule) in organic solvents could be explained by mean-field theory.<sup>[11]</sup> The transition of polymers in aqueous media, on the other hand, is different from organic solvents, because the hydrogen bonding as well as hydrophilic and hydrophobic interactions affect the solubility of polymer in water more than short range Van der Waals interactions.<sup>[12]</sup>

The change of Gibbs free energy  $\Delta G$ , which is the difference between the enthalpic and the entropic components, represents whether a process will happen spontaneously (Equation 1),

$$\Delta G = \Delta H - T\Delta S \quad (1)$$

where  $\Delta H$  and  $\Delta S$  represent the change in enthalpy and the change in entropy, respectively.

Polymers with LCST behavior dissolve in water at low temperature, the polymer hydrophilic moieties build hydrogen bonding with water and the hydrophobic moieties are surrounded with well-organized hydration shell.<sup>[13]</sup> (Figure 1-2) At high temperature, however, part of the hydrophilic moieties build hydrogen bonding with

## INTRODUCTION

each other and the hydrophobic moieties associate, liberating the water molecules in bulk. With increasing temperature, the enthalpic component  $\Delta H$  is positive due to breakage of the hydrogen bonding with water, so is the entropic component  $\Delta S$  because the well-organized hydration shells are released into bulk. This means that at a high temperature,  $\Delta G$  becomes negative and the phase separation happens spontaneously.

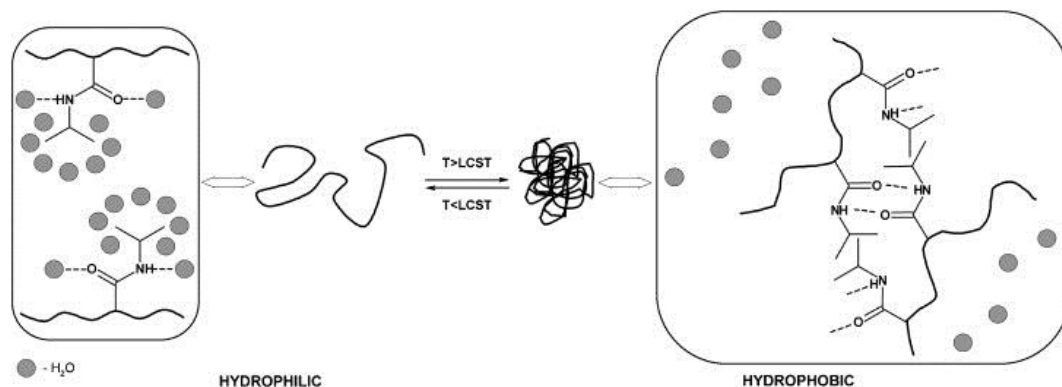


Figure 1-2. Schematic illustration of LCST-type phase separation of poly(*N*-isopropylacrylamide) (PNIPAM) in water.<sup>[13]</sup> (Reprinted with permission from Ref. [13]; Copyright 2007 Elsevier)

UCST polymers build strong hydrogen bonding with each other at low temperature. The hydrogen bonding turns weak when temperature increases.<sup>[14]</sup> Thus, at high temperature polymer-polymer hydrogen bonding are cleaved and the polymer hydrophilic moieties build hydrogen bonding with water, which leads to a positive enthalpic component  $\Delta H$ . The entropic component  $\Delta S$  is positive, because the polymer dissolves in the aqueous solution. This means at a high temperature,  $\Delta G$  becomes negative and the dissolution process happens spontaneously. Similar behavior was found for small inorganic compounds like sodium chloride or sugar, where the small molecules dissolve in water by destroying their crystal structures.<sup>[15]</sup>

The phase separation is normally monitored by a photometer, showing the cloudiness of the polymer solution at different temperatures. Cloud point ( $T_{CP}$ ) refers to the temperature where the solution transmittance changes. Thus, the definition of  $T_{CP}$  is depending on the shape of the turbidity curve. Generally,  $T_{CP}$  is defined as the inflection point of the turbidity curve or the temperature where the transmittance is 50%. Furthermore, polymer solutions show different cloud point on heating and cooling processes. The difference between the cloud point upon cooling and heating is defined as hysteresis. The cloud point is affected also by the rate of temperature changing as well as the polymer concentration. Other common characterization tools for

thermoresponsive polymer solution are differential scanning calorimetry (DSC) by monitoring the enthalpic effects<sup>[16–18]</sup> and light scattering by detecting the coil to globule transition<sup>[19]</sup>.

### Polymers with LCST-type thermoresponsivity in water

Many polymers show LCST-type thermoresponsivity in aqueous media. Among them, homo- and copolymer from *N*-substituted (meth)acrylamides, for example poly(*N*-isopropylacrylamide) (PNIPAM) and its copolymers are the most commonly studied LCST-type polymers.<sup>[4,12,20]</sup> PNIPAM displays a sharp phase transition in water with a small hysteresis on cooling and heating.<sup>[16–18,21]</sup> Gomes and coworkers found *via* light scattering that the  $T_{CP}$  of PNIPAM aqueous solution stayed at 32 °C in a concentration between 1 and 18 wt.%.<sup>[19]</sup> The sharp phase transition, small hysteresis and stable cloud point (32 °C) in broad polymer concentration range explained the wide use of PNIPAM for many varying applications. A typical turbidity curve of PNIPAM in aqueous solution is shown in Figure 1-3.

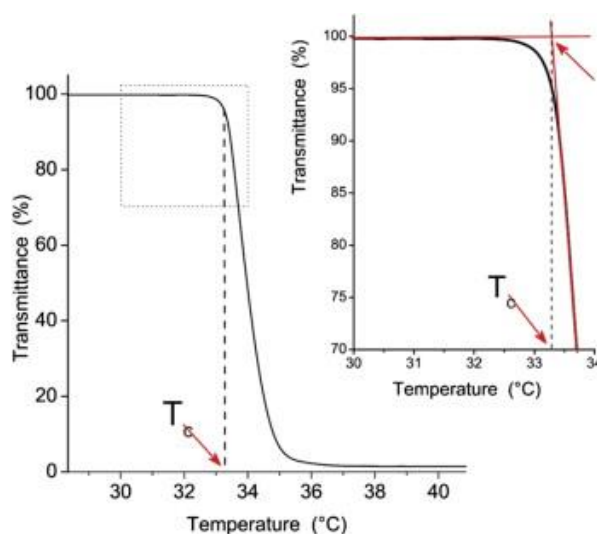


Figure 1-3. Typical turbidity curve of a LCST-type polymer solution, PNIPAM as example.<sup>[21]</sup> Here “ $T_C$ ” represented cloud point. (Reprinted with permission from Ref. [21]; Copyright 2015 Elsevier)

Beside PNIPAM, other *N*-substituted (meth)acrylamide homopolymers exhibiting LCST type phase separation behaviour in water were reviewed by Aseyev and coworkers<sup>[12]</sup> and are listed as follows: poly(*N*-isopropylmethacrylamide) (PiPMAAm), poly(*N*-ethylacrylamide) (PEAAm), poly(*N*-ethylmethacrylamide) (PEMAAm), poly(*N,N'*-ethylmethylacrylamide) (PEMAAm), poly(*N,N'*-diethylacrylamide) (PDEAAm), poly(*N*-n-propylacrylamide) (PnPAAm), poly(*N*-n-

propylmethacrylamide) (PnPMAAm), poly(*N*-cyclopropylacrylamide) (PcPAAm), poly(*N*-(*L*)-(1-hydroxymethyl)propylmethacrylamide (P(*L*-HMPMAAm)), poly(*N*-acryloylpyrrolidine (PAPR) and poly(*N*-acryloylpiperidine) (PAOPip). These polymers have both hydrophilic acrylamide and hydrophobic alkyl groups in the polymer side chain, which are responsible for the LCST properties in water, same as some poly(*N*-vinylamide)s, poly(methyl 2-alkylamidoacrylate)s and poly(oxazoline)s.

Other types of LCST polymers contain poly(ether)s such as poly(ethylene oxide)s (PEG,  $T_{CP}$  about 100 °C), poly(vinyl ether)s as well as poly(vinyl alcohol)s (PVA). Among them, PEO, also widely called poly(ethyleneglycol)s (PEG), is broadly applied in biomedical fields due to their excellent biocompatibility.<sup>[22,23]</sup>

### **Polymers with UCST-type thermoresponsivity in water**

In contrast to LCST materials, polymers with UCST property behave more like most inorganic solids in terms of dissolution process: the solubility of the polymer increases with temperature. Many proteins show UCST-type phase separation (crystallization) in aqueous buffer solution.<sup>[24]</sup> To the best of our knowledge, in 1967 Ranny showed the first example of oligomer with UCST behavior by studying the solubility of methyl ester of C<sub>10</sub> to C<sub>18</sub> fatty acids in DMSO.<sup>[25]</sup> In 1972 Patterson and coworkers showed the pressure effects in UCST polymer solution phase behavior.<sup>[26]</sup> A classic example of a synthetic UCST polymer is polystyrene (PS) in cyclohexane.<sup>[27,28]</sup> However, the UCST polymers in aqueous solution are rarely investigated compared to LCST ones.<sup>[29]</sup> Therefore, there are only few application examples of UCST polymers in literature.<sup>[30]</sup> It was in 2012 that polymers with UCST in aqueous solution were reviewed for the first time.<sup>[29]</sup>

Figure 1-4 displays the number of publications on UCST behavior of polymer aqueous solution as well as general UCST behavior, such as UCST behavior of small molecules or polymer blends and UCST behavior in organic solvents, in the last decade. It is clear that attention given on polymers with UCST behavior in water or electrolytes increased rapidly since year 2010. This is understandable because demands on thermoresponsive polymers for different applications are increasing and new polymer systems with UCST property in aqueous solution were found.

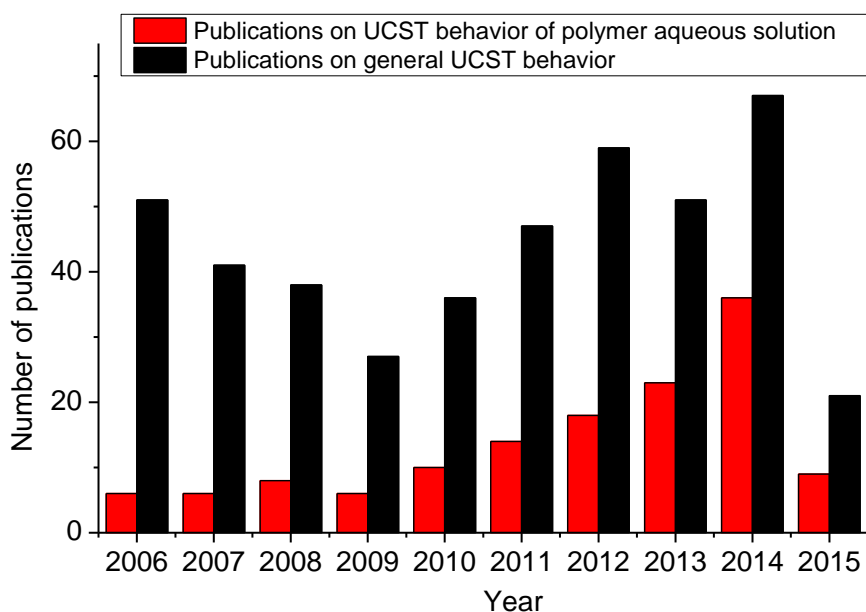


Figure 1-4. Number of publications per year in the last decade on general UCST behavior and UCST behavior of polymer in aqueous solution, respectively. (Based on a SciFinder search on February 26, 2015 with keyword: UCST)

There are polymers with UCST in water below zero or above 100 °C. For example, the UCST of poly(vinyl methyl ether) (PVME) in water is below -10 °C.<sup>[31,32]</sup> PEO with different molecular weights showed both UCST (between 250 and 300 °C) and LCST behavior (between 100 and 170 °C).<sup>[33]</sup> Some hydrophobically modified poly(vinyl alcohol)s showed UCST-type behavior at high temperatures.<sup>[34]</sup> Poly(hydroxyethyl methacrylate) (PHEMA), a well applied hydrogel material, can be also classified as hydrophobically modified PVA. PHEMA with molecular weight less than 5000 g/mol displayed a soluble-insoluble-soluble transition with temperature.<sup>[35]</sup> The cloud point for UCST-type transition was found to be above 100 °C.

Polymers with UCST in water within the 0-100 °C range are reviewed in the following sections.

### **Ionic polymers with UCST in water**

One family of ionic UCST polymers in aqueous solution are zwitterionic polymers, whose UCST-type phase separation is based on the intra- and intermolecular coulomb interactions. The ions increased the solubility of zwitterionic polymers. Thus the cloud points of zwitterionic polymers decreased significantly in the presence of salt.



## INTRODUCTION

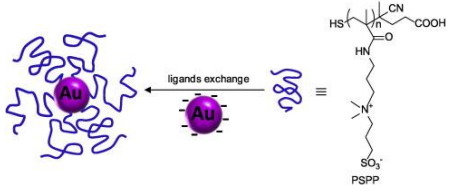
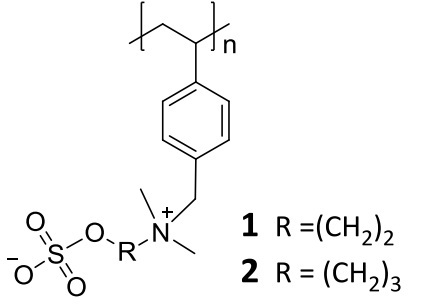
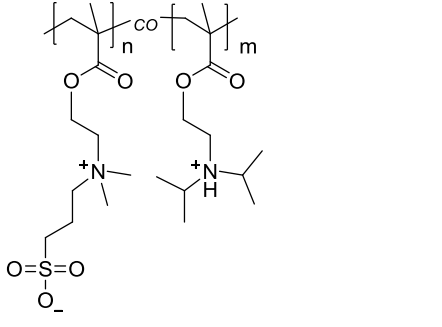
Examples of zwitterionic homopolymers are polybetaines like poly(3-dimethyl(methacryloyloxyethyl) ammonium propane sulfonate) (PDMAPS)<sup>[36,37]</sup> and poly(3-[*N*-(3-methacrylamidopropyl)-*N,N*-dimethyl]ammonio propane sulfonate) (PSPP)<sup>[38]</sup> as listed in the previous work.<sup>[29]</sup> Synthesis and the properties of ionic homo- and copolymers with UCST in water are shown in Table 1-1.

Table 1-1. Zwitterionic polymers with UCST in aqueous solution.

Polymer	Properties
<p style="text-align: center;">Polybetaine</p> <p style="text-align: center;"> <b>1</b> R = O(CH<sub>2</sub>)<sub>2</sub>  <b>2</b> R = NH(CH<sub>2</sub>)<sub>3</sub>  <b>3</b> R = O(CH<sub>2</sub>)<sub>11</sub> </p> <p>1: PDMAPS 2: PSPP 3: Polysoap</p>	<p>Homopolymers showed UCST behavior in pure water and the cloud points decreased in presence of salts. (Ref. [36–38])</p>
<p>Agarose-<i>graft</i>-PDMAPS block copolymer</p> <p>Prepared <i>via</i> atom transfer radical polymerization (ATRP) in DMSO, using CuBr-bpy as a catalyst system</p>	<p>Phase transition between 30 and 60 °C (<i>c</i> = 1 mg/mL)</p> <p>Aggregation of copolymer by cooling in pure water as well as in NaCl and urea solution with different concentrations.(Ref. [39])</p>
<p>RAFT polymerization of PDMAPS using water soluble CTA: 4-cyano-4-(phenylcarbonothioylthio)pentanoic acid (CPTA)</p>	<p>High molar mass polymer up to 500 kDa. Polymers with 5 kDa and 20 kDa molar mass showed no UCST in water (<i>c</i> = 1 mg/mL).</p> <p>Block copolymer of PDMAPS and hydrophilic PEGMA led to disappearance of UCST in water. (Ref. [40])</p>

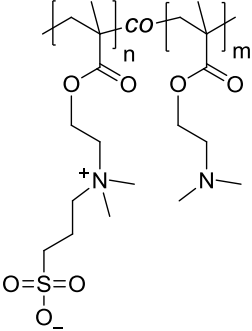
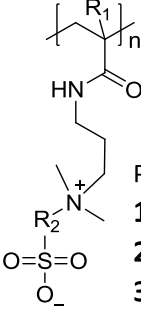
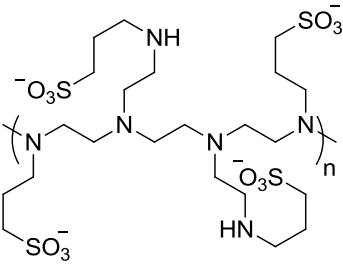
INTRODUCTION

Table 1-1. Zwitterionic polymers with UCST in aqueous solution. (continued)

Polymer	Properties
<p>PSPP@AuNP</p>  <p>(Scheme reprinted with permission from Ref. [41]; Copyright 2014 Elsevier)</p>	<p>PSPP prepared through RAFT polymerization; PSPP@AuNP hybrid <i>via</i> ligand exchange. PSPP@AuNP remained dispersed in pure water at any temperature even at low ionic strength. Free polymer chains in solution lead to an aggregation of PSPP@AuNP at low temperature. (Ref. [41])</p>
 <p>Halophilic polysulfobetaines PSB</p>	<p>Monomers were synthesized by ring opening reaction and the polymers were prepared <i>via</i> FRP using 4,4'-azobis(4-cyanovaleric acid) (ACVA) at 90 °C in 0.5 M aqueous NaBr solution. Polymers formed hydrogel by the polar action between zwitterions and water. UCST behavior was observed in presence of NaCl. (Ref. [42])</p>
<p>PEG-<i>b</i>-PSB</p> <p>Prepared by RAFT polymerization using PEG methyl ether (4-cyano-4-pentanoate dodecyl trithiocarbonate) as CTA</p>	<p>Polymers built self-assembled microspheres (~1µm) when the solution temperature was below the UCST. T<sub>CP</sub>: 20-60 °C Influence of NaCl was shown. (Ref. [43,44])</p>
 <p>PSBMA-<i>co</i>-DPA prepared <i>via</i> FRP using AIBN in DMF and water mixture.</p>	<p>Polymers with molar ratio of SBMA and DPA in copolymer =95/5 showed UCST behavior in pH 3 to pH 7. Cloud points decreased with higher pH value. With higher amount of DPA, the copolymer became insoluble in aqueous solutions between pH 5 and pH 7. (Ref. [45])</p>

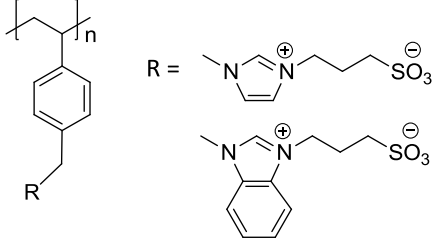
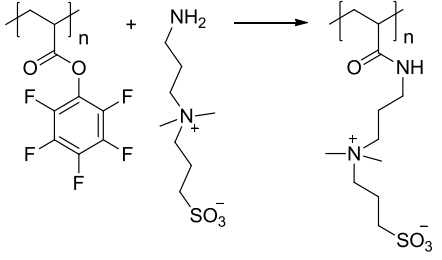
INTRODUCTION

Table 1-1. Zwitterionic polymers with UCST in aqueous solution. (continued)

Polymer	Properties
 <p>PSBMA-co-DMAEMA <i>via</i> ATRP on silica nanoparticles surface with CuBr<sub>2</sub>-bpy as a catalyst system in methanol/water mixture.</p>	<p>Copolymer with molar ratio of SBMA and DMAEMA =75/25 showed UCST and LCST in one. With higher amount of SBMA in copolymer, only UCST property remained. The cloud points increased up to 53 °C. (Ref. [46])</p>
 <p>Polybetaine  <b>1</b> R<sub>1</sub> = H, R<sub>2</sub> = (CH<sub>2</sub>)<sub>3</sub>  <b>2</b> R<sub>1</sub> = H, R<sub>2</sub> = (CH<sub>2</sub>)<sub>4</sub>  <b>3</b> R<sub>1</sub> = CH<sub>3</sub>, R<sub>2</sub> = (CH<sub>2</sub>)<sub>3</sub></p> <p>Polymer synthesis <i>via</i> FRP with KPS/TEMED redox pair in aqueous media.</p>	<p>Nanocomposite gel was prepared by adding inorganic clay platelets in the DMAA copolymers.</p> <p>The nanocomposite gel showed transparent/opaque transition with temperature (UCST-type) and good mechanic property. (Ref. [47–49])</p>
 <p><i>N</i>-sulfopropylated <i>b</i>-PEI (PS-PEI)</p>	<p>Polymers prepared through sulfopropylation of biopolymer branched PEI.</p> <p>T<sub>CP</sub> in water was between 19 and 85 °C and depended on molar ratio of sulfonate and PEI. A higher content of sulfonate increased the T<sub>CP</sub>. UCST behavior was highly pH-dependent. (Ref. [50])</p>

## INTRODUCTION

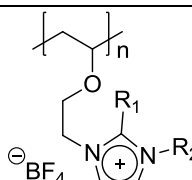
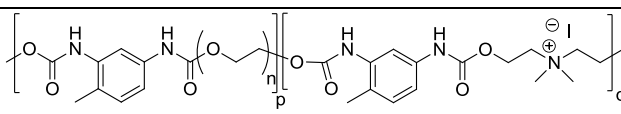
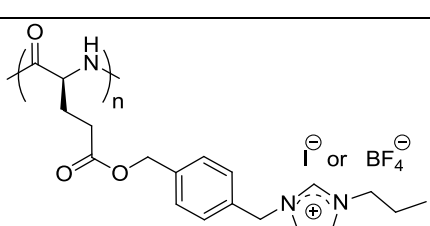
Table 1-1. Zwitterionic polymers with UCST in aqueous solution. (continued)

Polymer	Properties
 <p data-bbox="252 584 703 734">Polymers were prepared <i>via</i> FRP using ACVA at 90 °C in 25 wt% aqueous NaBr solution.</p>	<p data-bbox="730 322 1342 521">Polymers are stable against hydrolysis. Polymers behaved like hydrogels in water and showed UCST behavior in presence of NaCl with <math>T_{CP}</math> in the range 20-40 °C. (Ref. [51])</p>
	<p data-bbox="730 752 1342 1122">Polysulfobetaines and their copolymers <i>via</i> post-modification of poly-(pentafluorophenyl acrylate) (PPFPA) with 3-((3-aminopropyl)dimethylammonio)propane-1-sulfonate (ADPS) and pentylamine, benzylamine, or dodecylamine (insoluble), respectively (Ref. [52])</p>

### Polyelectrolytes in the presence of multivalent counterions

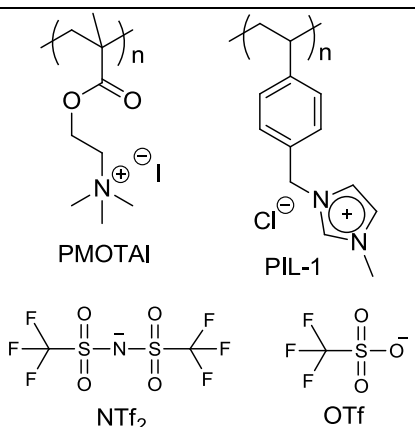
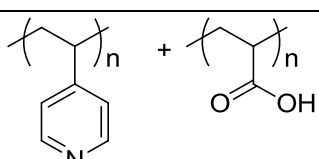
In analogy to zwitterionic polymers some polyelectrolytes show UCST behavior under certain ionic concentration and pH value. For instance, the micelles based on PEO and protonated poly(2-vinylpyridine) (PEO-*b*-P2VPH<sup>+</sup>) show reversible UCST-type micelles-solution transition in a temperature range of 38 to 70 °C, in presence of divalent peroxodisulfate ions (S<sub>2</sub>O<sub>8</sub><sup>2-</sup>) at pH 1.3.<sup>[53]</sup> Other examples are listed in Table 1-2.

Table 1-2. Polyelectrolytes with UCST in aqueous solution.

Polymer	Properties
 <p> <b>1</b> poly([MeIm][BF<sub>4</sub>])  R<sub>1</sub> = H R<sub>2</sub> = CH<sub>3</sub>  <b>2</b> poly([EtIm][BF<sub>4</sub>])  R<sub>1</sub> = H R<sub>2</sub> = C<sub>2</sub>H<sub>5</sub>  <b>3</b> poly([Me<sub>2</sub>Im][BF<sub>4</sub>])  R<sub>1</sub> = CH<sub>3</sub> R<sub>2</sub> = CH<sub>3</sub> </p> <p>Polymeric ionic liquids prepared <i>via</i> living cationic polymerization following post-modification and anion exchange reaction.</p>	<p>Polymers with M<sub>n</sub> ~ 15 kDa and PDI ~ 1.1.</p> <p>T<sub>CP</sub> between 5 to 15 °C with concentration of 2 wt.% in water.</p> <p>For polymer 1, T<sub>CP</sub> dependence on polymer concentration was shown. Up to 20 wt.% the T<sub>CP</sub> was about 25 °C. (Ref. [54])</p>
 <p>Polymer prepared <i>via</i> polyaddition and subsequent quaternization with (without) PEG<sub>2000</sub></p>	<p>Copolymers showed UCST behavior with p = 0, 1, 2, 3 (and 5 mol% of q).</p> <p>T<sub>CP</sub>: 48-84 °C (Ref. [55])</p>
 <p>α-helical polypeptide, prepared by ring-opening polymerization of <i>N</i>-carboxyanhydride with subsequent post-polymerization and ion-exchange reaction.</p>	<p>Biodegradable polymer</p> <p>T<sub>CP</sub>: 36 °C for I<sup>-</sup> (M<sub>n</sub> = 30.4 kDa, PDI = 1.5) and 69 °C for BF<sub>4</sub><sup>-</sup> (M<sub>n</sub> = 27.9 kDa, PDI = 1.5)</p> <p>(Ref. [56])</p>

## INTRODUCTION

Table 1-2. Polyelectrolytes with UCST in aqueous solution. (continued)

Polymer	Properties
Blend of P(NIPAM- <i>co</i> -2-acrylamido-glycolic acid) and PDMAEMA	LCST-UCST-type phase transition in acid solution; UCST behavior at high temperature based on the protonation of PDMAEMA (Ref. [57])
PEG- <i>b</i> -PDMAEMA	LCST-UCST in one at pH value of 10 and 12; thermoresponsive behavior was pH and salt dependent. (Ref. [58])
 <p>PMOTAI      PIL-1</p> <p>NTf<sub>2</sub>      OTf</p>	<p>Polymers prepared <i>via</i> RAFT polymerization</p> <p>PMOTAI: <math>M_n = 52</math> kDa,</p> <p>PIL-1: <math>M_n = 25</math> kDa</p> <p>UCST behavior dependence on polymer concentration, counterions and NaCl were studied.</p> <p><math>T_{CP}</math>: between 20-90 °C (Ref. [59])</p>
 <p>PAA/P4VP complex aqueous material</p>	UCST in pH between 1.7 and 2.5. The phase behaviors were characterized by FTIR and UV/Vis spectroscopy. (Ref.[60])

**Non-ionic polymers with UCST in water**

The non-ionic UCST polymers form very strong hydrogen bonding between polymer moieties and with water. The hydrogen bonding is more stable against ions, meaning that the UCST behaviors of non-ionic polymers are less sensitive to the salt concentration in water. For the applications in biological and biomedical areas, polymers with an inert UCST behavior against ions are of advantage. So far non-ionic polymers with UCST-type thermoresponsivity featured primary amide or ureido groups, which are responsible for the hydrogen bonding between polymer and water.<sup>[29]</sup> Some examples are discussed as follows and listed in Table 1-3.

Poly(*N*-acryloylglycinamide) (PNAGA) is the most studied UCST polymers so far. It was first synthesized by Haas in 1964 to produce a thermally reversible aqueous gels.<sup>[61]</sup> Later, they studied the gelation process and found that the gel remains dissolved in presence of small amount of urea or thiocyanate, which interrupts the hydrogen bonding.<sup>[62]</sup> The copolymerization of NAGA with acrylic acid was also investigated. It was concluded by calculating the average number of groups involved in a crosslink, that the gelation (also known as physical cross-linked gel) is based on the hydrogen bonding.<sup>[63,64]</sup> The aggregation of PNAGA in presence of sodium thiocyanate was studied by using dynamic and static light scattering and viscometer.<sup>[65]</sup> The local structural changes during sol-gel transition and in dilute solution was monitored using Raman spectroscopy. It was confirmed that the thermoresponsive hydrogen bonding is responsible for the transition.<sup>[66]</sup> The first controlled radical polymerization of NAGA was carried out by Glatzel and coworkers *via* RAFT polymerization by using ionic chain transfer agent and initiator.<sup>[67]</sup> The critical gelation concentration was found to decrease with increasing molecular weight. Another very recent work from Boustta and coworkers showed nicely the drug delivery experiment based on sol-gel transition of PNAGA, inspiring more application of PNAGA as well as UCST polymers.<sup>[68]</sup>

The UCST-type phase separation of PNAGA homopolymer made *via* FRP in DMSO using AIBN as initiator was first discovered by Agarwal and coworkers.<sup>[69]</sup> Later it was well discussed how the ionic groups can be introduced in the polymer chain before or after polymerization and thus could lead to a significant decrease or disappearance of cloud point.<sup>[70]</sup> In summary, the acrylic acid or acrylate impurities in the monomer, ionic initiator or/and chain transfer agent (in RAFT process) and hydrolysis caused by

high polymerization temperature or sample preparation should be avoided to get a PNAGA with UCST-type thermoresponsivity. These important hints are followed during the thesis.

Besides PNAGA homopolymer, a series of copolymers based on NAGA were synthesized and showed UCST behavior in aqueous solution: poly(*N*-acryloylglycinamide-*co*-*N*-acetylacrylamide) (PNAGA-*co*-NAAAm),<sup>[69]</sup> poly(*N*-acryloylglycinamide-*co*-butyl acrylate) (PNAGA-*co*-BA), poly(*N*-acryloylglycinamide-*co*-styrene) (PNAGA-*co*-St).<sup>[71]</sup> Furthermore, some derivatives of PNAGA also show UCST-type thermoresponsivity, for example poly(*N*-acryloylasparagineamide) (PNAAM), poly(*N*-acryloylglutamineamide) (PNAGAAm) and poly(methacryloyl-asparagineamide) (PNMAAM).<sup>[72]</sup>

Poly(acrylamide) (PAAm) is a well-known water soluble polymer. Copolymers based on acrylamide, however, could show UCST-type transition in water and electrolytes. Agarwal and coworkers have shown a series of copolymer of acrylamide (AAm) and acrylonitrile (AN) *via* free radical polymerization with cloud point from 5 to 60 °C by adjusting the content of AN in polymer.<sup>[71]</sup> A copolymer based on AAm and St could display UCST in water with homogeneous polymer composition.<sup>[73]</sup> Zhang and coworkers showed the reversible addition fragmentation chain-transfer (RAFT) polymerization of AAm and AN with different molar mass and content ratio.<sup>[74]</sup> The copolymer showed as expected UCST in aqueous solution. Thereafter, one sample was extended by hydrophobic (styrene), hydrophilic (dimethylacrylamide) and typical LCST monomer (*N,N'*-dimethylaminoethyl methacrylate), respectively. All synthesized block copolymers kept their UCST behavior in aqueous solution.

Polymethacrylamide (PMAAm) featured primary amide groups, same as PAAm, and additional methyl group at the polymer backbone that makes PMAAm more hydrophobic, which could work as AN or St in the examples mentioned above. This assumption was proved by Agarwal and coworkers who chose non-ionic initiator AIBN for the polymerization of MAAM and the polymer showed UCST-type transition in water, while the former studies failed to notice the property.<sup>[71,75]</sup>

Aoki and coworkers showed that the UCST-type phase separation of poly(6-(acryloyloxymethyl)uracil) (PAU) synthesized by free radical polymerization in DMF using AIBN as initiator.<sup>[76]</sup> They also observed the transition temperature dependence



## INTRODUCTION

of adenosine concentration, indicating the hydrogen bonding was the key for phase separation.

It was shown by Shimada and coworkers that ureido-derivatized polymers exhibited UCST behavior under physiological buffer condition.<sup>[30]</sup> They modified poly(allylurea) (PU) and poly(L-citrulline) derivatives with succinyl anhydride (PU-Su) and acetyl anhydride (PU-Ac) to adjust the cloud point and to control interactions between polymers and biocomponents. Very recently, Mishra and coworkers synthesized a series of ureido derivatized polymers *via* atom transfer radical polymerization (ATRP) and further quarternized with methyl iodide. The cloud point of the polymer in aqueous solution was found to be dependent on the degree of quaternization.<sup>[77]</sup>

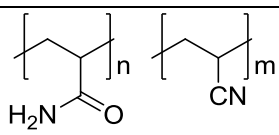
Ritter and coworkers showed the UCST-type transition of poly(*N*-vinylimidazole-*co*-1-vinyl-2-(hydroxymethyl)imidazole) and further modified the copolymer with small amounts of adamantyl groups to control the cloud point of the polymers in water.<sup>[78,79]</sup>

A low molecular weight poly(trimethylene ether) glycol (P03G,  $M_n = 300$  g/mol) was found to exhibit both LCST and UCST phase separation in water at low and high concentration, respectively.<sup>[80]</sup> This can be explained by the hydrophobicity of this polymer in comparison to PEO, leading to a shift of the LCST and UCST to 0-100 °C range.

Di and coworkers show the UCST behavior of poly(*N*-propionyl-aspartic acid/ethylene glycol) (PPAE) synthesized *via* polycondensation of L-aspartic acid and ethylene glycol, which could show promising applications in biomedical field.

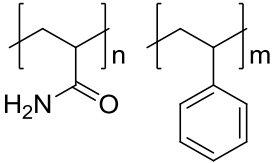
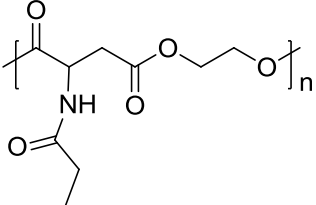
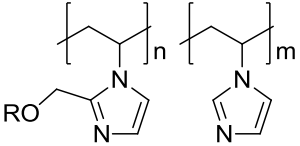
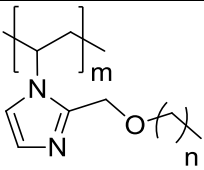
Recent review by Roth pointed out a new strategy for the preparation of stimuli-responsive materials by postpolymerization modifications.<sup>[81]</sup> As example, copolymers with UCST property was synthesized by modifying polyacrylate with appropriate amounts of aliphatic primary and secondary amines.

Table 1-3. Non-ionic polymers with UCST in aqueous solution.

Polymer	Properties
	<p>Copolymers prepared <i>via</i> FRP and RAFT polymerization. (Ref. [71,74])</p> <p><math>T_{CP}</math> could be controlled by varying the content of AN in polymer.<sup>[71]</sup></p>

INTRODUCTION

Table 1-3. Non-ionic polymers with UCST in aqueous solution. (continued)

Polymer	Properties
	<p>Copolymers prepared <i>via</i> FRP showed no UCST behavior, only the sample <i>via</i> RAFT polymerization showed UCST behavior. (Ref. [73])</p>
 <p>poly(<i>N</i>-propionyl-aspartic acid/ethylene glycol) (PPAE)</p>	<p><math>M_n</math>: 4~10 kDa,  PDI: <math>\approx 3</math>  <math>T_{CP}</math>: 27-32 °C in water  UCST behavior also in alcohol/water mixture (Ref. [82])</p>
 <p><b>1</b> R = H  <b>2</b> R = H, CONH-cyclodextrine</p> <p>1: poly(<i>N</i>-vinylimidazole-<i>co</i>-1-vinyl-2-(hydroxymethyl)-imidazole)  2: (1-Vinyl-2-yl)methyl-adamantan-1-ylcarbamate</p>	<p>polymers show UCST only if molar ratio of comonomer 1-Vinyl-2-(hydroxymethyl)-imidazole (polymer 1) is higher than 0.4 eq. <math>T_{CP}</math> between 18-40 °C in water, 4 wt.% in water  <math>T_{CP}</math> decreased with pH value: at pH 2 the copolymers are completely protonated and show no UCST  Terpolymer 2: with 0 mol% comonomer, <math>T_{CP}</math> = 41 °C. with 1 mol%, comonomer <math>T_{CP}</math> = 78 °C and with 2 mol% hydrophobic cyclodextrine side group <math>T_{CP}</math> over 100 °C  (polymer 1 Ref. [79] and polymer 2 Ref. [78])</p>
 <p>n = 0,1,2,3</p>	<p>Only if n = 1, LCST, <math>T_{CP}</math> = 23 °C  n = 0, polymer is water soluble  n = 2, 3 polymer is water insoluble  Copolymer with hydrophilic <i>N</i>-vinylimidazole also show LCST. (Ref. [83])</p>

## INTRODUCTION

Table 1-3. Non-ionic polymers with UCST in aqueous solution. (continued)

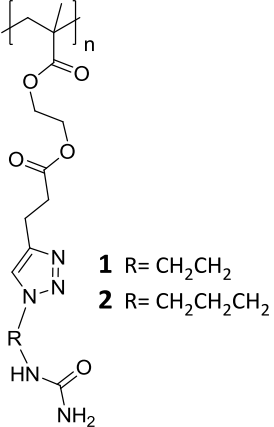
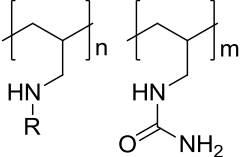
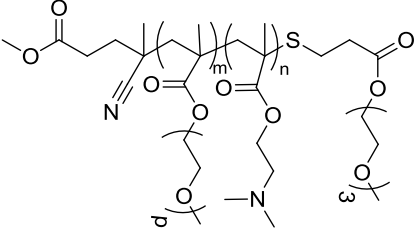
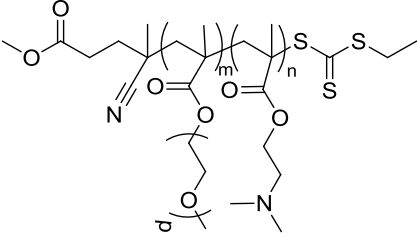
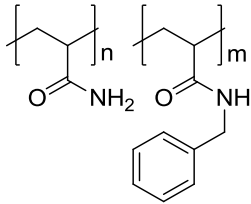
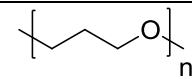
Polymer	Properties
<p>ureido-derivatized polymers</p>  <p><b>1</b> R = CH<sub>2</sub>CH<sub>2</sub> <b>2</b> R = CH<sub>2</sub>CH<sub>2</sub>CH<sub>2</sub></p>	<p>Polymer 1: T<sub>CP</sub> = 76 °C and polymer 2, T<sub>CP</sub> = 96 °C higher hydrophobicity results in higher T<sub>CP</sub>.</p> <p>Partly quaternization with methyl iodide decreased the T<sub>CP</sub>. (Ref. [77])</p>
 <p><b>1</b> R = H <b>2</b> R = COC<sub>2</sub>H<sub>4</sub>COOH <b>3</b> R = COCH<sub>3</sub></p>	<p>Copolymers with ionic groups were sensitive to buffer condition such as pH and salt condition. PU-Am7 selectively captured proteins. (Ref. [30])</p>
	<p>Schizophrenic diblock copolymer, From conventional micelles <i>via</i> unimers to reverse micelles and precipitated upon heating in presence of NaCl and [Co(CN)<sub>6</sub>]<sup>3-</sup> (Ref. [84])</p> <p>It should be noticed that in another example the authors showed a copolymer with methacrylic acid, which lead to disappearance of UCST in water, showed UCST only in alcohol–water solvent mixtures (Ref. [85])</p>
	<p>The influence of different counterions such as [Co(CN)<sub>6</sub>]<sup>3-</sup>, [Fe(CN)<sub>6</sub>]<sup>3-</sup>, [Cr(CN)<sub>6</sub>]<sup>3-</sup> on the LCST and UCST behavior of PDMAEMA. (Ref. [86])</p>

Table 1-3. Non-ionic polymers with UCST in aqueous solution. (continued)

Polymer	Properties
Supramolecular system from $\beta$ -CD trimer and naphthalene-terminated poly(ethylene glycol) (PEG-NP <sub>2</sub> )	Cyclodextrin (CD) inclusion complex Upside down bell-shaped UCST-LCST phase transition (Ref. [87])
	Copolymer of acrylamide (0.87 mol%) and benzylacrylamide (0.13 mol%) <i>via</i> post modification, showed T <sub>CP</sub> of 7 °C in water. (Ref. [88])
 ( M <sub>n</sub> =300 g/mol)	UCST behavior in water with concentration over 45 wt.%. (Ref. [80])

### Hydrogels with positive and negative thermoresponsive properties in water

Hydrogels are three-dimensionally crosslinked polymers, which absorb water and swell readily without dissolving. With excellent biocompatibility, hydrogels are perfect candidates for biological and biomedical applications, for instance cell immobilization<sup>[89]</sup>, sensors<sup>[90]</sup> and *on-off* release of molecules<sup>[7]</sup>. Hydrogels may swell or deswell dependent on the external environment and thus can be classified as pH, ionic strength, electromagnetic radiation and temperature responsive, based on the external stimuli.<sup>[91,92]</sup> Among them thermoresponsive hydrogels have gained more attentions because temperature could be easily controlled.<sup>[93,94]</sup>

Two most extensively investigated synthetic thermoresponsive hydrogels are based on PEG-polyester block copolymers and PNIPAMs.<sup>[95]</sup> PEG-polyester block polymers show a sol to gel transition with decrease in temperature if the concentration is above the critical gel concentration (CGC). These classes of polymers were recently nicely reviewed by Buwalda and coworkers.<sup>[95]</sup> The gelation of these polymers is due to micelle packing and hydrophobic interactions.<sup>[94]</sup> These are physically crosslinked hydrogels.

The most famous and well-studied thermoresponsive hydrogels with chemical crosslinking are based on the family of LCST polymers, such as PNIPAM mentioned

in the section above. Hydrogels made of polymers with a LCST-type transition shrink when the temperature is higher than the so-called volume phase transition temperature (VPTT) and swell when the temperature is lower than VPTT. Gels with this negative volume phase transition behavior are also called thermophobic hydrogels. Thermophobic hydrogels were well investigated in different areas, for instance thermoresponsive thin hydrogel-grafted surfaces for biomedical application,<sup>[96]</sup> drug delivery<sup>[97]</sup> as well as cell culture surfaces.<sup>[98]</sup>

The first observation of discontinuous phase transition of PNIPAM hydrogel was reported by Hirokawa and coworkers in 1984.<sup>[99]</sup> The first example of PNIPAM hydrogel with macroporous structures was prepared by Wu and coworkers in 1992 using dihydroxyethylene-bis-acrylamid (DHEBAAm) as crosslinker.<sup>[100]</sup> PNIPAM hydrogels have been found with two drawbacks: the release of loaded drugs was very quick within 24 hours and the swollen hydrogels have bad mechanical properties. Thus, interpenetrating polymer networks (IPNs) of PNIPAM were formed with *N,N'*-methylenebisacrylamide (MBAAm) as crosslinker,<sup>[101]</sup> or covalent copolymer system with hydrophilic or hydrophobic monomers for example AAc, propylacrylic acid (PAAc), PEO, and L-glutamic acid (L-Glu) to increase or decrease the volume transition temperature.<sup>[95]</sup>

Hydrogels based on polymers with UCST, however, show a positive volume phase transition and thus were defined as thermophilic hydrogels. Hydrogels with thermophilic behavior were reviewed very recently by Mah and coworkers.<sup>[102]</sup> Thermophilic hydrogels were less studied compared to their counterpart thermophobic hydrogels, similar like polymers with UCST in aqueous solution are rare.<sup>[103,104]</sup>

Thermophilic hydrogels based on ionic polymers, for instance polyelectrolyte polymers and polyzwitterions which contain positively and negatively charged side groups, have been widely studied.<sup>[105]</sup> The electrostatic forces between intra- or intermolecular ionic pairs are responsible for the volume transition behavior.<sup>[106]</sup> Examples are: Georgiev and coworkers prepared PDMAPS hydrogels with ethyleneglycol dimethacrylate (EGDM) as chemical crosslinker, showing reversible positive volume-phase transition with temperature.<sup>[106]</sup> Ning and coworkers. showed very recently a UCST-type transition of chemically crosslinked hydrogels based on zwitterionic sulfobetaine acrylamide.<sup>[49]</sup> As mentioned previously, the phase transition behavior of ionic

## INTRODUCTION

polymers are strongly affected by the low molecular weight electrolytes, for example salt as well as their concentrations and pH. The volume transition of the hydrogels based on these polymers are also found to be salt and pH sensitive.<sup>[107]</sup>

Besides ionic hydrogels, interpenetrating polymer networks (IPNs) show interpolymer complexation based on hydrogen bonding and thus provide volume transition behavior. A well-studied IPN system showing positive VPTT was based on AAm and acrylic acid (AAc). Interpolymer complex formation between PAAc, as a proton donor and PAAm, as proton acceptor in aqueous solution are formed due to hydrogen bonding.<sup>[108]</sup> Hydrogen bonding became weak with increasing temperature and thus lead to a dissociation of the complex.<sup>[109–111]</sup> A model of thermoreversible swelling changes induced by polymer complex formation and dissociation was introduced by Sakurai and coworkers.<sup>[112]</sup> (Figure 1-4)

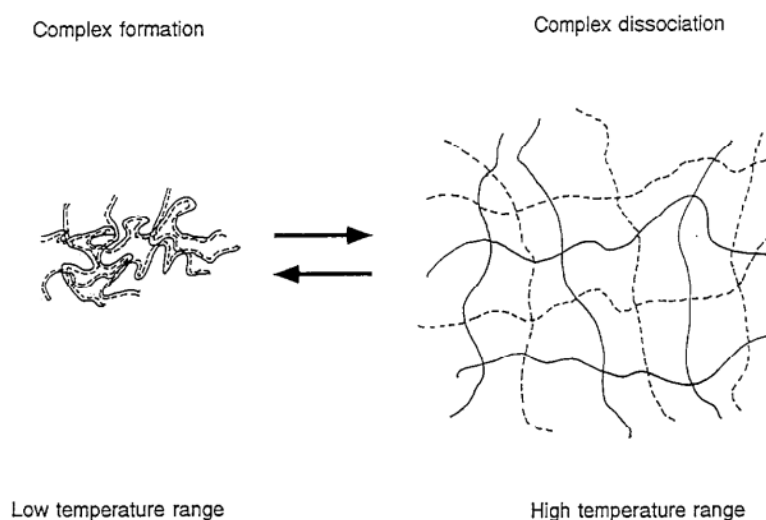


Figure 1-4. Model of thermoreversible swelling changes induced by polymer complex formation and dissociation.<sup>[112]</sup> (Reprinted with permission from Ref. [112]; Copyright 1991 Elsevier)

A comparison of P(AAc-AAm) IPNs and random copolymer particles was presented by Bouillot and coworkers. It was found that the IPNs display discontinuous volume change, while the copolymer particles show rather a linear increase of swelling ratio with increasing temperature.<sup>[110]</sup> (Figure 1-5) Katono and coworkers showed the first IPNs example using poly(AAm-co-MBA) gels as first component and PAAc as second component in 1991.<sup>[112]</sup> In the same work, it was found that, while the poly(AAm-co-MBA)/PAAc IPNs undergo an discontinuous volume transition behavior, the random copolymerized hydrogels from the same monomers exhibit a continuous volume

transition. Li and coworkers showed IPNs from poly(acrylic acid)-*graft*- $\beta$ -cyclodextrin (PAAc-*g*- $\beta$ -CD) and PAAm showing UCST behavior at 35 °C and the application in drug loading and release using ibuprofen as example.<sup>[113]</sup>

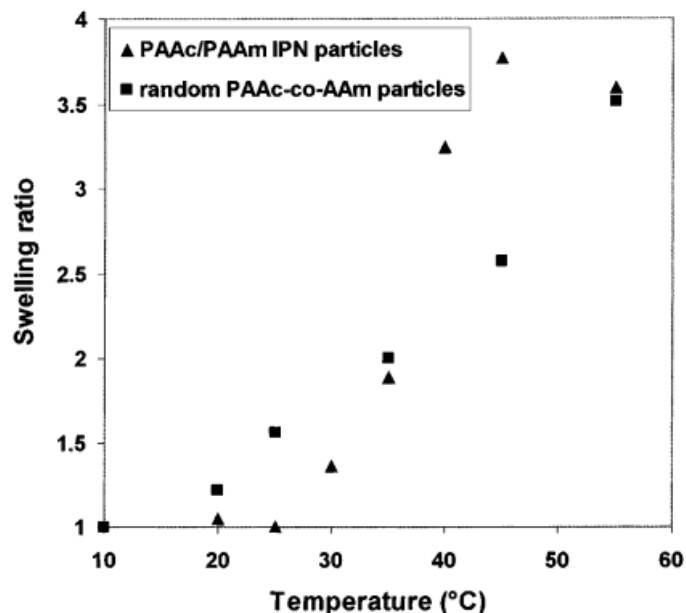


Figure 1-5. A direct comparison of swelling behaviour of P(AAc-AAm) copolymer and IPNs particle for an AAc/AAm molar ratio of 0.96.<sup>[110]</sup> (Reprinted with permission from Ref. [110]; Copyright 2000 Springer)

Similar to AAm, NAGA contains amide groups and thus is also suitable for IPNs. IPNs composed of PNAGA and PAAc were also reported in order to modulate volume phase-transition temperature.<sup>[114]</sup> (Figure 1-6)

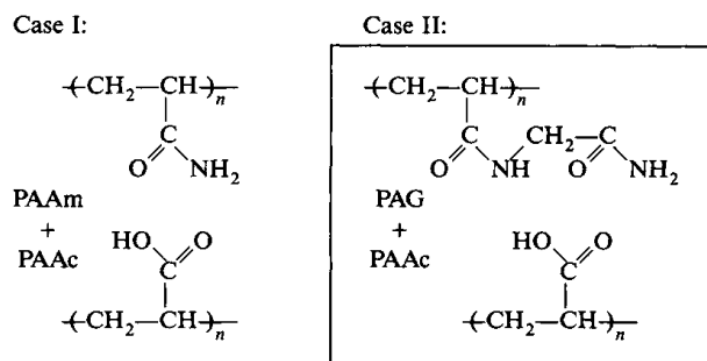


Figure 1-6. Two types of IPNs: Case I, PAAm/PAAc and case II, PNAGA/PAAc. (Reprinted with permission from Ref. [114]; Copyright 2003 John Wiley and Sons)

## Challenges

The previous contributions in the Agarwal group in recent years focused on the UCST behavior of homo- and copolymers in water like PNAGA, PAAm-*co*-AN, etc. For the first time UCST behavior of PNAGA and copolymer in water was shown in 2010.<sup>[69]</sup> These polymers were synthesized *via* FRP. In another contribution from Lutz and coworkers, RAFT polymerization of NAGA was shown.<sup>[67]</sup> They failed to observe UCST behavior in water. Later in 2012, the fact that traces of ionic groups in the polymer can reduce the  $T_{CP}$  or prevent phase transition of PNAGA was published by Agarwal and coworkers.<sup>[70]</sup> (Figure 1-7)

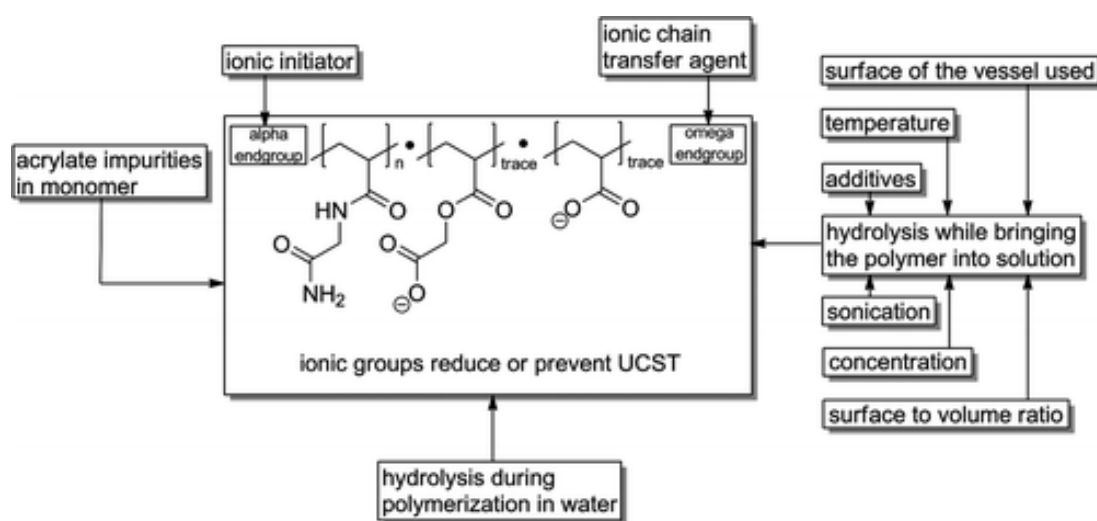


Figure 1-7. Traces of ionic groups in the polymer can reduce or prevent phase transition of PNAGA. (Reprinted with permission from Ref. [70]; Copyright 2012 American Chemical Society)

It has been further shown in this work, that the phase transition of PNAGA was broad and the hysteresis of cloud points on cooling and heating was around 10 °C. (Figure 1-8) Thus, it is important to understand the effect of polymer characters on the UCST behavior such as cloud point, hysteresis on cooling and heating, and sharpness of the phase transition. To achieve this, controlled radical polymerization methods are necessary to prepare polymers with well-defined structure, which was achieved in the present thesis.



## INTRODUCTION

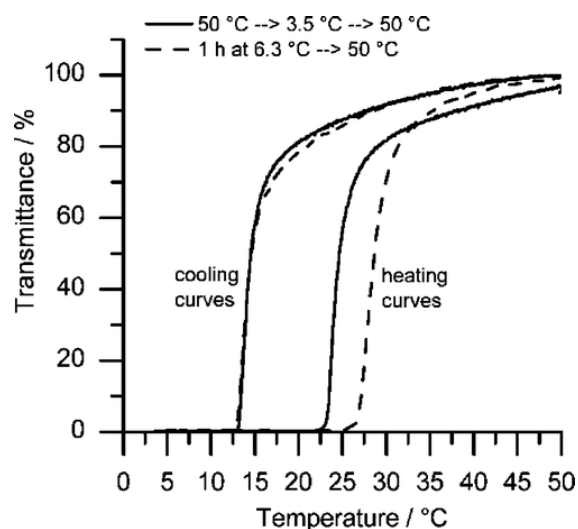


Figure 1-8. Turbidity curve of PNAGA in water with concentration of 1.0 wt.%. The hysteresis of cloud points on cooling and heating was around 10 °C. (Reprinted with permission from Ref. [70]; Copyright 2012 American Chemical Society)

In another contribution from the Agarwal group, copolymers with tunable UCST in water and electrolyte solution were introduced.<sup>[71]</sup> One copolymer system based on AAm and AN showed a very sharp phase transition in water and PBS. Another advantage of the PAAm-*co*-AN copolymer system is that the cloud point can be manipulated easily by varying the AN content in copolymer. (Figure 1-9) Based on the system, it is possible to produce photo cross-linkable polymers with UCST-type thermoresponsivity in my work.

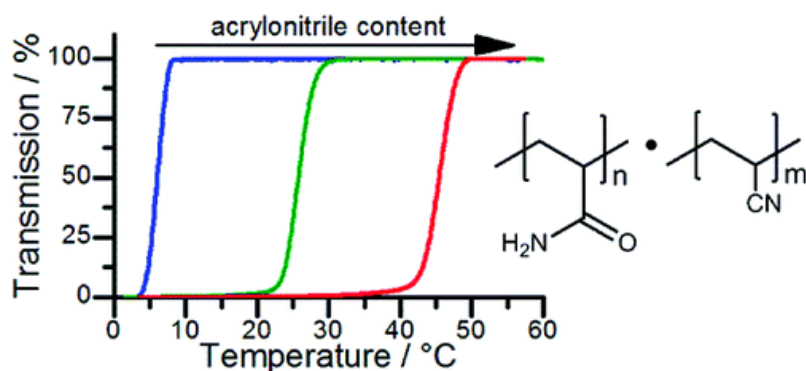


Figure 1-9. Turbidity curves of PAAm-*co*-AN copolymer in PBS. The cloud point can be manipulated easily by varying the AN content in copolymer. (Reprinted with permission from Ref. [71]; Copyright 2012 American Chemical Society)

### **1.2 Aims of the thesis**

Based on the previous understanding of UCST polymers, the aims of this work were to:

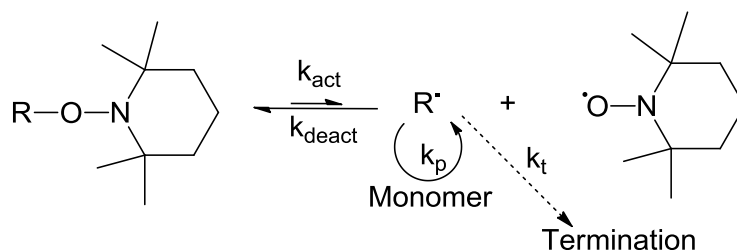
- study the effect of polymer characters such as chain end groups, molar mass and polydispersity on the UCST behavior, i.e. cloud point of the polymer aqueous solution, hysteresis on cooling and heating, and sharpness of the phase transition.
- establish the chemistry/methods of grafting UCST polymers on metal nanoparticles.
- study if UCST behavior can be retained in cross-linked polymer architectures and the influence of cross-linker amount (i.e. cross-linker density) on thermoresponsive behavior.
- provide photo cross-linkable UCST polymer based hydrogels for processing to fibers and films for applications like microactuators.

### 1.3 Controlled radical polymerization

Free radical polymerization (FRP) is the easily carried out and widely studied polymerization method. FRP can be applied for almost all vinyl monomers and shows excellent tolerance to impurities. Another advantage of FRP is that it is possible to access high molar mass polymers within short reaction times. However, based on its mechanism, FRP does have some limitations such as uncontrolled structure and broad polydispersity caused by transfer and termination reactions. Therefore controlled radical polymerization (CRP) was required in demand of well-defined polymers with controlled structure, for instance block copolymers or star polymers and polymers with compositional homogeneous chains.<sup>[73,115]</sup>

Theoretically, in a CRP the polymer chains remain active even if all monomers are exhausted until deliberately terminated. According to mechanism, CRP can be classified under two broad categories: reversible termination or reversible transfer. Nitroxide-mediated polymerization (NMP) and atom transfer radical polymerization (ATRP) are the two most studied examples of reversible termination, while reversible addition fragmentation chain transfer (RAFT) polymerization belongs to the latter one.

The main mechanism of NMP was the reversible equilibrium between the alkoxyamine as dormant species and the growing propagating radical as well as the nitroxide, acting as a control agent. (Scheme 1-1). The rapid equilibrium leads to propagation of all chains at approximately the same time and this theoretically results in chains of equal molar mass. The most widely used nitroxide was 2,2,6,6-tetramethylpiperidinyloxy (TEMPO) as shown in Scheme 1-1. With the new development of suitable nitroxides and particular experimental conditions in the last decades, the NMP could now be applied for almost all conventional vinyl monomers.<sup>[116]</sup>

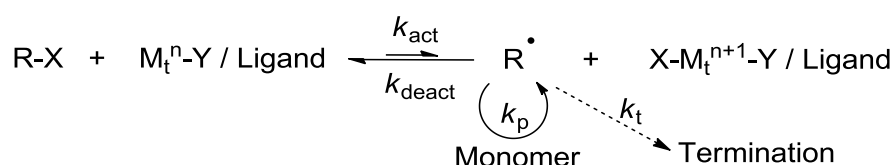


Scheme 1-1. General mechanism for NMP.

ATRP is one of the most investigated controlled radical polymerization system since it was first introduced by Matyjaszewski<sup>[117-119]</sup> and Sawamoto<sup>[120]</sup> independently in 1995.

## INTRODUCTION

Similar to NMP, the mechanism of ATRP was based on a reversible redox process: the dormant species alkyl halide (R-X) were catalyzed by a transition metal complex ( $M_t^n$ -Y/Ligand) to the propagating radical ( $R^\bullet$ ) and resulting in a corresponding higher oxidation state metal halide complex ( $X-M_t^{n+1}$ /Ligand). (Scheme 1-2) At the end of the polymerization the chain ends should (ideally) be a halogen atom and the alkyl part of the initiator. In the last two decades, ATRP has been developed extensively. Several different initiators, metal complex systems were developed for different purpose. Excellent review articles are given by Matyjaszewski and others.<sup>[115,121-124]</sup>

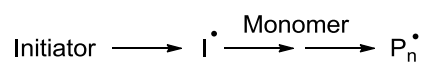


Scheme 1-2. General mechanism for ATRP.

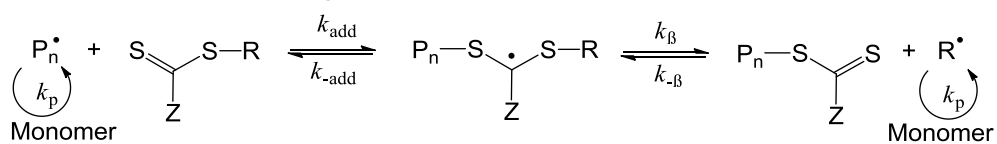
Another well applied CRP was the RAFT polymerization. The general mechanism of RAFT polymerization is shown in Scheme 1-3. Like conventional radical polymerization, the RAFT polymerization started with the initiation and ended with radical-radical termination process. The radical ( $P_n^\bullet$ ) added with thiocarbonylthio compounds (normally called as chain transfer agent, CTA) to form an intermediate radical, the fragmentation of which results in a new thiocarbonylthio compounds ( $P_n\text{-SC(Z)=S}$ ) and radical ( $R^\bullet$ ). The radical ( $R^\bullet$ ) propagated further to form radical ( $P_m^\bullet$ ). In the chain transfer and propagation step, the radical ( $P_m^\bullet$ ) added with the thiocarbonylthio compounds ( $P_n\text{-SC(Z)=S}$ ), similar as in the reversible chain transfer and propagation step, to form an intermediate radical ( $P_n\text{-SC}^\bullet(\text{Z})\text{S-P}_m$ ) and followed with the fragmentation. The reversible equilibrium between the polymeric thiocarbonylthio compounds as dormant species and the growing propagating radicals ( $P_n^\bullet$  and  $P_m^\bullet$ ) results in all chains growing with same rate. After the polymerization, the polymers are with thiocarbonylthio as end-group, which could be modified for further application. Since it was invented in 1998, RAFT was widely developed for almost all acrylic monomers.<sup>[125-129]</sup> The book “Handbook of RAFT Polymerization” of Barner-Kowollik was strongly recommended as an overview of RAFT polymerization.<sup>[130]</sup>

## INTRODUCTION

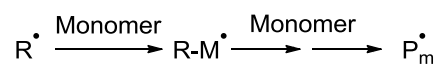
### Initiation



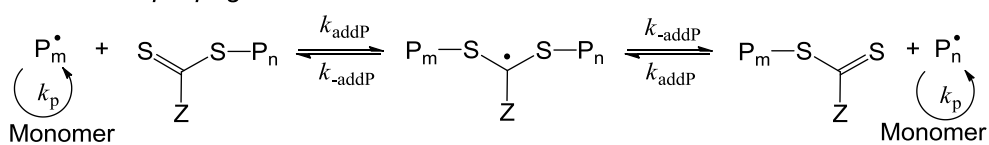
### Reversible chain transfer / propagation



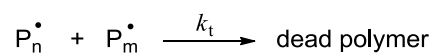
### Reinitiation



### Chain equilibration / propagation



### Termination



Scheme 1-3. General mechanism for RAFT polymerization.

#### 1.4 Gold nanoparticles stabilized with polymeric ligands

Gold nanoparticles (AuNPs) were used as colorant for glass or glittering pots from Egypt to India and China in history. In the last decades the interest in AuNPs increased significantly as they were found to exhibit different physical and chemical properties compared to bulk material. Therefore AuNPs are widely applied in catalytic and biological areas.<sup>[131]</sup> For many applications of AuNPs, it is important to protect the particle surface from chemical resistance as well as the modification of particle surface.<sup>[132]</sup> The surface modifications by the grafted materials influence the optical properties of the AuNPs.<sup>[133]</sup> Among many protecting materials for the metal nanoparticles, polymers are well established candidates to form a core-shell structure. Advantages of a polymer protecting film are: (a) the thickness of the film can be controlled by varying the chain length of polymer and the coating density of polymer on the nanoparticle surface; (b) the functional groups of polymers enable further chemistry for nanoparticles and (c) the functionalization of nanoparticles with a stimuli-responsive polymer results in “smart” materials. The use of stimuli-responsive polymer could enlarge the potential applications of nanoparticles in many areas.<sup>[134,135]</sup> AuNPs are normally prepared and *in situ* stabilized by inorganic compounds such as citrate. Two widely used approaches for functionalization of AuNPs with polymers are: 1<sup>st</sup> the “*grafting from*” approach, where the polymer chains directly grow from the initiators attached to the AuNP surfaces and 2<sup>nd</sup> “*grafting onto*”, where the polymer are attached onto AuNPs *via* ligand exchange.<sup>[136]</sup>

In detail, CRP methods such as surface-initiated atom transfer radical polymerization (SI-ATRP) or RAFT polymerizations are required in the “*grafting from*” strategy.<sup>[137–139]</sup> Therefore initiators are attached to AuNP surfaces at first. After polymerization polymer brushes are produced. Whereas, in the “*grafting onto*” approach polymers with anchor-groups such as thiol, thiocarbonate and AuNPs are prepared separately.<sup>[134,140]</sup> Functionalization of AuNPs with synthesized polymers is performed *via* ligand exchange process in one phase or two phases.

In literature, the combination of thermoresponsive polymers with AuNPs and the investigation of phase transition of the polymers on AuNPs are well known.<sup>[135,140–144]</sup> A well-studied system is based on PNIPAM; a polymer with LCST-type thermoresponsivity in water. Hybrid materials containing PNIPAM as ligand show

## INTRODUCTION

thermoresponsivity in water. Other known LCST polymers for nanoparticle functionalization are poly(*N*-vinyl caprolactam)<sup>[145]</sup>, ethylene oxide oligomers<sup>[141]</sup> and copolymer based on ethylene oxide<sup>[146]</sup>. Polymers with UCST behavior, on the other hand, are rarely investigated for protection of AuNPs. To the best of my knowledge only two zwitterionic polymers are known in literature: quarternized poly(*N,N*-dimethylaminoethyl methacrylate) (PDMAEMA)<sup>[135]</sup> and poly(*N,N*'-dimethyl(methacrylamido propyl)ammonium propanesulfonate) (PSPP).<sup>[41]</sup> Due to the fact, that the thermoresponsivity of zwitterionic polymers is based on the intra- and intermolecular coulomb interactions, the salt concentration influences the polymer coated AuNPs dramatically.<sup>[41]</sup> For this reason, non-ionic UCST polymers are of interest, as the phase transition are based on hydrogen bonds and the polymers show similar UCST-type phase transition in pure water and in electrolytes solution.<sup>[29]</sup>

**1.5 Literature**

- 1 H. Kanazawa, K. Yamamoto, Y. Matsushima, *Anal. Chem.* **1996**, *68*, 100–105.
- 2 N. S. Terefe, O. Glagovskaia, K. De Silva, R. Stockmann, *Food Bioprod. Process.* **2014**, *92*, 208–225.
- 3 M. Hrubý, S. K. Filippov, P. Štěpánek, *Eur. Polym. J.* **2015**, DOI 10.1016/j.eurpolymj.2015.01.016.
- 4 M. A. Ward, T. K. Georgiou, *Polymers* **2011**, *3*, 1215–1242.
- 5 J. P. Chen, A. S. Huffman, *Biomaterials* **1990**, *11*, 631–634.
- 6 A. Kondo, H. Kamura, K. Higashitani, *Biotechnol. Bioeng.* **1994**, *44*, 1–6.
- 7 R. H. and S. W. K. You Han Bae, Teruo Okano, *Macromol. Rapid Commun.* **1987**, *8*, 481–485.
- 8 Y. Oni, W. O. Soboyejo, *Mater. Sci. Eng. C. Mater. Biol. Appl.* **2012**, *32*, 24–30.
- 9 W. L. J. Hinrichs, N. M. E. Schuurmans-Nieuwenbroek, P. van de Wetering, W. E. Hennink, *J. Control. Release* **1999**, *60*, 249–259.
- 10 A. T. and E. P. Sevil Dincer, *Macromol. Chem. Phys.* **2002**, *203*, 1460–1465.
- 11 V. S. Khokhlov, Alexei R., Grosberg, Alexander Yu, Pande, *Statistical Physics of Macromolecules*, American Institute of Physics, **1994**.
- 12 V. Aseyev, H. Tenhu, F. M. Winnik, *Adv. Polym. Sci.* **2011**, *242*, 29–89.
- 13 I. Dimitrov, B. Trzebicka, A. H. E. Müller, A. Dworak, C. B. Tsvetanov, *Prog. Polym. Sci.* **2007**, *32*, 1275–1343.
- 14 F. Cordier, S. Grzesiek, *J. Mol. Biol.* **2002**, *317*, 739–752.
- 15 F. E. Young, F. T. Jones, *J. Phys. Colloid Chem.* **1949**, *53*, 1334–1350.



## INTRODUCTION

- 16 K. Van Durme, G. Van Assche, B. Van Mele, *Macromolecules* **2004**, *37*, 9596–9605.
- 17 F. Afroze, E. Nies, H. Berghmans, *J. Mol. Struct.* **2000**, *554*, 55–68.
- 18 M. Heskins, J. E. Guillet, *J. Macromol. Sci. Part A - Chem.* **1968**, *2*, 1441–1455.
- 19 R. Gomes de Azevedo, L. P. N. Rebelo, A. M. Ramos, J. Szydowski, H. C. de Sousa, J. Klein, *Fluid Phase Equilib.* **2001**, *185*, 189–198.
- 20 D. Roy, W. L. a Brooks, B. S. Sumerlin, *Chem. Soc. Rev.* **2013**, *42*, 7214–7243.
- 21 E. Karjalainen, V. Khlebnikov, A. Korpi, S.-P. Hirvonen, S. Hietala, V. Aseyev, H. Tenhu, *Polymer* **2015**, *58*, 180–188.
- 22 A. Aqil, S. Vasseur, E. Duguet, C. Passirani, J. P. Benoît, A. Roch, R. Müller, R. Jérôme, C. Jérôme, *Eur. Polym. J.* **2008**, *44*, 3191–3199.
- 23 J. Kim, S. Choi, K. M. Kim, C. H. Lee, H. S. Park, S. S. Hwang, S. M. Hong, S. Kwak, H.-O. Yoo, *Macromol. Symp.* **2006**, *245-246*, 565–570.
- 24 G. K. Christopher, a. G. Phipps, R. J. Gray, *J. Cryst. Growth* **1998**, *191*, 820–826.
- 25 M. Ranny, *Fette, Seifen, Anstrichm.* **1967**, *1*, 5–8.
- 26 L. Zeman, D. Patterson, *J. Phys. Chem. B* **1972**, *76*, 1214–1219.
- 27 G. Swislow, S.-T. Sun, I. Nishio, T. Tanaka, *Phys. Rev. Lett.* **1980**, *44*, 796–798.
- 28 I. Nishio, G. Swislow, S.-T. Sun, T. Tanaka, *Nature* **1982**, *300*, 243–244.
- 29 J. Seuring, S. Agarwal, *Macromol. Rapid Commun.* **2012**, *33*, 1898–1920.
- 30 N. Shimada, M. Nakayama, A. Kano, A. Maruyama, *Biomacromolecules* **2013**, *14*, 1452–1457.

## INTRODUCTION

- 31 K. Van Durme, G. Van Assche, E. Nies, B. Van Mele, *J. Phys. Chem. B* **2007**, *111*, 1288–1295.
- 32 G. Van Assche, B. Van Mele, T. Li, E. Nies, *Macromolecules* **2011**, *44*, 993–998.
- 33 Y. C. Bae, S. M. Lambert, D. S. Soane, J. M. Prausnitz, *Macromolecules* **1991**, *24*, 4403–4407.
- 34 T. Shiomi, K. Imai, C. Watanabe, M. Miya, *J. Polym. Sci. Part B-Polymer Phys.* **1984**, *22*, 1305–1312.
- 35 R. Longenecker, T. Mu, M. Hanna, N. A. D. Burke, H. D. H. Stöver, *Macromolecules* **2011**, *44*, 8962–8971.
- 36 D. N. Schulz, D. G. Peiffer, P. K. Agarwal, J. Larabee, J. J. Kaladas, L. Soni, B. Handwerker, R. T. Garner, *Polymer* **1986**, *27*, 1734–1742.
- 37 M. B. Huglin, M. A. Radwan, *Polym. Int.* **1991**, *26*, 97–104.
- 38 P. Mary, D. D. Bendejacq, M.-P. Labeau, P. Dupuis, *J. Phys. Chem. B* **2007**, *111*, 7767–7777.
- 39 M. Tian, J. Wang, E. Zhang, J. Li, C. Duan, F. Yao, *Langmuir* **2013**, *29*, 8076–8085.
- 40 H. Willcock, A. Lu, C. F. Hansell, E. Chapman, I. R. Collins, R. K. O'Reilly, *Polym. Chem.* **2014**, *5*, 1023–1030.
- 41 C. Durand-Gasselin, R. Koerin, J. Rieger, N. Lequeux, N. Sanson, *J. Colloid Interface Sci.* **2014**, *434*, 188–194.
- 42 V. A. Vasantha, S. Jana, A. Parthiban, J. G. Vancso, *RSC Adv.* **2014**, *4*, 22596–22600.
- 43 N. Morimoto, K. Muramatsu, T. Wazawa, Y. Inoue, M. Suzuki, *Macromol. Rapid Commun.* **2014**, *35*, 103–108.

- 44 N. Morimoto, T. Wazawa, Y. Inoue, M. Suzuki, *RSC Adv.* **2015**, *5*, 14851–14857.
- 45 C. Y. Chen, H. L. Wang, *Macromol. Rapid Commun.* **2014**, *35*, 1534–1540.
- 46 Z. Dong, J. Mao, D. Wang, M. Yang, W. Wang, S. Bo, X. Ji, *Macromol. Chem. Phys.* **2014**, *215*, 111–120.
- 47 J. Ning, G. Li, K. Haraguchi, *Macromol. Chem. Phys.* **2014**, *215*, 235–244.
- 48 J. Ning, G. Li, K. Haraguchi, *Macromolecules* **2013**, *46*, 5317–5328.
- 49 J. Ning, K. Kubota, G. Li, K. Haraguchi, *React. Funct. Polym.* **2013**, *73*, 969–978.
- 50 M. Noh, Y. Mok, D. Nakayama, S. Jang, S. Lee, T. Kim, Y. Lee, *Polymer* **2013**, *54*, 5338–5344.
- 51 V. A. Vasantha, S. Jana, A. Parthiban, J. G. Vancso, *Chem. Commun.* **2014**, *50*, 46–48.
- 52 P. a. Woodfield, Y. Zhu, Y. Pei, P. J. Roth, *Macromolecules* **2014**, *47*, 750–762.
- 53 X. Jia, D. Chen, M. Jiang, *Chem. Commun.* **2006**, 1736–1738.
- 54 H. Yoshimitsu, A. Kanazawa, S. Kanaoka, S. Aoshima, *Macromolecules* **2012**, *45*, 9427–9434.
- 55 F. Chen, J. Hehl, Y. Su, C. Mattheis, A. Greiner, S. Agarwal, *Polym. Int.* **2013**, *62*, 1750–1757.
- 56 Y. Deng, Y. Xu, X. Wang, Q. Yuan, Y. Ling, H. Tang, *Macromol. Rapid Commun.* **2015**, DOI 10.1002/marc.201400625.
- 57 B. Kim, D. Hong, W. V. Chang, *Colloid Polym. Sci.* **2014**, *293*, 699–708.
- 58 X. Han, X. Zhang, Q. Yin, J. Hu, H. Liu, Y. Hu, *Macromol. Rapid Commun.* **2013**, *34*, 574–580.

## INTRODUCTION

- 59 E. Karjalainen, V. Aseyev, H. Tenhu, *Macromolecules* **2014**, *47*, 7581–7587.
- 60 B. Li, X. Lu, Y. Ma, Z. Chen, *Eur. Polym. J.* **2014**, *60*, 255–261.
- 61 H. C. Haas, N. W. Schuler, *J. Polym. Sci. Part B Polym. Lett.* **1964**, *2*, 1095–1096.
- 62 H. C. Haas, R. D. Moreau, N. W. Schuler, *J. Polym. Sci. Part A-2 Polym. Phys.* **1967**, *5*, 915–927.
- 63 H. C. Haas, C. K. Chiklis, R. D. Moreau, *J. Polym. Sci. Part A-1 Polym. Chem.* **1970**, *8*, 1131–1145.
- 64 H. C. Haas, M. J. Manning, M. H. Mach, *J. Polym. Sci. Part A-1 Polym. Chem.* **1970**, *8*, 1725–1730.
- 65 O. Marstokk, B. Nyström, J. Roots, *Macromolecules* **1998**, *31*, 4205–4212.
- 66 D. Ostrovskii, P. Jacobsson, B. Nyström, O. Marstokk, H. B. M. Kopperud, *Macromolecules* **1999**, *32*, 5552–5560.
- 67 S. Glatzel, N. Badi, M. Päch, A. Laschewsky, J.-F. Lutz, *Chem. Commun.* **2010**, *46*, 4517–4519.
- 68 M. Boustta, P.-E. Colombo, S. Lenglet, S. Poujol, M. Vert, *J. Control. Release* **2014**, *174*, 1–6.
- 69 J. Seuring, S. Agarwal, *Macromol. Chem. Phys.* **2010**, *211*, 2109–2117.
- 70 J. Seuring, F. M. Bayer, K. Huber, S. Agarwal, *Macromolecules* **2012**, *45*, 374–384.
- 71 J. Seuring, S. Agarwal, *Macromolecules* **2012**, *45*, 3910–3918.
- 72 M. E. Hirokazu Nagaoka, Noriyuki Ohnishi, *Thermoresponsive Polymer And Production Method Thereof*, **2007**, US20070203313-A1.

## INTRODUCTION

- 73 B. A. Pineda-Contreras, F. Liu, S. Agarwal, *J. Polym. Sci. Part A Polym. Chem.* **2014**, *52*, 1878–1884.
- 74 H. Zhang, X. Tong, Y. Zhao, *Langmuir* **2014**, *30*, 11433–11441.
- 75 A. Silberberg, J. Eliassaf, A. Katchalsky, *J. Polym. Sci.* **1957**, *23*, 259–284.
- 76 T. Aoki, K. Nakamura, K. Sanui, A. Kikuchi, T. Okano, Y. Sakurai, N. Ogata, *Polym. J.* **1999**, *31*, 1185–1188.
- 77 V. Mishra, S.-H. Jung, H. M. Jeong, H. Lee, *Polym. Chem.* **2014**, *5*, 2411–2416.
- 78 G. Meiswinkel, H. Ritter, *Macromol. Chem. Phys.* **2013**, *214*, 2835–2840.
- 79 G. Meiswinkel, H. Ritter, *Macromol. Rapid Commun.* **2013**, *34*, 1026–1031.
- 80 H. N. Lee, B. M. Rosen, G. Fenyvesi, H. B. Sunkara, *J. Polym. Sci. Part A Polym. Chem.* **2012**, *50*, 4311–4315.
- 81 P. J. Roth, *Macromol. Chem. Phys.* **2014**, *215*, 825–838.
- 82 Y. Di, X. Ma, C. Li, H. Liu, X. Fan, M. Wang, H. Deng, T. Jiang, Z. Yin, K. Deng, *Macromol. Chem. Phys.* **2014**, *215*, 365–371.
- 83 G. Meiswinkel, H. Ritter, *Macromol. Chem. Phys.* **2014**, *215*, 682–687.
- 84 Q. Zhang, J.-D. Hong, R. Hoogenboom, *Polym. Chem.* **2013**, *4*, 4322–4325.
- 85 Q. Zhang, R. Hoogenboom, *Chem. Commun.* **2014**, *51*, 70–73.
- 86 Q. Zhang, F. Tosi, S. Ügdüler, S. Maji, R. Hoogenboom, *Macromol. Rapid Commun.* **2014**, DOI 10.1002/marc.201400550.
- 87 Z. Yang, X. Fan, W. Tian, D. Wang, H. Zhang, Y. Bai, *Langmuir* **2014**, *30*, 7319–7326.
- 88 Y. Zhu, A. B. Lowe, P. J. Roth, *Polymer* **2014**, *55*, 4425–4431.
- 89 A. C. Jen, M. C. Wake, A. G. Mikos, *Biotechnol. Bioeng.* **1996**, *50*, 357–364.

## INTRODUCTION

- 90 A. Richter, G. Paschew, S. Klatt, J. Lienig, K. Arndt, H. P. Adler, *Sensors* **2008**, 8, 561–581.
- 91 N. Peppas, *Eur. J. Pharm. Biopharm.* **2000**, 50, 27–46.
- 92 R. A. Siegel, B. A. Firestone, *Macromolecules* **1988**, 21, 3254–3259.
- 93 F. Hapiot, S. Menuel, E. Monflier, *ACS Catal.* **2013**, 3, 1006–1010.
- 94 M. R. Matanović, J. Kristl, P. A. Grabnar, *Int. J. Pharm.* **2014**, 472, 262–275.
- 95 S. J. Buwalda, K. W. M. Boere, P. J. Dijkstra, J. Feijen, T. Vermonden, W. E. Hennink, *J. Control. Release* **2014**, 190, 254–273.
- 96 J. Kobayashi, T. Okano, *React. Funct. Polym.* **2013**, 73, 939–944.
- 97 G. Li, S. Song, L. Guo, S. Ma, *J. Polym. Sci. Part A Polym. Chem.* **2008**, 46, 5028–5035.
- 98 M. Nakayama, T. Okano, T. Miyazaki, F. Kohori, K. Sakai, M. Yokoyama, *J. Control. Release* **2006**, 115, 46–56.
- 99 Y. Hirokawa, T. Tanaka, *J. Chem. Phys.* **1984**, 81, 6379–6380.
- 100 X. S. Wu, A. S. Hoffman, P. Yager, *J. Polym. Sci. Part A Polym. Chem.* **1992**, 30, 2121–2129.
- 101 X.-Z. Zhang, D.-Q. Wu, C.-C. Chu, *Biomaterials* **2004**, 25, 3793–3805.
- 102 E. Mah, R. Ghosh, *Processes* **2013**, 1, 238–262.
- 103 E. Gil, S. Hudson, *Prog. Polym. Sci.* **2004**, 29, 1173–1222.
- 104 N. Nath, A. Chilkoti, *Adv. Mater.* **2002**, 14, 1243–1247.
- 105 V. M. Monroy Soto, J. C. Galin, *Polymer* **1984**, 25, 254–262.
- 106 G. S. Georgiev, Z. P. Mincheva, V. T. Georgieva, *Macromol. Symp.* **2001**, 164, 301–312.

## INTRODUCTION

- 107 A. B. Lowe, C. L. McCormick, *Chem. Rev.* **2002**, *102*, 4177–4190.
- 108 E. A. Bekturov, L. A. Bimend, in *Adv. Polym. Sci. Vol. 41*, Springer Berlin Heidelberg, **1980**, pp. 99–147.
- 109 H. Katono, K. Sanui, N. Ogata, T. Okano, Y. Sakurai, *Polym. J.* **1991**, *23*, 1179–1189.
- 110 P. Bouillot, B. Vincent, *Colloid Polym. Sci.* **2000**, *278*, 74–79.
- 111 D. E. Owens, Y. Jian, J. E. Fang, B. V Slaughter, Y. Chen, N. A. Peppas, *Macromolecules* **2007**, *40*, 7306–7310.
- 112 H. Katono, A. Maruyama, K. Sanui, N. Ogata, T. Okano, Y. Sakurai, *J. Control. Release* **1991**, *16*, 215–227.
- 113 Q. Wang, S. Li, Z. Wang, H. Liu, C. Li, *J. Appl. Polym. Sci.* **2009**, *111*, 1417–1425.
- 114 H. Sasase, T. Aoki, H. Katono, K. Sanui, N. Ogata, R. Ohta, T. Kondo, Y. Sakurai, *Die Makromol. Chemie, Rapid Commun.* **1992**, *581*, 577–581.
- 115 V. M. C. Coessens, K. Matyjaszewski, *J. Chem. Educ.* **2010**, *87*, 916–919.
- 116 J. Nicolas, Y. Guillaneuf, C. Lefay, D. Bertin, D. Gigmes, B. Charleux, *Prog. Polym. Sci.* **2013**, *38*, 63–235.
- 117 J. Wang, K. Matyjaszewski, *Macromolecules* **1995**, *28*, 7572–7573.
- 118 J.-S. Wang, K. Matyjaszewski, *Macromolecules* **1995**, *28*, 7901–7910.
- 119 J. Wang, K. Matyjaszewski, *J. Am. Chem. Soc.* **1995**, *117*, 5614–5615.
- 120 M. Kato, M. Kamigaito, M. Sawamoto, T. Higashimuras, *Macromolecules* **1995**, *28*, 1721–1723.
- 121 K. Matyjaszewski, *Macromolecules* **2012**, *45*, 4015–4039.

## INTRODUCTION

- 122 M. Horn, K. Matyjaszewski, *Macromolecules* **2013**, *46*, 3350–3357.
- 123 W. Hadasha, B. Klumperman, *Polym. Int.* **2014**, *63*, 824–834.
- 124 K. Pangilinan, R. Advincula, *Polym. Int.* **2014**, *63*, 803–813.
- 125 A. E. Smith, X. Xu, C. L. McCormick, *Prog. Polym. Sci.* **2010**, *35*, 45–93.
- 126 D. J. Keddie, *Chem. Soc. Rev.* **2013**, *43*, 496–505.
- 127 G. Moad, E. Rizzardo, S. H. Thang, *Aust. J. Chem.* **2009**, *62*, 1402–1472.
- 128 G. Moad, E. Rizzardo, S. H. Thang, *Chem. - An Asian J.* **2013**, *8*, 1634–1644.
- 129 J. Chiefari, Y. K. B. Chong, F. Ercole, J. Krstina, J. Jeffery, T. P. T. Le, R. T. A. Mayadunne, G. F. Meijs, C. L. Moad, G. Moad, E. Rizzardo, S. H. Thang, C. South, *Macromolecules* **1998**, *31*, 5559–5562.
- 130 C. Barner-Kowollik, *Handbook of RAFT Polymerization*, WILEY-VCH, Weinheim, **2008**.
- 131 M. C. Daniel, D. Astruc, *Chem. Rev.* **2004**, *104*, 293–346.
- 132 L. Quaroni, G. Chumanov, *J. Am. Chem. Soc.* **1999**, *121*, 10642–10643.
- 133 L. Liz-Marzán, *Langmuir* **2006**, *22*, 32–41.
- 134 M. Liang, I. C. Lin, M. R. Whittaker, R. F. Minchin, M. J. Monteiro, I. Toth, *ACS Nano* **2010**, *4*, 403–413.
- 135 A. Housni, Y. Zhao, *Langmuir* **2010**, *26*, 12933–12939.
- 136 K. Saha, S. S. Agasti, C. Kim, X. Li, V. M. Rotello, *Chem. Rev.* **2012**, *112*, 2739–2779.
- 137 D. Li, Q. He, Y. Cui, J. Li, *Chem. Mater.* **2007**, *19*, 412–417.
- 138 T. K. Mandal, M. S. Fleming, D. R. Walt, *Nano Lett.* **2002**, *2*, 3–7.



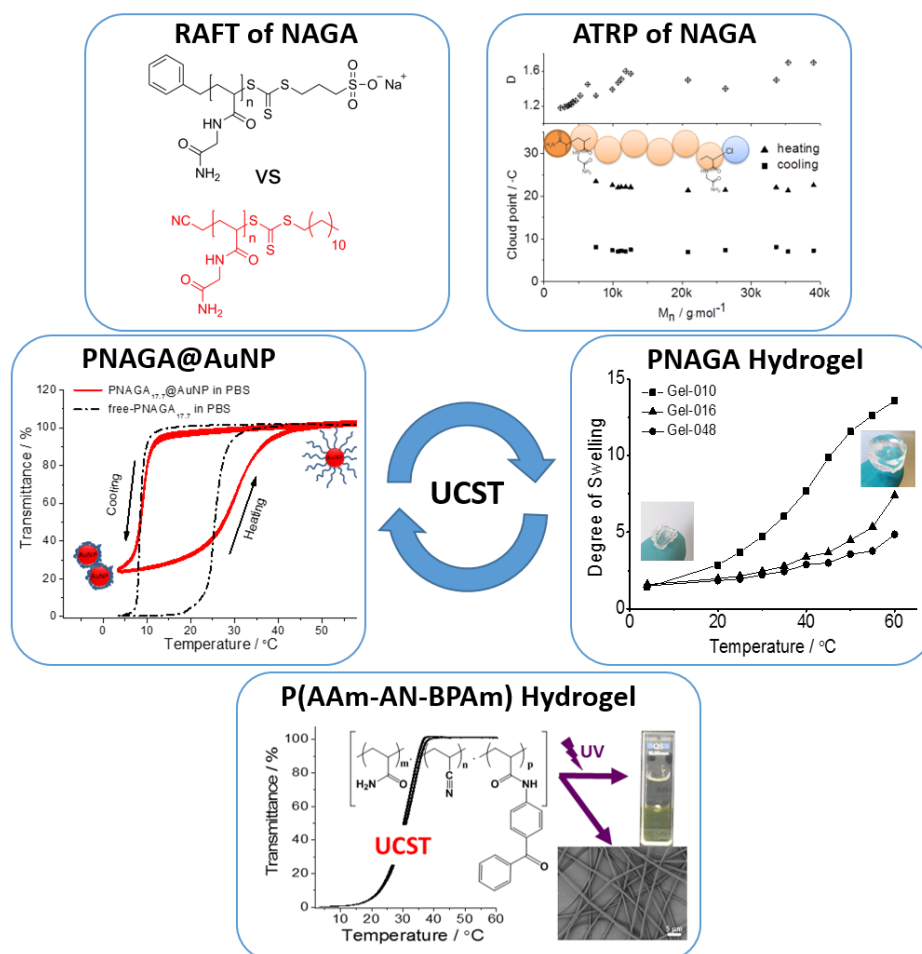
## INTRODUCTION

- 139 K. R. Yoon, B. Ramaraj, S. M. Lee, D. P. Kim, *Surf. Interface Anal.* **2008**, *40*, 1139–1143.
- 140 M. Q. Zhu, L. Q. Wang, G. J. Exarhos, A. D. Q. Li, *J. Am. Chem. Soc.* **2004**, *126*, 2656–2657.
- 141 C. Boyer, M. R. Whittaker, M. Luzon, T. P. Davis, *Macromolecules* **2009**, *42*, 6917–6926.
- 142 O. J. Cayre, N. Chagneux, S. Biggs, *Soft Matter* **2011**, *7*, 2211–2234.
- 143 S. Salmaso, P. Caliceti, V. Amendola, M. Meneghetti, J. P. Magnusson, G. Pasparakis, C. Alexander, *J. Mater. Chem.* **2009**, *19*, 1608–1615.
- 144 J. Shan, Y. Zhao, N. Granqvist, H. Tenhu, *Macromolecules* **2009**, *42*, 2696–2701.
- 145 M. Beija, J.-D. Marty, M. Destarac, *Chem. Commun.* **2011**, *47*, 2826–2828.
- 146 C. Durand-Gasselin, M. Capelot, N. Sanson, N. Lequeux, *Langmuir* **2010**, *26*, 12321–12329.



## 2 Synopsis

This dissertation focuses on the synthesis of polymers showing upper critical solution temperature (UCST)-type thermoresponsivity in water and electrolytes with different architectures and their properties. The dissertation consists of five interdependent chapters, all related to the key property of these polymers and materials: UCST. (Scheme 2-1)



Scheme 2-1. Schematic illustration of the thesis: Five interdependent chapters related to the key word of this dissertation: upper critical solution temperature (UCST).

Reversible addition fragmentation transfer (RAFT) polymerization (**Publication 1**, upper left in Scheme 2-1) and atom transfer radical polymerization (ATRP) (**Publication 2**, upper right in Scheme 2-1) were investigated as controlled radical polymerization methods for preparing PNAGA of linear structure. The influence of molar mass, polymer end-groups, polydispersity and salt concentration on the cloud point was analyzed and discussed by turbidimetry measurements to achieve better understanding of UCST behaviour in aqueous solution.

## SYNOPSIS

Polymers synthesized by controlled radical polymerization are of interest due to the possibility of post modification of polymer end-groups for further application. As one example, trithiocarbonate end-functionalized PNAGA synthesized *via* RAFT polymerization was grafted onto gold nanoparticles (AuNPs) by ligand exchange in phosphate buffered saline (PBS). (**Publication 3**, center left in Scheme 2-1) It was found that the hybrid material showed UCST-type phase transition.

A common example of cross-linked polymer structure was hydrogel, in which a chemical cross-linker was applied. Thus, chemically cross-linked PNAGA was synthesized to study its thermosensitivity in water and electrolytes. The hydrogel shows reversible positive swelling behaviour in pure water as well as in electrolytes, meaning the hydrogel swells at high temperature and shrink at low temperature. (**Publication 4**, center right in Scheme 2-1)

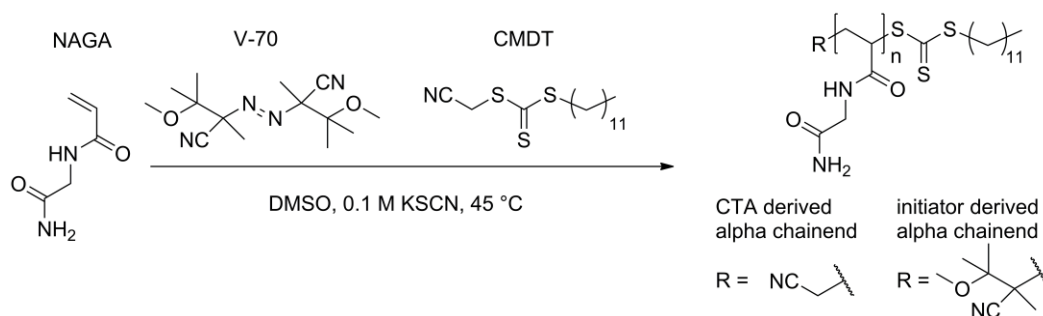
Further, a terpolymer with UCST-type thermoresponsivity has been investigated based on acrylamide (AAm), acrylonitrile (AN) and a photo cross-linkable comonomer. These terpolymers show stable and reproducible UCST behaviour in aqueous solution. The cloud points of the copolymers could be tuned by varying the content of AN in polymer. Another advantage of this system was the cross-linkable comonomer, which could be utilized as chemical cross-linker after UV irradiation. Thus, this copolymer was applied to perform films and fibrous membranes, which also show positive thermosensitivity in aqueous solution. (**Publication 5**, lower in Scheme 2-1)

## 2.1 Controlled radical polymerization of *N*-acryloylglycinamide and UCST-type phase transition of the polymers

The results of this part have been published by Fangyao Liu, Jan Seuring and Seema Agarwal in *Journal of polymer science part A: Polymer chemistry* **2012**, *50*, 4920-4928.

Reversible addition fragmentation transfer (RAFT) polymerization was investigated for preparing poly(*N*-acryloylglycinamide) (PNAGA) of linear structure. Non-ionic chain transfer agents (CTAs) and initiators were found necessary for keeping the upper critical solution temperature (UCST) property of the polymer in aqueous solution.

PNAGAs prepared by RAFT polymerizations using AIBN as initiator and dibenzyltrithiocarbonate (DBTC) or cyanomethyl dodecyl trithiocarbonate (CMTD) as CTAs at 70 °C showed UCST-type phase transition in water. However, the control of polymerization was insufficient: polydispersities were above 1.7. A good molar mass control was accomplished by choosing CMTD as CTA and 2,2'-Azobis(4-methoxy-2,4-dimethyl valeronitrile) (V-70) as initiator.(Scheme 2-2)



Scheme 2-2. Optimum conditions for the RAFT polymerization of NAGA to retain the polymer UCST behavior in water.

The successful control of polymerization was proved by low molar mass dispersity (between 1.3 and 1.4), linear dependence of molar masses on the conversion (Figure 2-1, left) and successful chain-extension experiment, in which a PNAGA prepared by RAFT polymerizations was used as macroinitiator and it disappeared in the GPC trace after the chain-extension (Figure 2-1, right).

## SYNOPSIS

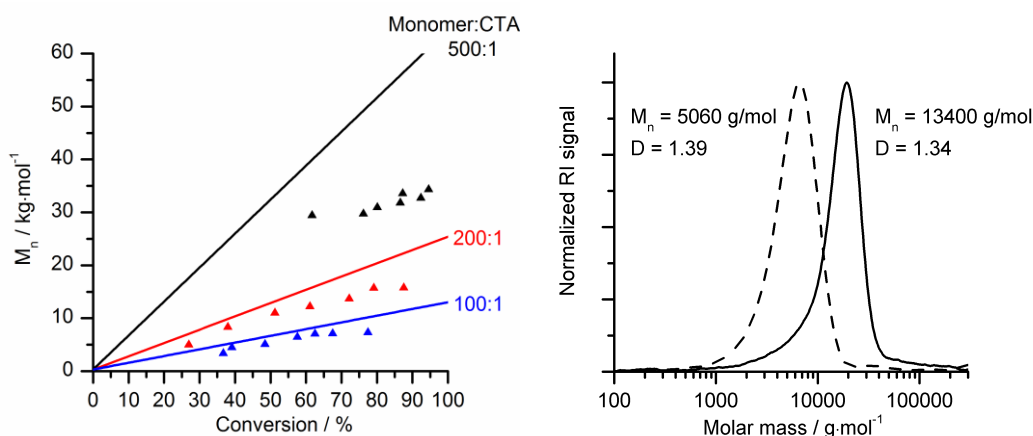


Figure 2-1. (Left) Molar masses determined by GPC as a function of conversion for different monomer:CTA ratios. Lines =  $M_{n,\text{theo}}$ ; triangles =  $M_{n,\text{exp}}$ . (Right) GPC traces of chain extension of poly(NAGA) synthesized by RAFT. Dotted line: polymer before chain extension; solid line: polymer after chain extension.

The influence of molar mass, polymer end-groups and salt concentration on the cloud point was analyzed by turbidity measurement. PNAGA showed a sharper turbidity curve in PBS than in pure water. Moreover, polymers with higher molar mass show sharper phase transition than the one with lower molar mass. The hydrophobic dodecyl end groups from the chain transfer agent caused an increase of cloud points of polymers at lower molar mass ( $M_n$  below  $10000 \text{ g/mol}$ , Figure 2-2). Furthermore, the influence of electrolytes on the cloud point of RAFT synthesized PNAGA was studied.

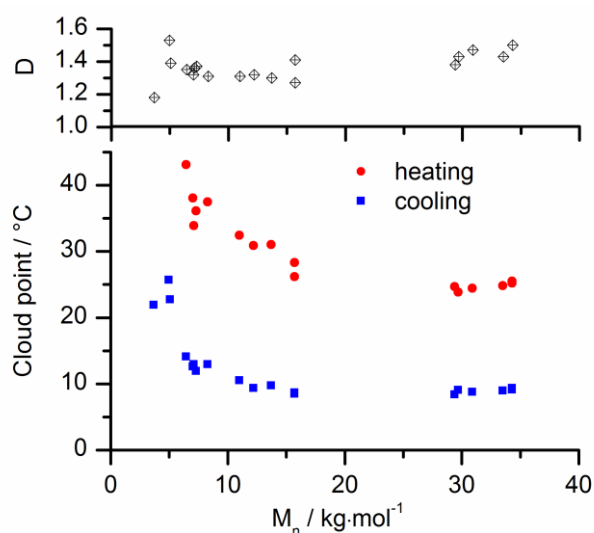
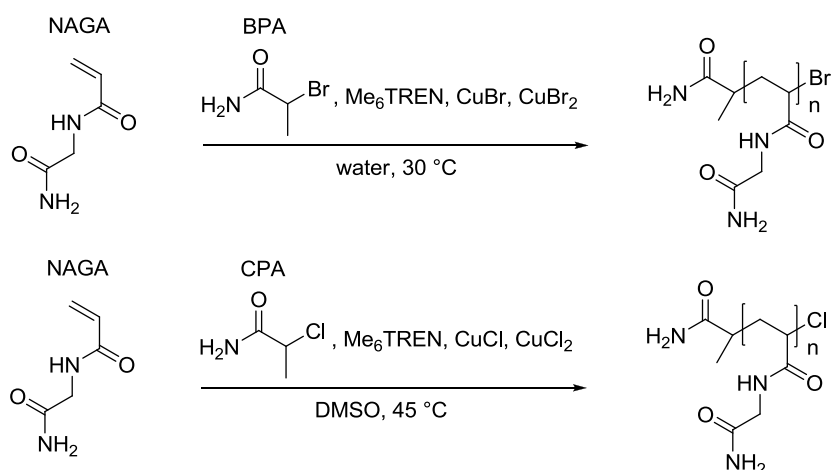


Figure 2-2. Cloud points of PNAGA synthesized by RAFT using CMDT as CTA as a function of molar mass.

## 2.2 Atom transfer radical polymerization as a tool for making poly(*N*-acryloylglycinamide) with molar mass independent UCST-type transitions in water and electrolytes

The results of this part have been published by Fangyao Liu, Jan Seuring and Seema Agarwal in *Polymer Chemistry* **2013**, *4*, 3123-3131.

Atom transfer radical polymerization (ATRP) of *N*-acryloylglycinamide (NAGA) has been used for preparing PNAGA with upper critical solution temperature (UCST)-type thermoresponsivity in water and electrolytes. The ATRP of NAGA can be carried out in water and DMSO, using 2-bromopropionamide (BPA) and 2-chloropropionamide (CPA) as initiator, CuBr/CuBr<sub>2</sub> and CuCl/CuCl<sub>2</sub> as catalyst as well as tris[2-(dimethylamino)ethyl]-amine (Me<sub>6</sub>TREN) as ligand, respectively. (Scheme 2-3)



Scheme 2-3. Optimum conditions for the ATRP of NAGA in aqueous media and DMSO to retain the polymer UCST behavior in water.

ATRP of NAGA in water at 30 °C was found extremely fast: the reaction conversion was already about 62 % after 1 min of reaction time (PDI = 1.29). The polymerization in DMSO was slower: after 1 hour of reaction time the conversion was 60 %, but a better control was achieved (PDI = 1.17). The molar masses increased linearly depending on the conversion and the number average molar masses ( $M_n$ ) agreed with the theoretical molar masses ( $M_{n,theo}$ ). The polymers are highly stable against hydrolysis both in water and in phosphate buffered saline. (Figure 2-3)

## SYNOPSIS

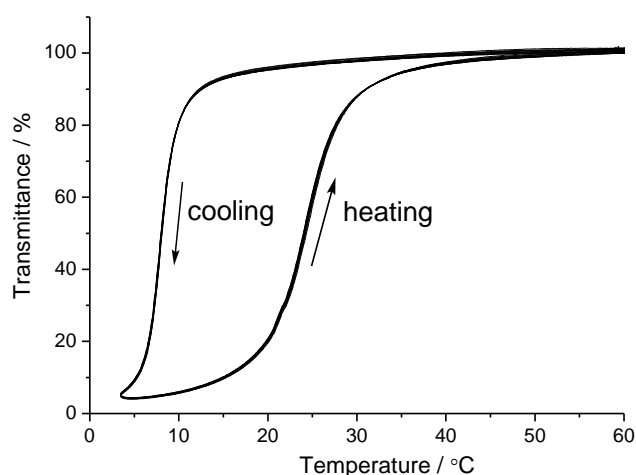


Figure 2-3. Nine consecutive turbidity measurements of poly(NAGA) synthesized by ATRP with a molar mass of  $M_n = 9600$  g/mol. The concentration was 0.2 wt% in PBS. The heating rate was 1.0 °C/min.

PNAGAs with different molar mass or polydispersity were prepared. It was found that by choosing monomer-like non-ionic initiators with primary amide groups (BPA and CPA), these polymers showed similar phase transition behaviour in aqueous solution ( $M_n$  above 5000 g/mol, Figure 2-4). Moreover, the influence of electrolytes on the cloud point of ATRP synthesized PNAGA was studied by measuring the turbidity of polymer solution with different amounts of salts like NaCl and Na<sub>2</sub>SO<sub>4</sub>.

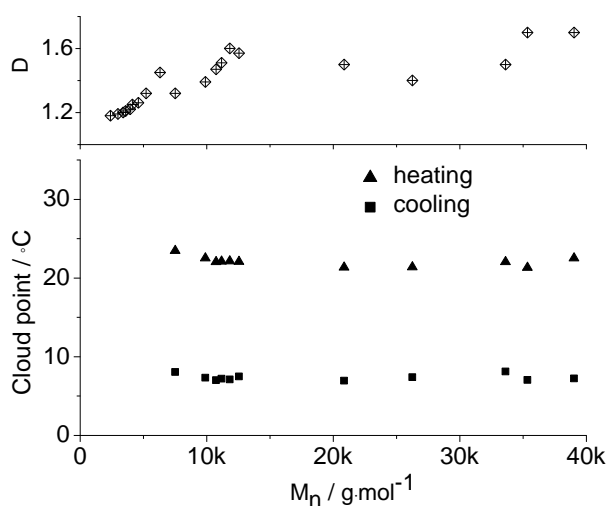


Figure 2-4. Cloud points of PNAGA synthesized by ATRP in DMSO using CPA:CuCl:CuCl<sub>2</sub>:Me<sub>6</sub>TREN as catalyst system at 45 °C as a function of molar mass.



### 2.3 Thermoresponsive gold nanoparticles with positive UCST-type thermoresponsivity

The results of this part have been published by Fangyao Liu and Seema Agarwal in *Macromolecular Chemistry and Physics*. **2015**, 216, 460-465.

Gold nanoparticles (AuNPs) that show positive thermoresponsivity of UCST-type at physiological condition were prepared. Trithiocarbonate end-functionalized poly(*N*-acryloylglycinamide) (PNAGA) synthesized *via* reversible addition fragmentation transfer (RAFT) polymerization of different molar masses (shown in **Section 2.1**) are grafted onto the AuNPs in phosphate buffered saline (PBS) by ligand exchange procedure. Three trithiocarbonate end-functionalized PNAGA samples with different  $M_n$ s (7100 g/mol, 17700 g/mol and 34000 g/mol) were investigated.

The grafting process had no negative effect on the cloud points, as the PNAGA@AuNPs showed similar phase transition behavior as that of the free-PNAGA sample used for grafting purpose. (Figure 2-5) The UCST-type transition of PNAGA@AuNPs hybrids was reversible with temperature for at least nine cooling/heating cycles. Moreover, no aggregation of PNAGA@AuNPs were observed in the transmission electron microscopy (TEM) images below cloud point.

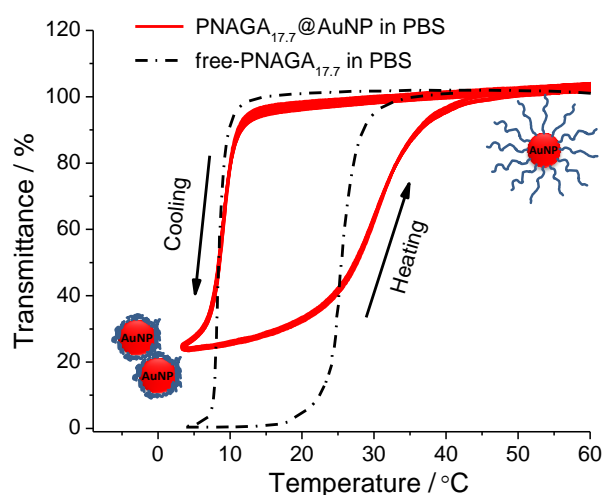


Figure 2-5 Phase transition behaviour of 0.2 wt% solution of PNAGA<sub>17.7</sub>@AuNPs (solid curves) and free-PNAGA<sub>17.7</sub> (dash curves) in PBS buffer. PNAGA<sub>17.7</sub>@AuNPs showed repeated reversible phase transitions at least for nine consecutive times.

## SYNOPSIS

The UCST-type thermoresponsivity of nanoparticle hybrid was further confirmed through DLS measurements by showing that the hydrodynamic radius increased simultaneously with increase in temperature of PNAGA@AuNPs.

The surface plasmon resonance (SPR) peak of PNAGA@AuNPs are at around 522 nm at room temperature. Molar mass of grafted polymers had no effect on the SPR peak. The effect of UCST-type thermoresponsivity on the SPR of PNAGA@AuNPs was studied by tracing the UV/Vis spectrum of PNAGA<sub>17.7</sub>@AuNPs in PBS at different temperatures. (Figure 2-6 A) By cooling the PNAGA@AuNPs in PBS solution from 30 to 3 °C, the absorption peak increased from 0.54 to 0.95. The SPR of AuNPs was at around 522 nm in the temperature range of 30 and 9 °C. Thereafter, the SPR peak increased from 522 nm to 525.5 nm. (Figure 2-6 B)

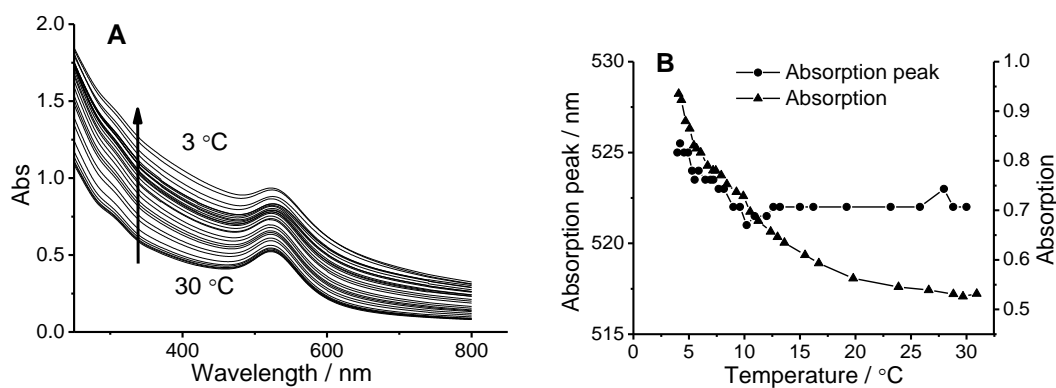


Figure 2-6. (A) UV/Vis spectra of PNAGA<sub>17.7</sub>@AuNPs in PBS at different temperatures; (B) Change in the position and intensity of the surface plasmon resonance peak of AuNPs in PNAGA<sub>17.7</sub>@AuNPs with temperature.

## 2.4 A non-ionic thermophilic hydrogel with positive thermosensitivity in water and electrolyte solution

The results of this part have been published by Fangyao Liu, Jan Seuring and Seema Agarwal in *Macromolecular Chemistry and Physics* **2014**, 215, 1466-1472.

Chemically cross-linked hydrogel was synthesized from *N*-acryloylglycinamide (NAGA) with *N,N'*-methylenebis(acrylamide) (MBAAm) as cross-linker *via* free radical polymerization in dimethyl sulfoxide. Three PNAGA hydrogel samples were prepared with different amount of cross-linker MBAAm, i.e. 0.01 eq (Gel-010), 0.016 eq (Gel-016) and 0.048 eq (Gel-048). The hydrogels showed positive volume transition with temperature in water and electrolyte solution: the degree of swelling increased with increasing temperature. (Figure 2-7) The stability of hydrogels with different cross-linker densities were studied. Gel-048 showed excellent stability in the temperature range of 4 to 70 °C.

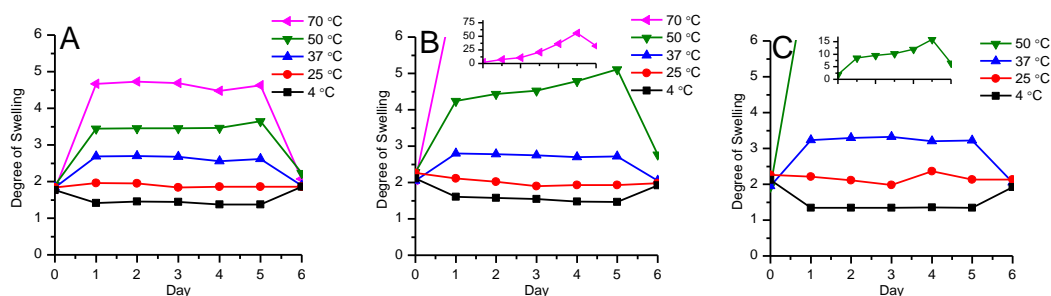


Figure 2-7. Degree of swelling of PNAGA hydrogels at different temperatures. The initial weight (day zero) and weight after temperature treatment for 6 days was recorded at RT for all gels. A: Gel-048, B: Gel-016, C: Gel-010.

The hydrogels showed reversible and reproducible UCST-type volume change in pure water as well as in phosphate buffered saline (PBS). As example, Figure 2-8 shows the swelling/deswelling process of Gel-010 by alternate heating and cooling for one day at 40 and 4 °C, respectively.

## SYNOPSIS

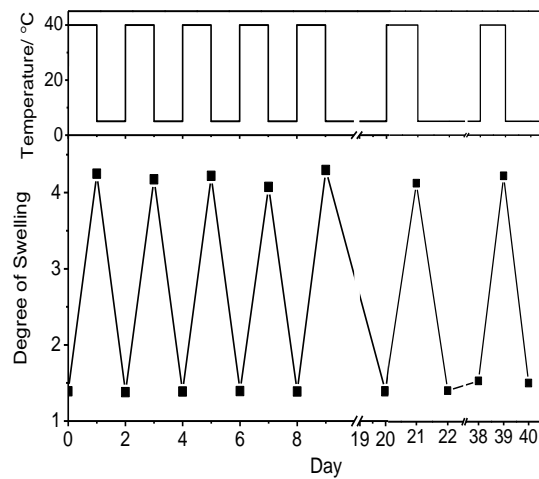


Figure 2-8. Reversibility volume-change of Gel-010 in water. The initial weight (day zero) was recorded at 4 °C. Temperature profile: 4/40. Between day 9 to 20 and day 22 to 38, the hydrogels were placed in water at 5 °C.

Further, the temperature dependence of the degree of swelling for hydrogels was investigated by incubating the hydrogels in water at 4, 20, 25, 30, 35, 40, 45, 50, 55, and 60 °C. (Figure 2-9) At 5 °C the degree of swelling was about 1.5 for all hydrogel samples and increased up to 13 (Gel-010), 7 (Gel-016) and 5 (Gel-048) at 60 °C, respectively. The study of volume phase transition behaviour dependency on temperature showed that the degree of hydrogel swelling could be tuned by varying the contents of cross-linkers.

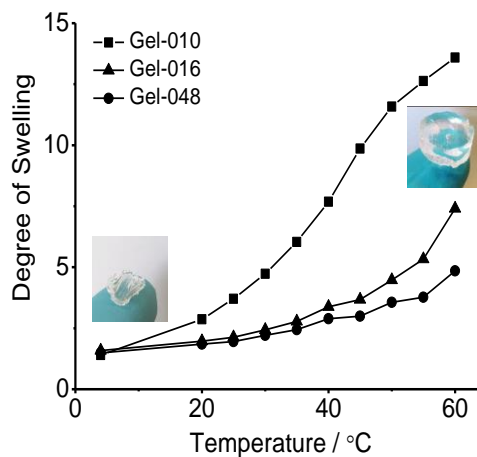
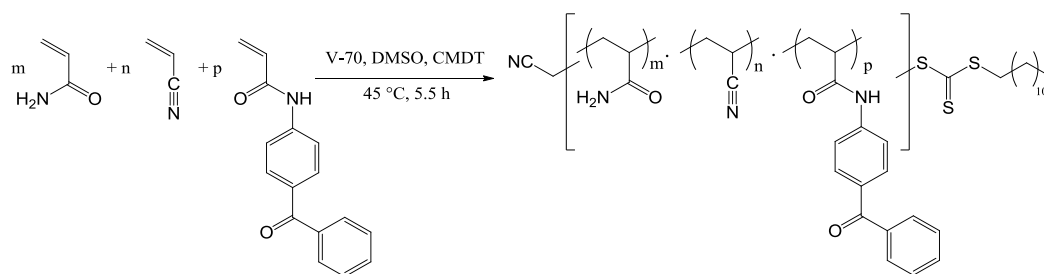


Figure 2-9. Degree of swelling as function of temperature for hydrogels with different contents of chemical cross linkers. (Squares = Gel-010, triangles = Gel-016 and circles = Gel-048)

## 2.5 Thermophilic films and fibers from photo cross-linkable UCST-type polymers

The results of this part have been published by Fangyao Liu, Shaohua Jiang, Leonid Ionov and Seema Agarwal in the journal: *Polymer Chemistry*, **2015**, DOI: 10.1039/C5PY00109A.

Polymers with UCST-type thermoresponsivity based on acrylamide (AAm), acrylonitrile (AN) and *N*-(4-benzoylphenyl) acrylamide (BPAm) as photo cross-linkable comonomer were synthesized *via* free radical and reversible addition fragmentation chain-transfer (RAFT) polymerization. (Scheme 2-4)



Scheme 2-4. Formation of photo cross-linkable UCST-type polymer with *N*-(4-benzoylphenyl) acrylamide (BPAm) as cross-linker by RAFT polymerization.

The UCST-type phase transition of polymer aqueous solution was monitored by turbidity measurement. The cloud points could be manipulated by varying the amount of AN in the feed. The cloud point of 0.1 wt.% polymer solutions increased with increase in AN amount in the feed: from 30 °C (8% AN) via 40 °C (10% AN) to 52 °C (12% AN). The terpolymers were stable against hydrolysis and showed almost no hysteresis during cooling and heating cycles for at least nine cycles. (Figure 2-10)

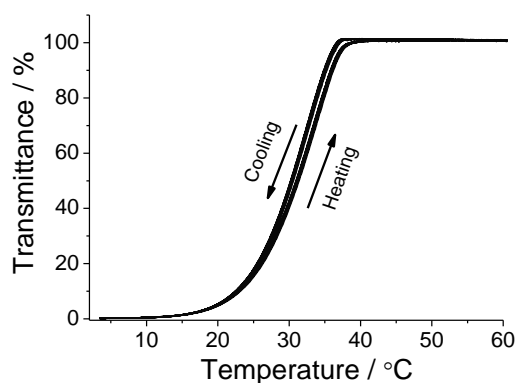


Figure 2-10. Nine consecutive measurements of 0.1 wt.% solution of poly(AAm-AN-BPAm) made by RAFT. The copolymer showed excellent hydrolytic stability and reproducible cloud point with very negligible hysteresis (cloud point on cooling: 32.8 °C; cloud point on heating: 33.5 °C).

## SYNOPSIS

Further, chemically cross-linked films and nanofibers (average diameter around 500 nm, Figure 2-11) were successfully made from these terpolymers by solution casting and electrospinning followed by UV irradiation as cross-linking process. The films and nanofibers showed temperature dependent positive volume transitions that were unitized for design of microactuators. (Figure 2-12)

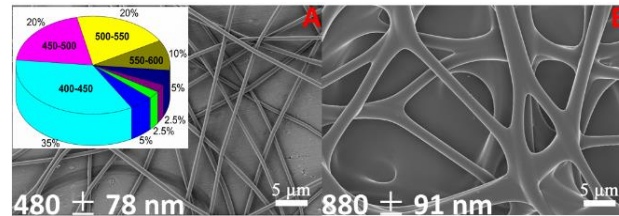


Figure 2-11. SEM images of polymer nanofibers in (A) dried and (B) wet state. Insert: pie chart of the fiber diameter distribution.

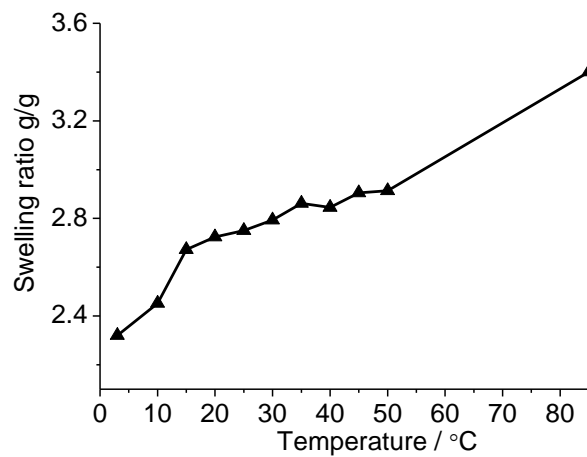


Figure 2-12. Temperature dependency of swelling ratio of hydrogels in water prepared by UV irradiation from terpolymer DMSO solution. The measurements were started from 50 °C followed by cooling to 3 °C. The swelling ratio data at 85 °C was obtained by testing an extra sample to avoid the effect of possible hydrolysis of the hydrogel. At each temperature the samples were equilibrated for 30 min.

## 2.6 Individual contributions to joint publications

### **Publication 1: Controlled radical polymerization of *N*-acryloylglycinamide and UCST-type phase transition of the polymers**

Dr. Jan Seuring and I contributed equally to this work. Kinetic experiments, turbidity measurements and chain extensions were conducted by me. Preliminary experiments and writing of the manuscript was done primary by Dr. Jan Seuring. I helped in finalization and correction of the manuscript. Prof. Dr. Seema Agarwal (corresponding author) was responsible for supervision, designing the concept and correction of the manuscript.

### **Publication 2: Atom transfer radical polymerization as a tool for making poly(*N*-acryloylglycinamide) with molar mass independent UCST-type transitions in water and electrolytes**

I designed the concept, performed all synthetic and analytic experiments and wrote the manuscript. Dr. Jan Seuring provided helpful discussions during the work and corrected the manuscript. Prof. Dr. Seema Agarwal (corresponding author) was responsible for supervision, participating in discussion, design of concept and correction of the manuscript.

### **Publication 3: Thermoresponsive gold nanoparticles with positive UCST-type thermoresponsivity**

I designed the concept, performed all synthetic and analytic experiments and wrote the manuscript. Prof. Dr. Seema Agarwal (corresponding author) was responsible for supervision, participating in discussion, designing concept and correction of the manuscript.

**Publication 4: A non-ionic thermophilic hydrogel with positive thermosensitivity in water and electrolyte solution**

I performed the synthetic and analytic experiments and wrote the manuscript. Dr. Jan Seuring did preliminary experiments and corrected the manuscript. Prof. Dr. Seema Agarwal (corresponding author) was responsible for supervision, participating in discussion, designing concept and correction of the manuscript.

**Publication 5: Thermophilic films and fibers from photo cross-linkable UCST-type polymers**

I designed the concept, performed all synthetic and analytic experiments and wrote the manuscript except that Dr. Shaohua Jiang produced the nanofiber mat and performed experiments and measurements related to the electrospinning part together with me. Dr. Leonid Ionov did the self-rolled polymer films experiment and wrote the part of manuscript related to this experiment and Prof. Dr. Seema Agarwal (corresponding author) was responsible for supervision, participating in discussion, designing concept and correction of the manuscript.



### **3 Reprints of Publications**

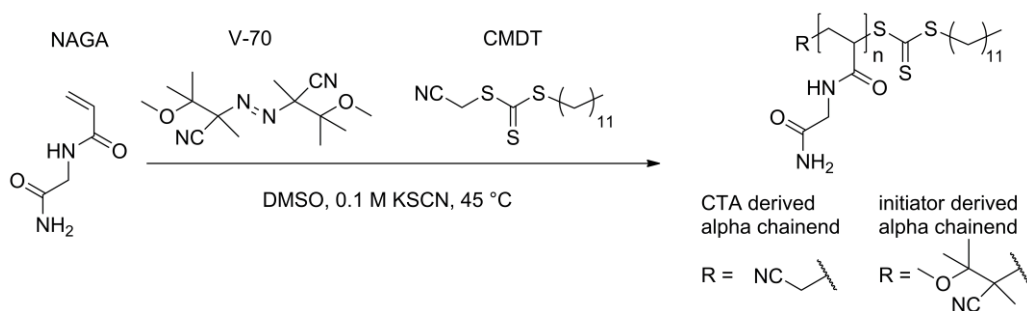
The manuscripts are reprinted in the form of journal articles with permission of the respective publisher.

The corresponding author is marked with an asterisk.

**Publication 1: Controlled Radical Polymerization of *N*-Acryloylglycinamide and UCST-Type Phase Transition of the Polymers**

**Fangyao Liu**, Jan Seuring and Seema Agarwal\*, Controlled Radical Polymerization of *N*-Acryloylglycinamide and UCST-Type Phase Transition of the Polymers, *Journal of polymer science part A: Polymer chemistry* **2012**, 50, 4920-4928.

Reprinted with permission; Copyright 2012 John Wiley and Sons



## Controlled Radical Polymerization of *N*-Acryloylglycinamide and UCST-Type Phase Transition of the Polymers

Fangyao Liu, Jan Seuring, Seema Agarwal

Department of Chemistry, Scientific Center for Materials Science, Philipps-Universität Marburg, Hans-Meerwein Strasse, D-35032 Marburg, Germany

Correspondence to: S. Agarwal (E-mail: agarwal@staff.uni-marburg.de)

Received 18 May 2012; accepted 28 July 2012; published online 20 August 2012

DOI: 10.1002/pola.26322

**ABSTRACT:** *N*-Acryloylglycinamide was polymerized via the reversible addition fragmentation transfer process without sacrificing its key property, the upper critical solution temperature in water. This could be achieved by choosing an appropriate nonionic initiator [2,2'-azobis(4-methoxy-2,4-dimethyl valeronitrile) (V-70)] and nonionic chain-transfer agent (cyanomethyl dodecyl trithiocarbonate). A good molar mass control was accomplished as proved by the linear increase of molar mass with conversion, a chain extension experiment, and low dispersity. The influence

of molar mass, polymer end groups, or salt concentration on the cloud point was analyzed by turbidimetry. Polymer end groups exerted a distinct effect on the cloud points, whereas the influence increased with decreasing molar masses. © 2012 Wiley Periodicals, Inc. *J Polym Sci Part A: Polym Chem* 50: 4920–4928, 2012

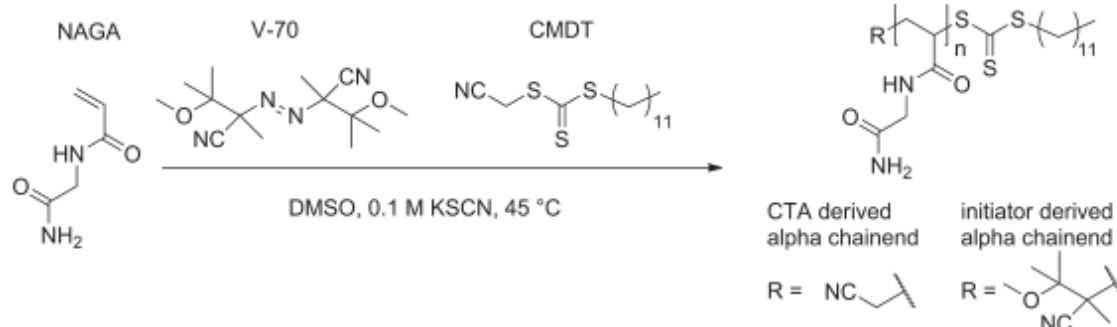
**KEYWORDS:** *N*-acryloylglycinamide; RAFT; smart polymers; thermoresponsive polymers; upper critical solution temperature

**INTRODUCTION** Although the general term water-soluble "thermoresponsive polymer" is frequently applied, it actually represents a synonym for polymers with lower critical solution temperature (LCST), as only very few examples of polymers with an upper critical solution temperature (UCST) in water under practically relevant conditions were reported, that is, with phase transitions between 0 and 100 °C, atmospheric pressure, and relevant ionic strength (from pure water to physiological milieu). This is supported by a 2010 review and survey on nonionic water-soluble thermoresponsive polymers.<sup>1</sup> The UCST of all known examples is based either on Coulomb interactions or on thermally reversible hydrogen bonding. The first applies for some zwitterionic polymers like poly(betaine)s.<sup>2–6</sup> However, Coulomb interactions are disturbed in the presence of electrolytes. The very strong sensitivity of the phase transition temperature to electrolyte concentration and polymer concentration makes them unsuitable for most applications. If the polymers are nonionic and the UCST is due to hydrogen bonding, the phase transition temperature is less sensitive to both electrolytes (except for specifically hydrogen bond-breaking agents like thiocyanates) and polymer concentration, and therefore, they represent promising candidates for many fields of applications. Yet, very few examples of nonionic, hydrogen-bonding UCST polymers were reported.<sup>7–9</sup> Poly(*N*-acryloylglycinamide) [poly(NAGA)] is one of these polymers. For the first time, it was synthesized by Haas and Schuler in 1964.<sup>10(a)</sup>

They found that poly(NAGA) can form thermoreversible gels in concentrated aqueous solutions.<sup>10(a–f)</sup> Haas and Schuler furthermore reported that hydrogen bond-interrupting agents like thiocyanate or urea can prevent the gel formation.<sup>10(b)</sup> Poly(NAGA) also does not exhibit thermoreversible gelation behavior in dilute solutions; however, it contains polymer aggregates despite of its transparent and homogeneous appearance. This was initially evidenced by a nonlinear dependency among reduced viscosity and polymer concentration in pure water, along with the fact that the viscosity dropped significantly on addition of sodium thiocyanate.<sup>10(b)</sup> Later, the conclusions of Haas and Schuler were confirmed by light scattering and Raman spectroscopy.<sup>11,12</sup> We would like to emphasize in this context that although both thermoreversible gelation and aggregate formation in dilute solution are due to hydrogen bonding, these phenomena differ considerably from a UCST-type phase separation. For UCST behavior, the occurrence of phase separation is a stringent requirement.<sup>13</sup> In contrast, in the thermoreversible gelation of concentrated poly(NAGA) solutions, no phase separation takes place as the gel is only in one phase with homogenous properties. The formation of aggregates in dilute solution can be regarded as a form of microphase separation. However, a preliminary temperature-dependent light scattering study of poly(NAGA) suggested that these aggregates are thermodynamically stable above the phase transition temperature and no macrophase separation sets in.<sup>14</sup> It is yet

Fangyao Liu and Jan Seuring have contributed equally to the experimental part.

© 2012 Wiley Periodicals, Inc.



**SCHEME 1** Schematic representation of the optimum conditions developed in this work for the RAFT polymerization of *N*-acryloylglycinamide while retaining the UCST of the resulting polymers in water.

unclear whether there is a distinct temperature where aggregates form/break; however, most likely these aggregates are just thermosensitive rather than thermoresponsive. Based on this, a behavior comparable with micelles that comprise a gradual decrease of the aggregation number with temperature would be most likely. Thus, despite numerous contributions focused on the thermoreversible gelation of poly(NAGA), a UCST-type phase separation has not been reported in the publications mentioned above. We recently revealed the reason for this:<sup>14</sup> it has been failed to notice the UCST in the past because ionic groups were introduced unintentionally either by acrylate impurities in the monomer, hydrolysis of the polymer side chains, and/or usage of ionic initiators or chain-transfer agents (CTAs). Ionic groups in polymers contribute strongly exothermic to the enthalpy of mixing.<sup>15,16</sup> The effect on the UCST of poly(NAGA) is extreme because the enthalpy change of the phase transition is already two magnitudes smaller than for most LCST polymers such as PNiPAAm.<sup>17–19</sup> The proof for these conclusions along with a procedure to obtain stable aqueous solutions of nonionic poly(NAGA) that allows exploitation of UCST in pure water as well as physiological milieu was published.<sup>14</sup> Most recently, the synthesis of thermoresponsive poly(acrylamide-co-acrylonitrile)s and poly(methacrylamide) indicated that the knowledge gained for poly(NAGA) is valid for the whole polymer class of nonionic hydrogen-bonding UCST polymers.<sup>20</sup>

Recent work of Lutz and coworkers<sup>21</sup> regarding the controlled radical polymerization of NAGA by reversible addition fragmentation transfer (RAFT) polymerization gave additional support to our findings. The fact that poly(NAGA) prepared via RAFT polymerization did not comprise a cloud point in water can most likely be deduced to the usage of an ionic radical initiator (VA-044) and an ionic CTA [sodium 3-(((benzylthio)-carbonothioyl)thio)propane-1-sulfonate]. The cloud point suppressing effect of the ionic end groups could be compensated by the addition of electrolytes; however, it is preferable to obtain polymers that exhibit the desired functionality in pure water as well and are not strongly influenced by the electrolyte concentration.

This work was carried out with the aim to provide controlled radical polymerization of NAGA by the RAFT process

without sacrificing the most interesting property of the polymers, the UCST in water. The underlying concept of this work was to use nonionic radical initiators and nonionic CTAs to achieve molar mass control and well-defined chain ends without sacrificing the thermoresponsivity in water (Scheme 1). Although this concept has been developed in our previous work, we could not achieve good molar mass control ( $D > 2$ ), and therefore, an appropriate correlation of properties with the molar mass distribution was not possible. There were two motivations for this study: on one hand, the determination of molar mass dependence of the phase transition required control over the molar mass—this can be achieved by RAFT; and on the other hand, RAFT represents an excellent method for a precise functionalization of polymer end groups. Besides allowing both grafting from and grafting onto various substrates, it enables straightforward preparation of complex macromolecular architectures such as (multi)block copolymers, dendrimers, star polymers, comb polymers, and so forth.<sup>22</sup> This will be important for the development of smart materials with UCST-type thermoresponsivity of poly(NAGA) in the future.

## EXPERIMENTAL

### Materials

Azobisisobutyronitrile (Fluka) was recrystallized from ethanol. Acrylate-free *N*-acryloylglycinamide [NAGA;  $m_p$ (DSC) = 143 °C, residual potassium < 5 ppm] was synthesized according to a recently published procedure.<sup>14</sup> 3-(((Benzylthio)carbonothioyl)thio)propane-1-sulfonate (BCPS) and dibenzyltrithiocarbonate (DBTC) were synthesized according to the literature.<sup>21,23</sup> 2,2'-Azobis(4-methoxy-2,4-dimethyl valeronitrile) (V-70; Wako), cyanomethyl dodecyl trithiocarbonate (CMTD, 98%; Aldrich), and potassium thiocyanate (99%, p.a.; Grüssing) were used as received. Solvents were distilled before use. Ultrapure water was obtained from a TKA Micro UV system model 08.1005 (conductivity = 0.06  $\mu\text{S}/\text{cm}$ , filtered through 200 nm filter, UV treated). Phosphate buffered saline (PBS) was prepared using precalibrated tablets (Aldrich).

### Analytical Techniques

<sup>1</sup>H spectra were recorded on a Bruker Avance DRX-500 (500 MHz) either in D<sub>2</sub>O at 80 °C or DMSO-*d*<sub>6</sub> at 100 °C.

**TABLE 1** RAFT Polymerization of NAGA with AIBN as Initiator and Dibenzyltrithiocarbonate (DBTC) as CTA

Entry	Time (min)	Yield (%)	$M_{n, \text{theo}}$ (g/mol)	$M_n$ (g/mol)	D	Cloud point in PBS <sup>a</sup> (°C)	
						Cooling	Heating
1	200	19	15,100	7,260	3.0	18.8	30.1
2	230	32	25,200	9,450	2.9	17.3	28.1
3	300	51	39,300	12,600	2.7	17.3	29.1
4	635	48	37,500	12,600	3.0	16.9	28.8

The Mono:CTA:In ratio was 600:1:0.2 with a monomer concentration of 0.59 M.

<sup>a</sup>  $c = 0.2$  wt %; heating rate = 1.0 °C/min.

Turbidity measurements were performed on a custom-modified Tepper turbidity photometer TP1-D at a wavelength of 670 nm, a cell path length of 10 mm, and magnetic stirrer. The polymer solutions (above phase transition temperature) were filtered through a warm 1.2- $\mu\text{m}$  PET syringe filter before measurement. The heating program started at 60 °C and proceeded via cooling to 3.5 °C at a constant rate of 1.0 °C/min followed by reheating to the starting temperature with the same rate. The inflection point of the transmittance curve was considered as cloud point. It was graphically determined by the maximum of the first derivative of the heating or cooling curve, respectively. For sample preparation, the polymers were weighed into 2-mL polypropylene tubes. The dissolution parameters for poly(NAGA) in PBS (pH 7.4) and salt solutions were as follows:  $c = 1.0$  wt %,  $T = 70$  °C inside the tubes, and  $t = 90$  min without sonication. The parameters in pure water were as follows:  $c = 1.0$  wt %,  $T = 70$  °C inside the tubes, and  $t = 60$  min with sonication. For sonication, a heated Bandelin Sonorex RK 102 H ultrasound device (HF power = 120 W, HF peak performance = 480 W, HF frequency = 35 kHz) was used. The samples were diluted to 0.2 wt %, and the hot samples were quickly filtered through a preheated 1.2- $\mu\text{m}$  PET-filter into the cuvette.

Molar masses and molar mass distributions of the polymers were determined by gel permeation chromatography (GPC) with dimethyl sulfoxide as eluent. Two PL-Gel Mixed-D columns (particle size 5  $\mu\text{m}$ , dimension 7.5 mm  $\times$  300 mm) calibrated with narrow Pullulan standards and a differential refractive index detector were used. The flow rate was 1.0 mL/min. The molar mass distributions were calculated using the software Cirrus 3.3. The theoretically number-average molar mass  $M_{n, \text{theo}}$  was calculated using the following equation:

$$M_{n, \text{theo}} = [c_0(\text{monomer})/c_0(\text{CTA})] \times x_p \times M_{\text{NAGA}} + M_{\text{CTA}} \quad (1)$$

where  $c_0(\text{monomer})$  and  $c_0(\text{CTA})$  refer to the initial concentrations of monomer and RAFT CTA, respectively;  $x_p$  denotes monomer conversion; and  $M_{\text{NAGA}}$  and  $M_{\text{CTA}}$  are the molar masses of the monomer and CTA.

## Syntheses

### General Procedure for the Purification and Isolation of Polymers

The reactions were stopped by air contact. Thereafter, the polymers were precipitated from the 10-fold excess volume of methanol. Subsequent to centrifugation (10 min, 8000 rpm) and decantation, the sediment was thoroughly slurried with methanol using a glass rod. The centrifugation-wash cycles were repeated three times. Subsequently, the polymer was dried in the vacuum oven at 70 °C for 24 h. The brittle pellet was grinded to a powder using a glass rod and further dried for another 24 h to obtain a powdery white polymer.

### Example of RAFT Polymerization of NAGA with DBTC as CTA

In a 25-mL nitrogen flask, 1 g NAGA (200 equiv) and 11.3 mg DBTC (1 equiv) were dissolved in 11.2 mL distilled DMSO. The solution was degassed by three freeze-pump-thaw cycles. One hundred microliters of a separately degassed DMSO solution containing 1.3 mg of AIBN (0.2 equiv) was added, and the flask was placed into an oil bath that was preheated to 70 °C. Further details are given in Table 1.

<sup>1</sup>H NMR (500 MHz, D<sub>2</sub>O,  $T = 80$  °C; the HDO peak was calibrated to  $\delta = 4.20$  ppm): 1.3–1.8 (polymer backbone,  $-\text{CH}_2-$ ), 2.0–2.3 (polymer backbone,  $-\text{CH}-$ ), 2.5 (S- $\text{CH}_2$ -Ph), 3.6–4.05 (NH- $\text{CH}_2$ -CONH<sub>2</sub>), 7.05–7.3 (Ar-H).

### Example of RAFT Polymerization of NAGA with CMDT as CTA

In a 50-mL nitrogen flask, 2 g NAGA (200 equiv) was dissolved in 24.7 mL distilled DMSO containing 0.1 M KSCN. One milliliter of a CTA-stock solution in the same solvent containing 24.8 mg CMDT (1 equiv) was added. This solution was degassed by three freeze-pump-thaw cycles. A V-70 stock solution was prepared by dissolving V-70 in separately degassed DMSO with 0.1 M KSCN. From this stock solution, 800  $\mu\text{L}$  solution containing 1.93 mg of V-70 (0.08 equiv) was quickly added to the reaction mixture. The mixture was placed into a preheated oil bath and stirred for 4 h at 45 °C. Further details are given in Table 3.

<sup>1</sup>H NMR (500 MHz, DMSO- $d_6$ ,  $T = 100$  °C; the DMSO peak was calibrated to  $\delta = 2.50$  ppm): 0.87 (alkyl- $\text{CH}_3$ ), 1.27

**TABLE 2** RAFT Polymerization of NAGA with AIBN as Initiator and CMDT as CTA

Entry	Time (min)	Yield (%)	$M_{n, \text{theo}}$ (g/mol)	$M_n$ (g/mol)	$D$
1	25	5	4,110	4,450	1.69
2	65	12	9,670	8,610	1.69
3	140	28	21,300	12,600	1.95

The Mono:CTA:In ratio was 600:1:0.2 with a monomer concentration of 0.59 M.

(alkyl), 1.3–1.8 (polymer backbone,  $-\text{CH}_2-$ ), 1.9–2.3 (polymer backbone,  $-\text{CH}-$ ), 2.3–2.4 ( $\text{S}-\text{CH}_2$ -alkyl), 3.35 ( $\text{S}-\text{CH}_2-\text{CN}$ ), 3.4–4.05 ( $\text{NH}-\text{CH}_2-\text{CONH}_2$ ), 6.5–7.3 ( $\text{CONH}_2$ ), 7.3–7.4 ( $\text{CONH}-$ ).

#### Chain Extension of the RAFT Polymer

Poly(NAGA) (79 mg; synthesized by RAFT polymerization, 1 equiv based on  $M_{n, \text{theo}} = 6524$  g/mol) was dissolved at 75 °C in 2 mL distilled DMSO solution containing 0.1 M KSCN in a 10-mL nitrogen flask. After cooling to room temperature, 151 mg NAGA (100 equiv) was added. The solution was degassed by three freeze-pump-thaw cycles. A V-70 stock solution was prepared by dissolving V-70 in separately degassed 0.1 M KSCN containing DMSO. From this stock solution, 200  $\mu\text{L}$  solution containing 0.29 mg of V-70 (0.08 equiv) was quickly added to the reaction mixture. The mixture was placed into a preheated oil bath and stirred for 4 h at 45 °C. The chain extension was followed by  $^1\text{H}$  NMR and GPC (Figs. 5 and 6).

## RESULTS AND DISCUSSION

### RAFT Polymerization of NAGA

It has been previously shown that even trace amounts of ionic groups in the polymer repeating units or at the chain ends of poly(NAGA) cause an extreme depression of the cloud point until the phase separation is completely suppressed.<sup>14</sup> At least up to a  $P_n$  of 200, polymers with  $\alpha$ -chain ends—derived from the initiator 2,2'-azobis[2-(2-imidazolin-2-yl)propane]dihydrochloride (VA-044)—or polymers with a sulfonate group at the  $\omega$ -chain ends, based on the CTA sodium BCPS, did not exhibit a cloud point in dilute aqueous solution. In this work, nonionic initiators and CTAs were used to obtain poly(NAGA) with thermoresponsivity. Most of these nonionic reagents are insoluble in water, and therefore, dimethyl sulfoxide was chosen as polymerization medium. First attempts were carried out using nonionic DBTC as CTA and AIBN as nonionic radical initiator, and indeed, the resulting polymer showed a cloud point (Table 1). However, at a reaction temperature of 70 °C, an inhibition period of about 150 min was observed besides an insufficient molar mass control with broad dispersities (Table 1). The occurrence of an inhibition period during the RAFT process indicates a slow re-initiation by the R-group.<sup>22</sup> In the case of DBTC, the benzyl radical is too stable for a fast re-initiation.

These results suggested a change of the R-group of the CTA. Cyanomethyl dodecyl trithiocarbonate (CMDT) was chosen as

new CTA, and polymerization of NAGA was carried out using the same conditions (Table 2). In this case, no inhibition was observed but the dispersities were relatively high, i.e. about 1.7. In general, free radical polymerization of water-soluble acrylamides in organic solvents such as DMSO does not yield very high molar masses. For instance, the  $k_p k_0^{0.5}$  ratio of acrylamide in DMSO is 12 times lower than in water.<sup>24</sup> When NAGA is polymerized with AIBN as initiator at 70 °C for 2 h and a monomer concentration of 0.59 M, the molar mass is  $M_n = 64,300$  g/mol. It is not possible to conduct a well-controlled radical polymerization beyond the molar mass that is achieved by free radical polymerization under the same conditions. Therefore, the focus was changed to optimize the conditions for free radical polymerization. For acrylamide, it has been observed that the molar mass increases with decreasing reaction temperature.<sup>24,25</sup> The same was found for the free radical polymerization of NAGA. By using the nonionic radical initiator V-70 with a half life decomposition temperature of 30 °C, the reaction temperature could be decreased from 70 to 45 °C. The obtained molar mass was significantly higher with a number-averaged molecular weight of 88,200 g/mol. Therefore, further RAFT polymerizations were carried out using V-70 as radical initiator. At 45 °C with V-70 as initiator and CMDT as CTA, RAFT polymerization of NAGA led to improved polydispersities of about 1.4 for the main peak of the elugram. However, the GPC elugrams comprised shoulders in the region of 64,300 g/mol where free radically polymerized polymer is expected (Fig. 1).

It is known that poly(NAGA) can form physical aggregates in DMSO,<sup>21</sup> and therefore, aggregation might have interfered during the RAFT polymerization. Shoulders from high molar mass impurities were previously observed for the RAFT polymerization of NiPAAm;<sup>26</sup> however, the reasons are unclear. Although no physical aggregates were observed in the GPC ( $c = 2$  mg/mL), one could assume that an insufficient

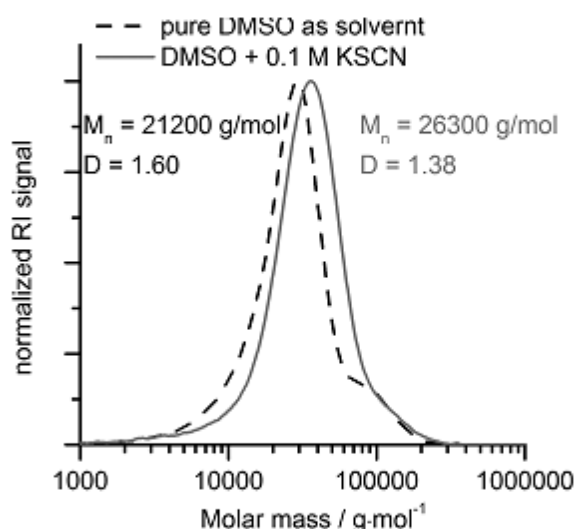


**FIGURE 1** Influence of potassium thiocyanate additive in the polymerization medium on the molar mass distribution of poly(NAGA) synthesized by RAFT.

**TABLE 3** RAFT Polymerization of NAGA with V-70 as Initiator and CMDT as CTA

Entry	Mono:CTA:In	<i>t</i> (h)	Yield (%)	$M_{n, \text{theo}}$ (g/mol)	$M_n$ (g/mol)	<i>D</i>	Cloud points in PBS <sup>a</sup> (°C)	
							Cooling	Heating
1	50:1:0.1	20	68	4,674	3,670	1.18	22	n.d. <sup>b</sup>
2	100:1:0.04	0.67	37	5,015	3,340	1.41	n.d. <sup>b</sup>	n.d. <sup>b</sup>
3		0.83	39	5,330	4,470	1.32	n.d. <sup>b</sup>	n.d.
4		1	49	6,527	5,060	1.39	23	n.d. <sup>b</sup>
5		1.5	58	7,690	6,440	1.35	14.1	43
6		2	63	8,332	7,030	1.32	12.6	38
7		3	68	8,965	7,100	1.36	13.0	37
8		6	78	10,246	7,290	1.37	11.9	36
9	200:1:0.08	0.33	27	7,224	4,960	1.53	26	n.d. <sup>b</sup>
10		0.5	38	10,055	8,270	1.31	12.9	38
11		0.75	51	13,452	11,000	1.31	10.5	32
12		1	61	15,978	12,200	1.32	9.3	30.9
13		1.5	72	18,806	13,700	1.27	9.7	31.0
14		3	79	20,600	15,700	1.41	8.5	28.3
15		5.33	88	22,762	15,700	1.33	8.7	26.2
16	500:1:0.2	1	62	39,915	29,400	1.38	8.4	24.7
17		1.5	76	49,202	29,700	1.43	9.1	23.9
18		2	80	51,699	30,900	1.47	8.8	24.5
19		3	87	56,307	33,500	1.43	9.0	24.8
20		5	92	59,584	32,700	1.65	9.1	25.2
21		6	95	61,000	34,300	1.50	9.4	25.5

The monomer concentration was 0.59 M. The V-70 concentration was 0.24 mM except for the first entry where it was 1.2 mM.

<sup>a</sup> Polymer concentration was 0.2 wt %.

<sup>b</sup> Cloud point not determined due to very broad transition.

solubilization in the concentrated reaction mixture (75 mg/mL) leads to hindered accessibility of the growing chain ends, and therefore, hindered chain equilibration and inevitably resulted in less control. Based on this hypothesis, 0.1 M potassium thiocyanate was added to the polymerization medium to break intramolecular and intermolecular hydrogen bonds. Using this additive, the shoulder in the GPC elugrams disappeared, and a controlled RAFT polymerization of NAGA could be achieved (Fig. 1). Kinetic studies were conducted with monomer:CTA ratios of 100:1, 200:1, and 500:1 (Table 3). The absolute monomer and initiator concentrations were held constant at 0.59 M and 0.24 mM, respectively. Constant concentration of the growing polymer chains was supported by the first-order kinetic plots (Fig. 2). A slight retardation was observed at higher CTA concentrations, which resulted in lower conversions. In a single experiment with a monomer:CTA ratio of 50, the initiator concentration was increased to 1.2 mM.

Molar masses increased linearly depending on the conversion (Figs. 3 and 4); the dispersity was 1.3–1.4. Number-averaged molar masses  $M_n$  were always lower when compared with the theoretical molar masses  $M_{n, \text{theo}}$ . Pullulan was used as standard for GPC calibration, and the molar masses determined were not absolute. Therefore, a deviation

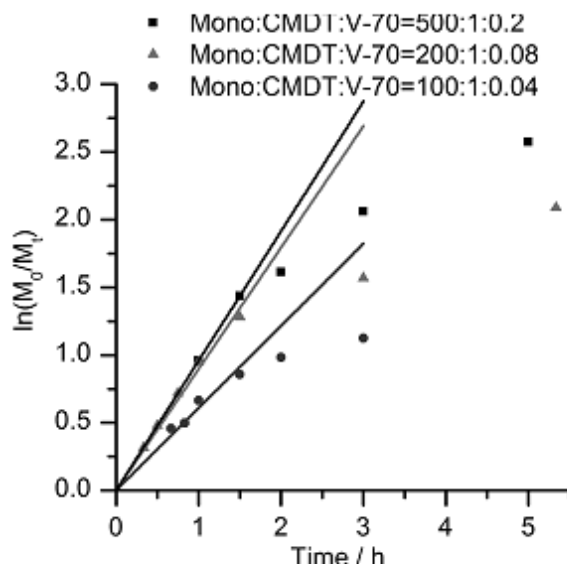


**FIGURE 2** First-order kinetic plots of the RAFT polymerization of NAGA with different monomer:CTA ratios. The monomer concentration was 0.59 M, and the initiator concentration was 0.24 mM.

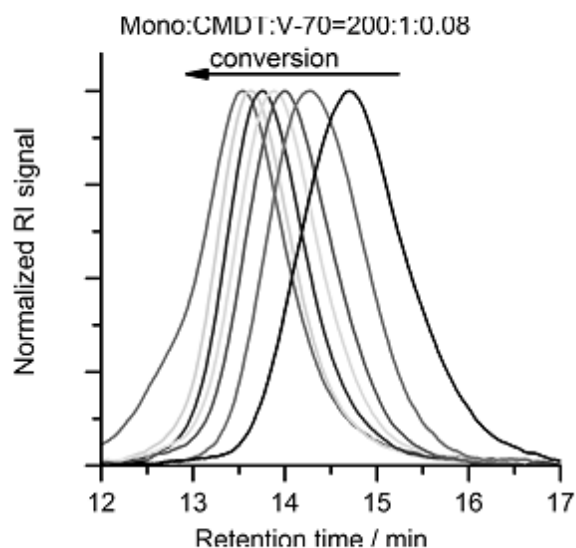


**FIGURE 3** GPC elugrams of poly(NAGA) synthesized by RAFT using Mono:CMDT:V-70 in the ratio 200:1:0.08. Conversion from right to the left: 27, 38, 51, 61, 72, 79, and 88%.

of  $M_n$  from  $M_{n, \text{theo}}$  is not unusual. At higher Mono:CTA:In ratios (500:1:0.08), the deviation from  $M_{n, \text{theo}}$  increased, despite of the proceeding increase of molar mass with conversion. Nearly quantitative functionalization of the polymer chain ends by the RAFT agent could be demonstrated by a chain extension experiment (Fig. 5). Here, a polymer with  $M_n = 5060$  g/mol (Table 3, entry 4) was prepared by RAFT. This polymer was subsequently used as macroinitiator for the polymerization of new NAGA monomer to obtain a chain-extended polymer of  $M_n = 13,400$  g/mol. Disappearance of the macroinitiator was evident from the corresponding GPC elugram, thereby almost quantitative end-group functionalization via the RAFT process was proven. More-

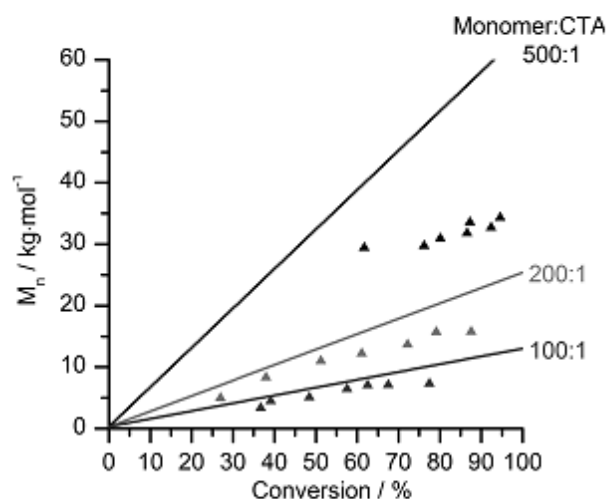


**FIGURE 4** Molar masses determined by GPC as a function of conversion for different monomer:CTA ratios. Lines =  $M_{n, \text{theo}}$ ; triangles =  $M_n$ .

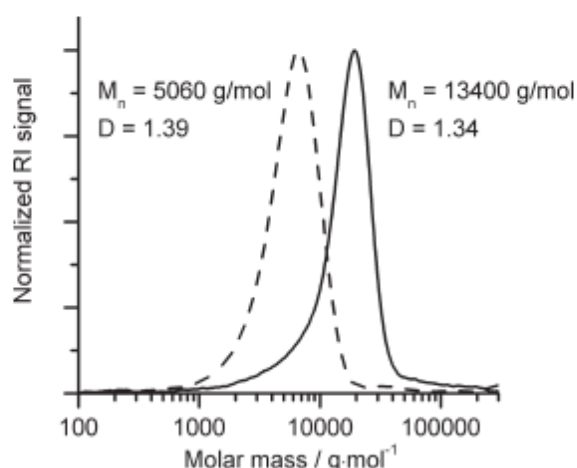


**FIGURE 5** GPC traces illustrating the successful chain extension of poly(NAGA) synthesized by RAFT. Dotted line: polymer before chain extension; solid line: polymer after chain extension.

over, this is in agreement with the decreasing end-group signals in the  $^1\text{H}$  NMR spectra (Fig. 6).

#### Molar Mass and End-Group Dependence of the Cloud Points of Poly(NAGA)

Polymers synthesized by controlled radical polymerization were used to prepare 0.2 wt % solutions in either pure water or PBS. The advantage of the RAFT system developed in this work is that the polymers show a UCST in pure water, media with low ionic strength, and media with higher ionic strength like PBS. For instance, the sample with  $M_n = 29,400$  g/mol (Table 3, entry 16) displayed cloud points in pure water of 11.8 °C on cooling and 28.8 °C on heating, respectively. In PBS, the cloud points were 8.4 °C on cooling and 24.7 °C on heating. A more detailed discussion concerning salt effects is given in "Influence of Electrolytes on the Cloud Point of Poly(NAGA) Synthesized by RAFT" section. Figure 7 depicts nine consecutive turbidity measurements of a representative sample with  $M_n = 29,400$  g/mol (Table 3, entry 16); reversibility of the phase transitions was excellent. To analyze the dependence of cloud points on the molar mass, PBS was adopted as solvent. This choice was based on the fact that sonication was required to dissolve nonionic poly(NAGA) in pure water; however, as this procedure bears the risk of molar mass degradation, it should be avoided. This appears to be a particular drawback of the long dodecyl chain of CMDT and could be overcome in the future by using derivatives with shorter alkyl chains instead. All samples could be dissolved in PBS by heating to 70 °C for 90 min. Subsequently, the cloud points of these solutions were determined by turbidimetry and plotted as a function of the molar mass (Fig. 8). At molar masses from  $M_n = 15$ –35 kg/mol, cloud points were independent of the molar mass. However, below  $M_n = 15$  kg/mol, the influence of the polymer end group was significant. In the case of RAFT polymerization with CMDT as CTA, the dodecyl end groups are hydrophobic, which gives a reason for the observed increasing



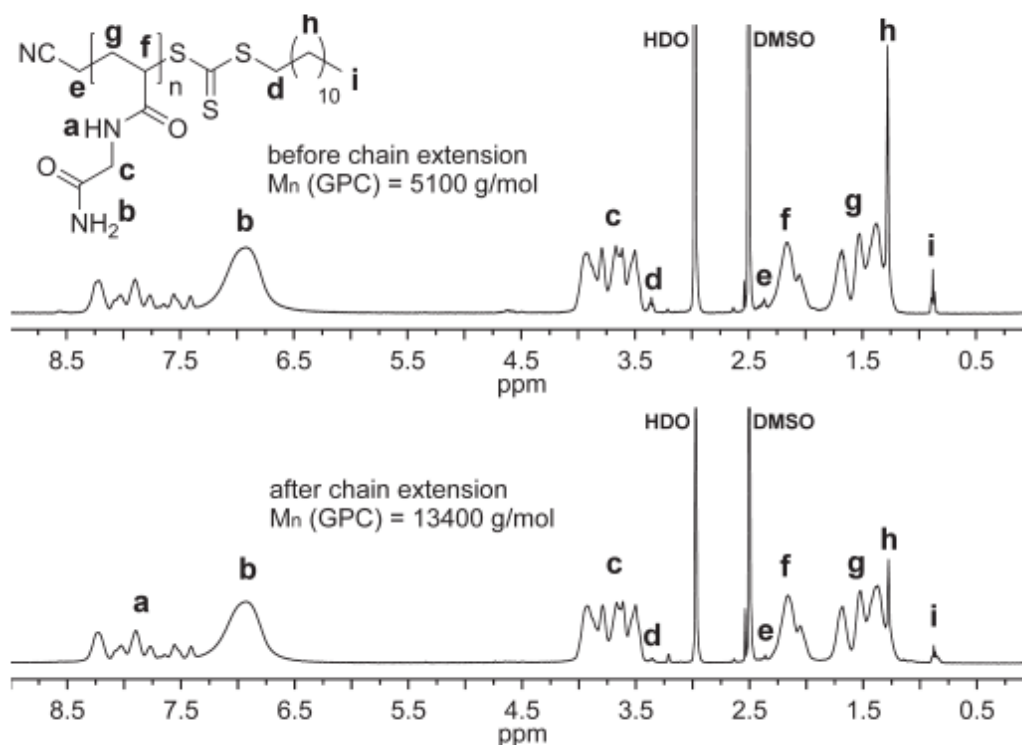


**FIGURE 6**  $^1\text{H}$  NMR spectra of poly(NAGA) synthesized by RAFT before and after chain extension. The spectra were measured in  $\text{DMSO-}d_6$  at  $100^\circ\text{C}$ .

cloud points toward lower molar masses. The cloud points on cooling increased steadily from  $T_c = 9^\circ\text{C}$  at  $M_n = 15,700$  g/mol to  $T_c = 22^\circ\text{C}$  at  $M_n = 3670$  g/mol.

From the molar mass dependence, it can be deduced that the broadness of the molar mass distribution (represented by dispersity  $D$ ) does not exert any influence on the cloud points as long as the low molar mass region is not reached. However, if molar masses cover this range, a mixture of polymers with different cloud points is present and consequently results in a broadening of the phase transition zone. Furthermore, this conclusion

is supported by the fact that the phase transitions become broader at lower molar masses when compared with polymers exhibiting similar  $D$ -values (samples with  $M_n = 8270$ ,  $13,700$ , and  $29,400$  g/mol in Fig. 9). The temperature intervals in which the transmission dropped from 90% to 10% during cooling and increased from 10% to 90% during heating were taken as a measure of the sharpness of transition. For poly(NAGA) synthesized by RAFT with  $M_n = 29,400$  g/mol and a  $D$  value of 1.38, the intervals were  $2.1^\circ\text{C}$  on cooling and  $6.6^\circ\text{C}$  on heating. Toward decreasing molar masses of  $M_n = 13,700$  and  $8270$  g/mol with  $D$ -values of 1.27 and 1.31, the corresponding intervals increased

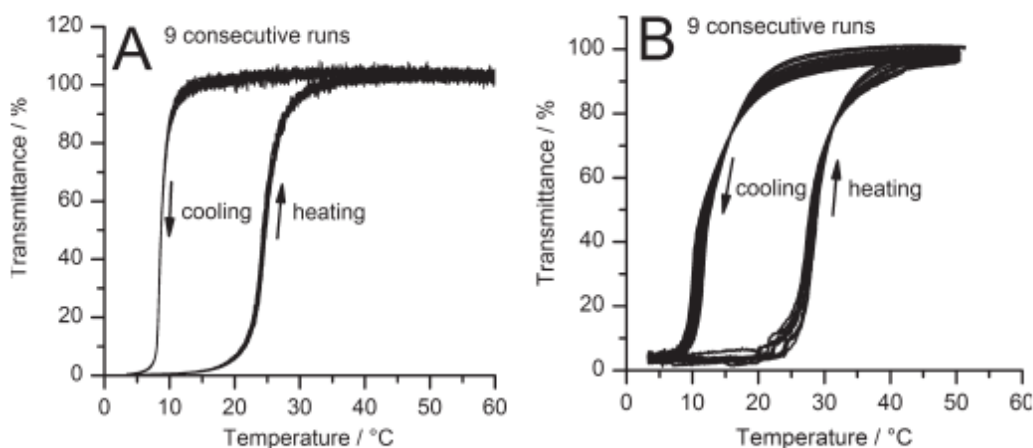


**FIGURE 7** Nine consecutive turbidity measurements of poly(NAGA) synthesized by RAFT with a molar mass of  $M_n = 29,400$  g/mol. The concentration was 0.2 wt % in (A) PBS and (B) pure water.

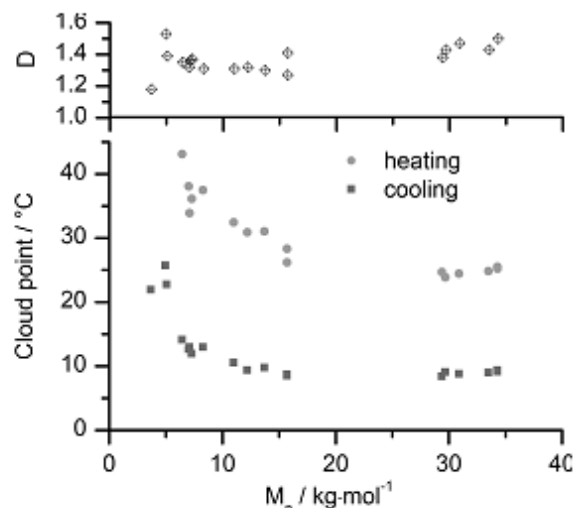


**FIGURE 8** Cloud points of poly(NAGA) synthesized by RAFT using CMDT as CTA as a function of molar mass.

to 4.5 and 8.8 °C on cooling and 11.9 and 18.1 °C on heating, respectively. Below  $M_n = 5000$  g/mol, the transitions became very broad and were not fully reversible in the time frame of one measurement cycle. To fully redissolve, they required further heating to 70 °C for a couple of minutes. Apparent deviations from the cloud point trend in the lower molar mass region, for instance, entries 1 and 9 of Table 3, can also be explained by dispersity effects. All effects discussed above should be less pronounced when CTAs with shorter alkyl groups are used, for example, cyanomethyl ethyltrithiocarbonate.

In analogy with our observations, the inverse influence of the end-group polarity was reported for polymers with LCST. Huber et al.<sup>27</sup> showed for poly(2-isopropyl-2-oxazoline) with a molar mass of about 3000 g/mol that a change of the terminal groups from a methyl to a nonyl moiety decreased the cloud point by 19 °C from 47 °C for P*i*PrOx<sub>25</sub> to 28 °C for Non-P*i*PrOx<sub>25</sub>. Xia et al.<sup>28</sup> performed ATRP of NiPAAm using the hydrophilic initiator chloropropionamide (CP). The cloud

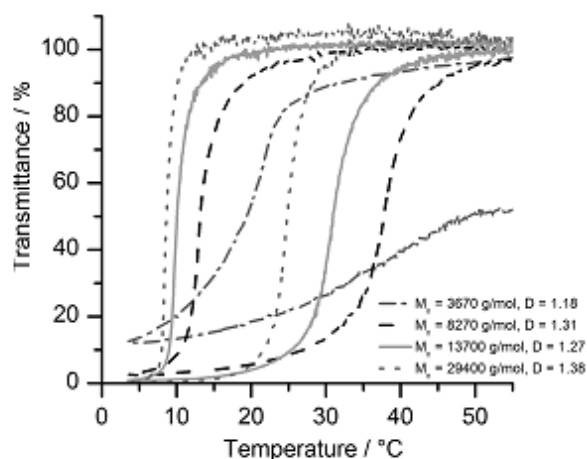


**FIGURE 9** Influence of the molar mass distribution on the turbidity curve of poly(NAGA) with hydrophobic end groups.

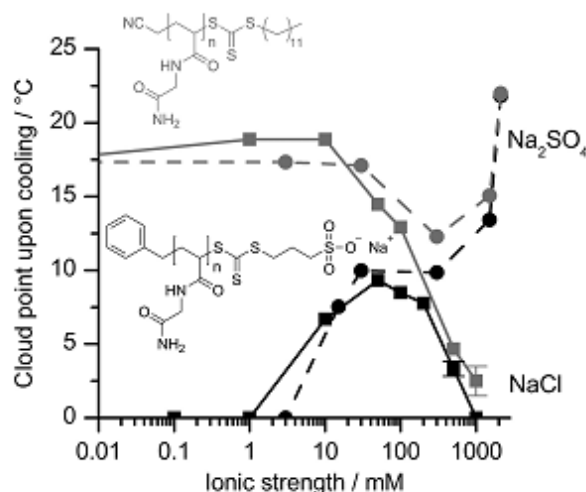


**FIGURE 10** Cloud points of poly(NAGA) with ionic or nonionic end groups as a function of ionic strength. Here, cloud point of zero means that the polymer was water soluble at 0 °C.

point (50%T) of PNiPAAm-CP polymers thereby dropped from 45.3 to 34.4 °C as the  $M_{n, theo}$  increased from 3000 to 16,300 g/mol. As expected, the end-group effect was most significant for the low molar mass samples and considerably less remarkable for longer chains.

#### Influence of Electrolytes on the Cloud Point of Poly(NAGA) Synthesized by RAFT

In a recent contribution, we showed that RAFT polymerization with an ionic CTA led to a polymer that does not exhibit a UCST in pure water but in PBS.<sup>14</sup> However, RAFT polymerization with a nonionic CTA resulted in a polymer that exhibited a UCST in both media. In this work, the influence of salt additives on both types of polymers is analyzed in detail. Two samples were synthesized using different CTA/initiator systems: poly(NAGA) with a sulfonate omega end group was synthesized according to Lutz and coworkers<sup>21</sup> using BCPS as CTA and V-044 as initiator, and on the contrary, nonionic poly(NAGA) was prepared with CMDT as CTA and V-70 as initiator. In both cases, a monomer:CTA ratio of 200:1 was used. Figure 10 displays the cloud points on cooling as a function of salt concentration. In pure water, the nonionic polymer with dodecyl omega end group showed a cloud point on cooling of 17.4 °C and a cloud point on heating of 34.6 °C. For the poly(NAGA) with a sulfonate (ionic) omega end group, no cloud point could be detected in pure water. However, cloud points were observed at sodium chloride concentrations above 1 mM and increased considerably with NaCl concentration as the end group got shielded by sodium cations. A further increase in NaCl concentration caused a steady decrease of the cloud points until they disappeared at around 1000 mM NaCl. At high concentrations of NaCl, the same trend was observed for nonionic poly(NAGA). This is an effect specific to sodium chloride; the influence of sodium sulfate was more complex. In case of nonionic poly(NAGA), there was a local minimum of the cloud points at around 100 mM sodium sulfate, which is even lower than the cloud point in

pure water. Beyond this concentration, the cloud points steadily increased for both polymers. This increase is in agreement with the Hofmeister series of ions, which was established to describe the effect of ions on the solubility of proteins.<sup>29</sup> Such correlations according to the Hofmeister series were also reported for LCST polymers like PNIPAAm. Here, the effect of salts was thoroughly investigated and even contributed to revision of the underlying mechanism of the Hofmeister series.<sup>30,31</sup> Now it is unambiguous that ions act via polarization effects, surface tension, as well as direct ion binding and therefore could affect thermoresponsivity in a different manner. Real biological fluids are complex and contain both chaotropic and kosmotropic agents, and hence, the UCST behavior is very difficult to predict. However, it was previously shown that poly(NAGA) retains its UCST in human blood serum.<sup>14</sup>

### CONCLUSIONS

NAGA was polymerized by a controlled radical polymerization with good molar mass control, as demonstrated by the linear increase of molar mass with conversion and a chain-extension experiment. This was achieved without sacrificing its key property, the UCST in water. Because of the molar mass control, it was possible to analyze the molar mass dependence of the cloud points. In analogy to LCST-polymers, it was detected that polymer end groups exerted a strong effect on the cloud points with increasing influence toward lower molar masses. The hydrophobic dodecyl end groups derived from the CTA caused an increase in the cloud points. Furthermore, with RAFT a well-established method of controlled polymerization enables precise end-group functionalization, grafting reactions, and synthesis of block copolymers. This allows the design of smart materials with UCST-type thermoresponsivity, a class of materials that is largely underrepresented because of the limited number of available materials with such behavior.

### ACKNOWLEDGMENTS

The authors thank the Philipps-Universität Marburg for financial support, the group of Prof. Barner-Kowollik (KIT) for the provision of dibenzyltrithiocarbonate, and Anna Fichtner for assisting with preliminary experiments for the RAFT polymerization.

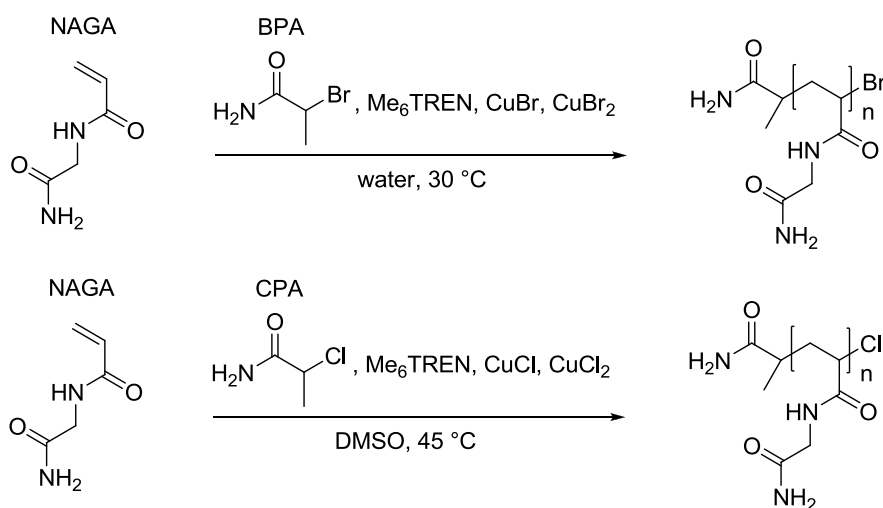
### REFERENCES AND NOTES

- Aseyev, V.; Tenhu, H.; Winnik, F. M. *Adv. Polym. Sci.* **2010**, *242*, 29–89.
- Schulz, D. N.; Pfeiffer, D. G.; Agarwal, P. K.; Larabee, J.; Kaladas, J. J.; Soni, L.; Handwerker, B.; Garner, R. T. *Polymer* **1986**, *27*, 1734–1742.
- Huglin, M. B.; Radwan, M. A. *Polym. Int.* **1991**, *26*, 97–104.
- Chen, L.; Honma, Y.; Mizutani, T.; Liaw, D.; Gong, J. P.; Osada, Y. *Polymer* **2000**, *41*, 141–147.
- Arotcarena, M.; Heise, B.; Ishaya, S.; Laschewsky, A. *J. Am. Chem. Soc.* **2002**, *124*, 3787–3793.
- Virtanen, J.; Arotcarena, M.; Heise, B.; Ishaya, S.; Laschewsky, A.; Tenhu, H. *Langmuir* **2002**, *18*, 5360–5365.
- Aoki, T.; Nakamura, K.; Sanui, K.; Ogata, N.; Kikuchi, A.; Okano, T.; Sakurai, Y. *Proc. Int. Symp. Controlled Release Bioactive Mater.* **1996**, *23*, 767.
- Nagaoka, H.; Ohnishi, N.; Eguchi, M. Thermoresponsive Polymer and Production Method Thereof. U.S. Patent 2007/0203313-A1, August 30, 2007.
- Shimada, N.; Ino, H.; Maie, K.; Nakayama, M.; Kano, A.; Maruyama, A. *Biomacromolecules* **2011**, *12*, 3418–3422.
- (a) Haas, H. C.; Schuler, N. W. *Polym. Lett.* **1964**, *2*, 1095–1096; (b) Haas, H. C.; Moreau, R. D.; Schuler, N. W. *J. Polym. Sci. Part A-2: Polym. Phys.* **1967**, *5*, 915–927; (c) Haas, H. C.; Chiklis, C. K.; Moreau, R. D. *J. Polym. Sci. Part A-1: Polym. Chem.* **1970**, *8*, 1131–1145; (d) Haas, H. C.; MacDonald, R. L.; Schuler, A. N. *J. Polym. Sci. Part A-1: Polym. Chem.* **1970**, *8*, 1213–1226; (e) Haas, H. C.; Manning, M. J.; Mach, M. H. *J. Polym. Sci. Part A-1: Polym. Chem.* **1970**, *8*, 1725–1730; (f) Haas, H. C.; MacDonald, R. L.; Schuler, A. N. *J. Polym. Sci. Part A-1: Polym. Chem.* **1970**, *8*, 3405–3415.
- Marstokk, O.; Nyström, B.; Roots, J. *Macromolecules* **1998**, *31*, 4205–4212.
- Ostrovskii, D.; Jacobsson, P.; Nyström, B.; Marstokk, O.; Kopperud, H. B. M. *Macromolecules* **1999**, *32*, 5552–5560.
- IUPAC. In Compendium of Chemical Terminology, 2nd ed. (the “Gold Book”; compiled by A. D. McNaught and A. Wilkinson); Blackwell Scientific Publications: Oxford, **1997**. XML online corrected version: <http://goldbook.iupac.org> (2006) created by M. Nic, J. Jirat, and B. Kosata; updates compiled by A. Jenkins. ISBN 0-9678550-9-8; doi:10.1351/goldbook.
- Seuring, J.; Frank, F. M.; Huber, K.; Agarwal, S. *Macromolecules* **2012**, *45*, 374–384.
- Feil, H.; Bae, Y. H.; Feijen, J.; Kim, S. W. *Macromolecules* **1993**, *26*, 2496–2500.
- Kunugi, S.; Tada, T.; Yamazaki, Y. *Langmuir* **2000**, *16*, 2042–2044.
- Schild, H. G.; Tirrell, D. A. *J. Phys. Chem.* **1990**, *94*, 4353–4356.
- Mumick, P. S.; Mc Cormick, C. L. *Polym. Eng. Sci.* **1994**, *34*, 1419–1428.
- Ding, Y.; Ye, X.; Zhang, G. *Macromolecules* **2005**, *38*, 904–908.
- Seuring, J.; Agarwal, S. *Macromolecules* **2012**, *45*, 3910–3918.
- Glatzel, S.; Badi, N.; Päch, M.; Laschewsky, A.; Lutz, J. *Chem. Commun.* **2010**, *46*, 4517–4519.
- Handbook of RAFT Polymerization; Barner-Kowollik, C., Ed.; Wiley-VCH: Weinheim, **2008**.
- Wood, M. R.; Duncalf, D. J.; Rannard, S. P.; Perrier, S. *Org. Lett.* **2006**, *8*, 553–556.
- Kurenkov, V. F.; Abramova, L. I. *Polym. Plast. Technol. Eng.* **1992**, *31*, 659–704.
- Wu, X.; Lu, C.; Wu, G.; Zhang, R.; Ling, L. *Fibers Polym.* **2005**, *6*, 103–107.
- Schilli, C.; Lanzendörfer, M. G.; Müller, A. H. E. *Macromolecules* **2002**, *35*, 6819–6827.
- Huber, S.; Hutter, N.; Jordan, R. *Colloid Polym. Sci.* **2008**, *286*, 1653–1661.
- Xia, Y.; Burke, N. A. D.; Stöver, H. D. H. *Macromolecules* **2006**, *39*, 2275–2283.
- Hofmeister, F. *Arch. Exp. Pathol. Pharmacol.* **1888**, *24*, 247–260.
- Zhang, Y.; Furyk, S.; Bergbreiter, D. E.; Cremer, P. S. *J. Am. Chem. Soc.* **2005**, *127*, 14505–14510.
- Zhang, Y.; Cremer, P. S. *Curr. Opin. Chem. Biol.* **2006**, *10*, 658–663.

**Publication 2: Atom transfer radical polymerization as a tool for making poly(*N*-acryloylglycinamide) with molar mass independent UCST-type transitions in water and electrolytes**

**Fangyao Liu, Jan Seuring and Seema Agarwal\***, Atom transfer radical polymerization as a tool for making poly(*N*-acryloylglycinamide) with molar mass independent UCST-type transitions in water and electrolytes, *Polymer Chemistry* **2013**, *4*, 3123-3131.

Reproduced by permission of The Royal Society of Chemistry



Cite this: *Polym. Chem.*, 2013, 4, 3123

## Atom transfer radical polymerization as a tool for making poly(*N*-acryloylglycinamide) with molar mass independent UCST-type transitions in water and electrolytes

Fangyao Liu,<sup>a</sup> Jan Seuring<sup>b</sup> and Seema Agarwal<sup>\*a</sup>

Atom transfer radical polymerization (ATRP) of *N*-acryloylglycinamide has been used as a tool to make poly(NAGA) showing UCST-type phase transitions in water and electrolytes independent of molar mass and end-groups. We hypothesized that similarity in the structure of polymer chain ends with the repeat unit of poly(NAGA) could help in eliminating the effect of molar mass dependence of the cloud point especially in the low molar mass region. The monomer-like end-groups were introduced by choosing an appropriate initiator for ATRP like chloropropionamide (CPA). The catalyst system CuCl/CuCl<sub>2</sub> and tris-[2-(dimethylamino)ethyl]-amine (Me<sub>6</sub>TREN) as a ligand provided controlled polymerization of NAGA in DMSO at 45 °C with UCST-type transitions retained in water and electrolytes without being influenced by chain ends/molar mass and high concentration of salts like NaCl and Na<sub>2</sub>SO<sub>4</sub>.

Received 12th February 2013

Accepted 4th March 2013

DOI: 10.1039/c3py00222e

www.rsc.org/polymers

### Introduction

Poly(*N*-acryloylglycinamide) (poly(NAGA)) is a nonionic polymer showing UCST (upper critical solution temperature)-type transitions in water based on reversible hydrogen bonding.<sup>1</sup> This is one of the few examples of a polymer showing UCST-type phase transitions in water and electrolytes in contrast with many examples known for polymers having LCST (lower critical solution temperature)-type phase transitions. Although the topic of polymers having UCST-type phase transitions especially in water and electrolytes is highly relevant for many applications, unfortunately there are not many examples and the basic studies for such behaviour are missing. A recent review article published in *Macromolecular Rapid Communications* is a good reference to details of existing polymers showing UCST in water.<sup>2</sup> Although poly(NAGA) was first synthesized by Haas and Schuler in 1964 in a water-alcohol mixture with potassium peroxodisulfate as an initiator and showed thermoreversible gel in concentrated aqueous solutions, a UCST-type phase separation remained unnoticed for more than three decades.<sup>3</sup> Recently we carried out detailed studies and showed that the presence of trace amounts of ionic groups introduced unintentionally by either acrylate impurities in the monomer, hydrolysis of the polymer side chains and/or usage of ionic initiators or chain transfer agents could lead to loss of UCST

behavior.<sup>4</sup> The effect of ionic groups on the UCST of poly(NAGA) was extreme because of their strongly exothermic contribution to the enthalpy of mixing, and the enthalpy change of the phase transition is about two orders of magnitude smaller than for most LCST-polymers like, *e.g.*, poly(*N*-isopropylacrylamide) (poly(NiPAAm)).<sup>5–7</sup> Proof of these conclusions along with a procedure to obtain stable aqueous solutions of nonionic poly(NAGA) to exploit UCST in pure water as well as in a physiological milieu was recently published.<sup>4</sup>

Controlled radical polymerization of NAGA by reversible addition fragmentation transfer (RAFT) polymerization reported in ref. 8 was an additional support to our findings.<sup>8</sup> The poly(NAGA) made by RAFT polymerization did not show a UCST in water most probably because an ionic radical initiator (VA-044) and an ionic chain transfer agent (sodium 3-(((benzylthio)carbonothioyl)thio)propane-1-sulfonate) were used. To confirm this fact, we used nonionic radical initiators and nonionic chain transfer agents (CTAs) for RAFT polymerization of NAGA and provided the corresponding polymer with controlled molecular masses without sacrificing the most interesting property, the UCST in water as well as in phosphate buffered saline (PBS) solution.<sup>9</sup> Although poly(NAGA) of different molar masses showed cloud points (measures of UCST-type transitions) in water, end groups had a strong effect on the cloud points with increasing influence towards lower molar masses. The cloud point of poly(NAGA) with molar mass more than 20 000 ( $M_n$  = number average molar mass) was almost the same but increased with a decrease in the molar mass below 20 000. The hydrophobic end groups derived from the CTA caused an upshift of the cloud points with a decrease in molar mass.

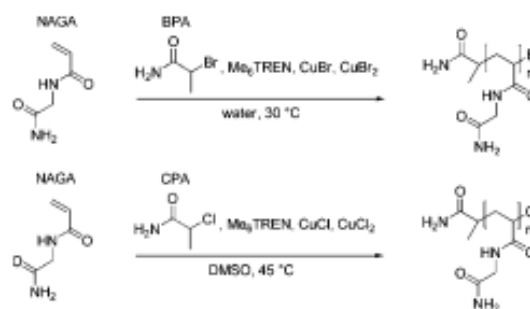
<sup>a</sup>University of Bayreuth, Macromolecular Chemistry II, Bayreuth Center for Colloids and Interfaces, Universitätsstrasse 30, D-95440 Bayreuth, Germany. E-mail: agarwal@uni-bayreuth.de; Fax: +49-921-553393; Tel: +49-921-553397

<sup>b</sup>Fb. Chemie, Philipps-Universität Marburg, D-35032, Germany

We present here controlled radical polymerization of NAGA by atom transfer radical polymerization (ATRP) with an aim to have a system with a cloud point independent of molar mass and ready for end group functionalization, grafting reactions and synthesis of block copolymers for future studies. This will allow the design of smart materials with UCST-type thermoresponsivity, a class of materials that is largely underrepresented due to the limited number of available materials with such behaviour.

We hypothesize that similarity in the structure of polymer chain ends with the repeat unit of poly(NAGA) could help in eliminating the effect of molar mass dependence of the cloud point. This is relatively easy to accomplish in ATRP as compared to RAFT by choosing an appropriate initiator.

In the last decade a lot of progress has been made concerning the ATRP of *N*-substituted acrylamides like poly(diacetoneacrylamide) (poly(DAAM)) or poly(*N*-isopropylacrylamide) (poly(NiPAAM)). Good results could be obtained by employing PMDETA or Me<sub>6</sub>TREN as ligands for the catalyst.<sup>10</sup> However, monomers with a primary amide group remained a problem. Inactivation of the catalyst and displacement of the terminal halogen atom by the nucleophilic nitrogen containing group are some of the side reactions shown for (meth)acrylamides.<sup>11</sup> Acrylamide might be the closest relative to NAGA in the sense that both bear a primary amide as a potential coordination site. Therefore, it is worthwhile to briefly review the important literature related to the ATRP of acrylamide. ATRP of acrylamide in glycerol–water mixtures was studied in 2003 by Jewrajka and Mandal using water soluble halopropionamides as an initiator and CuBr/CuBr<sub>2</sub> with bipyridine ligand as a catalyst.<sup>12</sup> However, even under optimized conditions the PDI (polydispersity index) was high (1.6–1.7). Later improved PDI of about 1.5 was shown by changing to PMDETA as a ligand.<sup>13</sup> In 2008 Lu *et al.* showed PDIs between 1.03 and 1.58 but with low conversions of 8 to 66% after 48 h using *N,N,N',N'*-tetramethylethylenediamine (TMEDA) as a ligand.<sup>14</sup> Further, higher conversions (about 50%) with PDIs of 1.2–1.3 could be achieved by AGET ATRP using chloropropionamide as an initiator, ascorbic acid as a reducing agent and Me<sub>6</sub>TREN as a ligand only at 25 °C.<sup>15</sup> In contrast, higher temperature like 80 °C led to completely uncontrolled polymerizations. In 2011 An and Song claimed a conventional ATRP of acrylamide with both high conversion and very narrow PDIs of around 1.1. They used chloropropionamide/CuCl/CuCl<sub>2</sub>/Me<sub>6</sub>TREN as a catalyst system.<sup>16</sup> Recently Broekhuis and co-workers reported ATRP of acrylamide in water with methyl 2-chloropropionate as an initiator and Me<sub>6</sub>TREN/copper halogenide as a catalyst system at room temperature but obtained good correlation of theoretical and obtained molar mass only for low to medium monomer-initiator ratios but with relatively high polydispersities (1.4–1.8).<sup>17</sup> The continuous efforts to provide controlled polymerization of acrylamide clearly showed it to be a non-trivial system. Finding suitable reaction conditions for ATRP of NAGA, the targeted monomer for the present studies, was still more challenging because there were a number of other restrictions. To date only DMSO and water above the phase transition temperature (cloud point) have been known solvents for poly(NAGA). In water the temperature must not exceed 60 °C for



**Scheme 1** Reaction scheme and optimum conditions observed in this work for the ATRP of *N*-acryloylglycinamide (NAGA) in aqueous media and DMSO.

longer time intervals because even a little hydrolysis of the amide bonds of NAGA drastically changes the thermoresponsive behavior of the resulting polymer. Additionally, the temperature must not drop below the phase transition temperature of the polymer, *e.g.* ~30 °C for a 5 wt% solution to ensure homogeneous dispersion of the polymer chains. At higher concentrations poly(NAGA) can form physically cross-linked thermoreversible gels in water as well as DMSO which is unfavourable for a controlled polymerization. The gel melting temperature increases with polymer concentration, thus forbidding high monomer concentrations that are usually employed in controlled polymerizations in order to minimize side reactions like transfer reactions to the solvent.

In this work we provide controlled polymerization of NAGA in water and DMSO using chloropropionamide (CPA) as an initiator, CuCl/CuCl<sub>2</sub> and Me<sub>6</sub>TREN as a ligand, respectively as evidenced by molar mass control, low polydispersities and chain extension experiments. The resulting polymer showed UCST-type transitions in water and electrolytes independent of molar mass (Scheme 1).

## Experimental section

### Materials

Acrylate free *N*-acryloylglycinamide ( $T_m$ (DSC) = 143 °C, residual potassium < 5 ppm) was synthesized according to the procedure published by us previously.<sup>4</sup> Tris[2-(dimethylamino)ethyl]amine (Me<sub>6</sub>TREN) was synthesized according to the literature.<sup>18</sup> Copper(i) bromide (Aldrich, 98%), copper(ii) bromide (Merck, >98%), copper(i) chloride (Aldrich, 97%), copper(ii) chloride (Aldrich, 99%), 2-bromopropionamide (BPA, Aldrich, 99%), and 2-chloropropionamide (CPA, Aldrich, 98%) were used as received. Solvents were distilled prior to use. Ultra-pure water was obtained from a TKA Micro UV system model 08.1005 (conductivity = 0.06 μS cm<sup>-1</sup>, filtered through a 200 nm filter, UV treated). Phosphate buffered saline was prepared using precalibrated tablets (Aldrich).

### Analytical techniques

<sup>1</sup>H spectra were recorded on a Bruker Avance DRX-500 (500 MHz) in d<sub>6</sub>-DMSO at 100 °C.

Turbidity measurements were performed on a custom-modified Tepper turbidity photometer TP1-D at a wavelength of

670 nm with a cell path length of 10 mm while stirring the solution. The polymer solutions (above phase transition temperature) were filtered through a warm 1.2  $\mu\text{m}$  PET syringe filter before measurement. The heating program started at 60  $^{\circ}\text{C}$  and proceeded *via* cooling to 3.5  $^{\circ}\text{C}$  at a constant rate of 1.0  $^{\circ}\text{C min}^{-1}$  followed by reheating to the starting temperature with the same rate. The inflection point of the transmittance curve was considered as the cloud point. It was graphically determined by the maximum of the first derivative of the heating or cooling curve, respectively. For sample preparation the polymers were weighed into 2 mL polypropylene tubes. The dissolution parameters for poly(NAGA) in phosphate buffered solution (pH 7.4) and salt solutions were:  $c = 1.0 \text{ wt\%}$ ,  $T = 70 \text{ }^{\circ}\text{C}$  inside the tubes,  $t = 90 \text{ min}$ , no sonication. The parameters in pure water were:  $c = 1.0 \text{ wt\%}$ ,  $T = 70 \text{ }^{\circ}\text{C}$  inside the tubes,  $t = 60 \text{ min}$  with sonication. For sonication a heated Bandelin Sonorex RK 102 H ultrasound device (HF power = 120 W, HF peak performance = 480 W, HF frequency = 35 kHz) was used. The samples were diluted to 0.2 wt% and the hot samples were quickly filtered through a preheated 1.2  $\mu\text{m}$  PET-filter into the cuvette.

Molar masses and molar mass distributions of the polymers were determined by gel permeation chromatography (GPC) with dimethyl sulfoxide as eluent. Two PL-Gel Mixed-D columns (particle size 5  $\mu\text{m}$ , dimension 7.5 mm  $\times$  300 mm) calibrated with narrow Pullulan standards and a differential refractive index detector were employed. The flow rate was 1.0  $\text{mL min}^{-1}$ . The molar mass distributions were calculated using the software Cirrus 3.3. The theoretical number-average molar mass  $M_{n,\text{theo}}$  was calculated using eqn (1):

$$M_{n,\text{theo}} = \left[ \frac{c_0(\text{monomer})}{c_0(\text{initiator})} \right] \times x_p \times M_{\text{NAGA}} + M_{\text{initiator}} \quad (1)$$

where  $c_0(\text{monomer})$  and  $c_0(\text{initiator})$  refer to the initial concentrations of the monomer and ATRP initiator, respectively;  $x_p$  denotes monomer conversion,  $M_{\text{NAGA}}$  and  $M_{\text{initiator}}$  are the molar masses of the monomer and ATRP initiator.

#### Example of ATRP of *N*-acryloylglycinamide in water with CuBr as catalyst and BPA as initiator

NAGA (200 mg, 1.57 mmol, 50 eq.) CuBr<sub>2</sub> (7.01 mg, 0.031 mmol, 1 eq.) and Me<sub>6</sub>TREN (16.8  $\mu\text{L}$ , 0.062 mmol, 2 eq.) were dissolved in 3 mL of H<sub>2</sub>O in a nitrogen flask. In another nitrogen flask 2-bromopropionamide (47.7 mg, 0.31 mmol) was dissolved in 10 mL of H<sub>2</sub>O. These solutions were degassed by three freeze-thaw-cycles. CuBr (4.50 mg, 0.031 mmol, 1 eq.) was then added into the monomer solution under an argon atmosphere and it was placed into a preheated oil bath and stirred at 30  $^{\circ}\text{C}$ . Thereafter 2-bromopropionamide solution (0.031 mmol, 1 eq.) was added to the reaction system. It was polymerized at 30  $^{\circ}\text{C}$  for 1 h.

#### Example of ATRP of *N*-acryloylglycinamide in DMSO with CuCl/CuCl<sub>2</sub> as catalyst and CPA as initiator

500 mg of NAGA (50 eq.), 10.5 mg of copper(II) chloride (1 eq.) and 42  $\mu\text{L}$  of Me<sub>6</sub>TREN (2 eq.) were added into a nitrogen-flask and dissolved in 2.10 mL of DMSO. A CPA stock solution with

$c = 16.78 \text{ mg mL}^{-1}$  was prepared separately. Both solutions were degassed by three freeze-pump-thaw cycles. In an argon atmosphere 7.7 mg of CuCl (1 eq.) was added to the monomer solution. The mixture was placed in a preheated oil bath and stirred at 45  $^{\circ}\text{C}$ . Thereafter, 0.5 mL of the stock solution containing 8.39 mg of CPA (1 eq.) was added to the monomer solution.

#### General procedure for the purification and isolation of polymers

The reactions were stopped by air contact. Thereafter, the polymers were precipitated from the 10-fold excess volume of methanol. Subsequent to centrifugation (10 min, 8000 rpm) and decantation, the sediment was thoroughly slurried with methanol using a glass rod. The centrifugation-wash cycles were repeated three times. Subsequently the polymers were dried in a vacuum oven at 70  $^{\circ}\text{C}$  for 24 h.

#### Chain extension of the ATRP polymer in DMSO

In a two-step method of chain extension, first NAGA was polymerized using the ATRP method as described above. The polymer was isolated after 1 h by precipitation in methanol and characterized. In the second step, 150 mg of NAGA (50 eq.), 3.15 mg of CuCl<sub>2</sub> (1 eq.) and 12.5  $\mu\text{L}$  of Me<sub>6</sub>TREN (2 eq.) were dissolved in 0.97 mL of DMSO in a 10 mL nitrogen flask (solution 1). In a second 10 mL nitrogen flask 100 mg poly(NAGA) was dissolved in 1 mL of DMSO (solution 2). Both solutions were degassed by three freeze-pump-thaw cycles. In an argon atmosphere 2.33 mg of CuCl (1 eq.) was added to the monomer solution. The mixture was placed in a preheated oil bath and stirred at 45  $^{\circ}\text{C}$ . Thereafter, 0.9 mL of the stock solution containing 90 mg of CPA (1 eq.) was added to the monomer solution and polymerized for a definite interval of time.

For the *in situ* method, 300 mg of NAGA (50 eq.), 6.3 mg of CuCl<sub>2</sub> (1 eq.) and 25.05  $\mu\text{L}$  of Me<sub>6</sub>TREN (2 eq.) were dissolved in 1.06 mL of DMSO in a 10 mL nitrogen flask (solution 1). In a second 10 mL nitrogen flask 20.16 mg of CPA was dissolved in 2 mL of DMSO (solution 2). In a third 10 mL nitrogen flask 200 mg of NAGA was dissolved in 1.04 mL of DMSO (solution 3). All solutions were degassed by three freeze-pump-thaw-cycles. Thereafter, 64 mg of CuCl (1 eq.) was added to solution 1 under an argon atmosphere and the mixture was placed in a preheated oil bath and stirred at 45  $^{\circ}\text{C}$ . Then 500  $\mu\text{L}$  of solution 2 was added to solution 1 to start the reaction. After 1 h, 0.78 mL was removed from the reaction mixture and the polymer was precipitated in an excess of methanol to obtain 77 mg (57%) of polymer. 0.78 mL of solution 3 containing 25 eq. of NAGA was added to the reaction mixture and it was further stirred for 1 h until the chain extended polymer was precipitated in excess methanol to obtain 150.8 mg (50%) of polymer.

## Results and discussion

### ATRP of NAGA in water

Initial experiments for controlled radical polymerization of NAGA were carried out at 30  $^{\circ}\text{C}$  using a monomer concentration

of 0.39 M (5 wt%) in water. As a catalyst system 2-bromopropionamide (BPA) : CuBr : CuBr<sub>2</sub> : Me<sub>6</sub>TREN was used in the ratio 1 : 1 : 1 : 2 (Table 1). The use of Cu(I) is well known in the literature for providing better control during polymerization.<sup>12,16,19,20</sup>

The polymerization proceeded extremely fast. The reaction conversion was already about 62% after 1 min of reaction time with a polydispersity of 1.29. Further reactions were carried out for different intervals of time. The conversion changed from 62% to 94% on increasing the time of polymerization to 60 minutes with the systematic increase in molar mass but also with an increase in the polydispersity to 1.48 (entries 1–7; Table 1). The fast reaction rate in water was in accordance with the theoretical and experimental observations of free radical polymerization of vinyl monomers like *N,N*-dimethylacrylamide, acrylamide and methacrylamide in the literature.<sup>21–24</sup> This could be attributed to many different factors, such as the existence of a radical-solvent complex, hydrogen bonds between water and the different species involved in the polymerization, conformation of polymer coils *etc.*

Interestingly, a relatively good match was found between the theoretical molar mass and the number average molar mass, although the molar masses determined were not absolute and Pullulan was used as standard for GPC calibration. Also, a molar mass control by changing the monomer : initiator (M : In) ratio was possible (entries 8–10; Table 1; Fig. 1). In a representative reaction for improving the control, the change of the catalyst system from BPA, CuBr and CuBr<sub>2</sub>, to CPA, CuCl and CuCl<sub>2</sub> for a M : In ratio of 50 : 1 did not significantly affect the yield, molar mass or the polydispersity (entry 11; Table 1). A chain extension experiment in water at 30 °C showed an increase in the molar mass but a minor fraction of dead chain ends left as indicated by the shoulder in the GPC elugram (Fig. 2).

#### ATRP of NAGA in DMSO

Further to achieve better control during ATRP of NAGA, reactions were carried out in DMSO at 45 °C using different monomer concentrations and different reaction times using

**Table 1** ATRP of NAGA in water using BPA as an initiator, CuBr/CuBr<sub>2</sub> and Me<sub>6</sub>TREN as a catalyst system. *c*(monomer) = 0.39 M (5 wt%), *T* = 30 °C<sup>a</sup>

Entry	M : In : Cu(I) : Cu(II) : L	<i>t</i> /min	Yield/%	<i>M</i> <sub>n,theor</sub> / g mol <sup>-1</sup>	<i>M</i> <sub>n</sub> (GPC)/ g mol <sup>-1</sup>	PDI
1	50 : 1 : 1 : 1 : 2	1	62	4141	4560	1.29
2	50 : 1 : 1 : 1 : 2	2	69	4600	4610	1.38
3	50 : 1 : 1 : 1 : 2	3	70	4647	4830	1.40
4	50 : 1 : 1 : 1 : 2	4	72	4792	4850	1.49
5	50 : 1 : 1 : 1 : 2	5	73	4813	5010	1.48
6	50 : 1 : 1 : 1 : 2	10	74	4904	5650	1.50
7	50 : 1 : 1 : 1 : 2	60	94	6170	6250	1.48
8	100 : 1 : 1 : 1 : 2	60	88	11427	10600	1.54
9	150 : 1 : 1 : 1 : 2	120	88	17065	16100	1.76
10	200 : 1 : 1 : 1 : 2	180	72	18603	20900	2.88
11	50 : 1 : 1 : 1 : 2 <sup>b</sup>	5	65	4270	4960	1.34

<sup>a</sup> L = ligand, PDI = *M*<sub>w</sub>/*M*<sub>n</sub>. <sup>b</sup> CPA : CuCl : CuCl<sub>2</sub> : Me<sub>6</sub>TREN as a catalyst system.

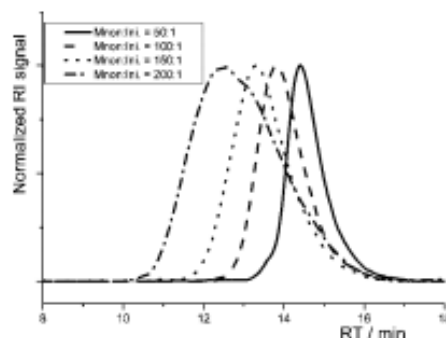


**Fig. 1** GPC elugrams of poly(NAGA) synthesized by ATRP with different monomer : initiator ratios. The polymerization was carried out at 30 °C with a monomer concentration of 0.39 M (5 wt%) in water. As a catalyst system BPA : CuBr : CuBr<sub>2</sub> : Me<sub>6</sub>TREN was used in the ratio 1 : 1 : 1 : 2 (entries 7–10, Table 1).

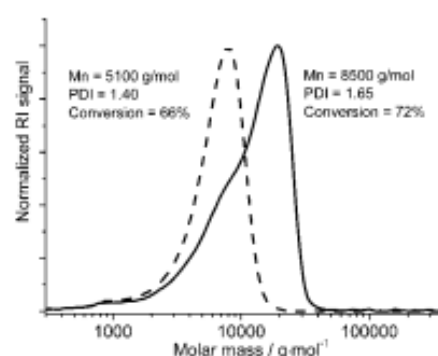


**Fig. 2** The *in situ* chain extension experiment of ATRP in water. The polymerization was carried out at 30 °C with a monomer concentration of 0.39 M (5 wt%) and BPA : CuBr : CuBr<sub>2</sub> : Me<sub>6</sub>TREN = 1 : 1 : 1 : 2 as a catalyst system. Dotted line: polymer before chain extension; solid line: polymer after chain extension (a second batch of NAGA, catalyst and ligand was added and the system was further polymerized for another 5 min).

Me<sub>6</sub>TREN as a ligand, BPA or CPA as an initiator and CuBr/CuBr<sub>2</sub> or CuCl/CuCl<sub>2</sub> as a catalyst, respectively. Compared to aqueous media, the ATRP of NAGA using a BPA/CuBr/CuBr<sub>2</sub>/Me<sub>6</sub>TREN catalyst system in DMSO was slower. A maximum yield of about 21% and 36% was achieved after about 18 h of polymerization time with a moderate polydispersity of 1.32–1.39 for a 1.5 M and 2.5 M solution, respectively (entries 1 and 2; Table 2). There was no significant increase in the yield on increasing the reaction time from 4 h to 18 h and obvious difference in theoretical and observed molar masses was also seen (entries 1–4; Table 2). Based on these preliminary reactions in DMSO and studies in water as described above, a mixed solvent of water and DMSO was used in further reactions. The effect of different reaction parameters, for example, ratio of water : DMSO, type of catalyst and reaction time, was studied in providing controlled ATRP of NAGA. Adding a small amount of water (water : DMSO; 1 : 9 (v/v)) enhanced the rate of polymerization in comparison to the reaction in pure DMSO as measured by the amount of polymer formed (yield was 53% in 4 h; compare entries 4 and 5; Table 2). The yield was already



**Table 2** Comparison of molar mass, yield and polydispersity index of poly(NAGA) made by ATRP under different conditions

Entry	Solvent	Initiator	Temp./°C	Time/h	Conc./M	Yield/%	$M_n$ (GPC)	$M_n$ (Calc.)	PDI
1	DMSO	BPA	45	18.5	2.5	36	3360	2480	1.39
2	DMSO	BPA	45	18.5	1.5	21	2940	1480	1.32
3	DMSO	BPA	45	4	2.5	34	3410	2330	1.28
4	DMSO	BPA	45	4	1.5	17	2800	1160	1.24
5	H <sub>2</sub> O/DMSO 0.1/0.9	BPA	45	4	1.5	53	4870	3550	1.39
6	H <sub>2</sub> O/DMSO 0.1/0.9	BPA	45	1	1.5	38	4290	2550	1.32
7	H <sub>2</sub> O/DMSO 0.1/0.9	CPA	45	1	1.5	65	5540	4270	1.31
8	DMSO	CPA	45	1	1.5	60	4510	3950	1.17
9	DMSO <sup>a</sup>	CPA	45	1	1.5	86	6390	5620	1.33

<sup>a</sup> The catalyst system was: CPA : CuCl : Me<sub>6</sub>TREN (without CuCl<sub>2</sub>).

much higher (38%) after 1 h of reaction time in comparison to the reaction in DMSO (compare entries 4 and 6; Table 2) but the addition of a small amount of water in the reaction medium also led to increased polydispersities and deviation in theoretical and observed molar masses. These experiments clearly showed uncontrolled reactions either in the presence of water or water : DMSO as the reaction medium using BPA/CuBr/CuBr<sub>2</sub>/Me<sub>6</sub>TREN as a catalyst system and slow polymerization in DMSO.

Further change of the initiator system to CPA/CuCl/CuCl<sub>2</sub>/Me<sub>6</sub>TREN for the polymerization of NAGA in water : DMSO showed an interesting effect. Chlor in 2-chloropropionamide (CPA) in contrast to Brom in 2-bromopropionamide (BPA) showed a significant effect, and not only was the rate of polymerization increased (compare entries 6 and 7; Table 2) but a relatively good correlation was seen between the observed and theoretical molar mass with moderate polydispersity (1.31).

This experiment gave us a hint to use a CPA/CuCl/CuCl<sub>2</sub>/Me<sub>6</sub>TREN system in DMSO (without water) for enhancing the

rate of polymerization and getting a controlled ATRP of NAGA. Therefore for further optimizations, polymerizations were carried out in DMSO using CPA as an initiating system. The polymerization of 1.5 M NAGA solution using a CPA/CuCl/CuCl<sub>2</sub>/Me<sub>6</sub>TREN system at 45 °C in 1 h gave a 60% yield which was significantly higher in comparison to the BPA/CuBr/CuBr<sub>2</sub>/Me<sub>6</sub>TREN system (compare entries 4 and 8; Table 2). The resulting poly(NAGA) had a very low polydispersity (1.17) and showed a very good correlation of theoretical and observed molar masses. The <sup>1</sup>H NMR of the resulting polymer is shown in Fig. 3. The same reaction carried out without the addition of CuCl<sub>2</sub> (entry 9; Table 2) showed uncontrolled reaction with increased polydispersity and significant difference in theoretical and observed molar masses.

The polymerization kinetics was further studied in DMSO using optimized conditions of using a CPA/CuCl/CuCl<sub>2</sub>/Me<sub>6</sub>TREN initiating system at 45 °C. Kinetic studies were conducted with M : In ratios of 50 : 1, 200 : 1 and 500 : 1 (Table 3). The monomer concentration was 1.5 M. First-order kinetic plots

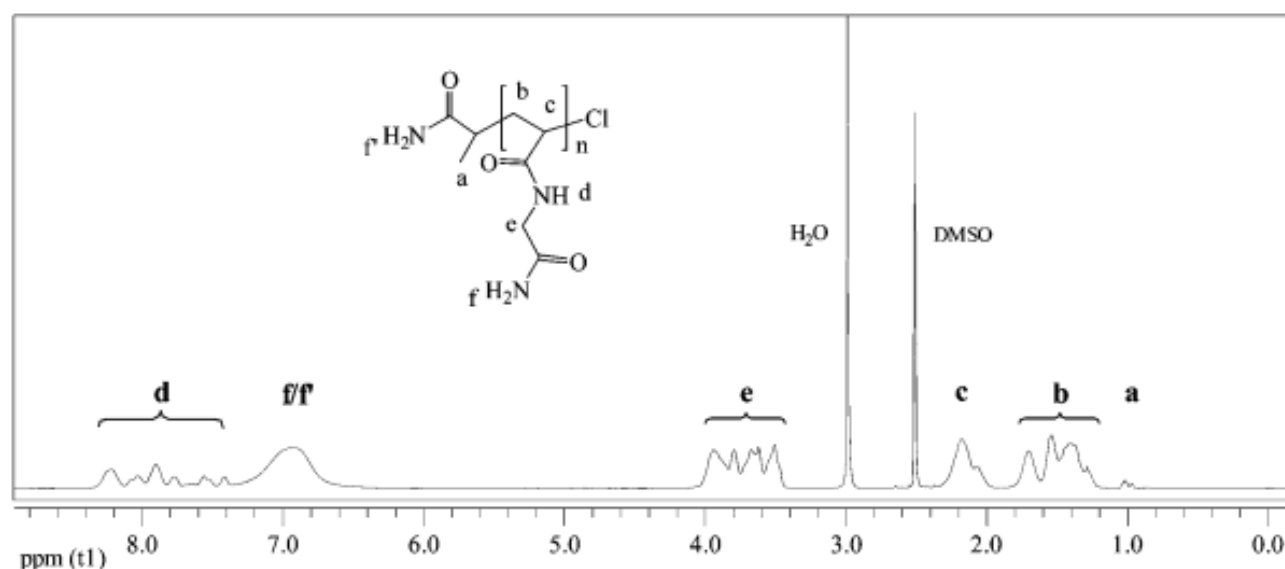


**Fig. 3** <sup>1</sup>H NMR spectrum of poly(NAGA) synthesized by ATRP using a CPA/CuCl/CuCl<sub>2</sub>/Me<sub>6</sub>TREN catalyst system at 45 °C in DMSO. The spectrum was measured in DMSO-d<sub>6</sub> at 100 °C.

**Table 3** ATRP of NAGA with CPA as an initiator, CuCl/CuCl<sub>2</sub> as a catalyst and Me<sub>6</sub>TREN as a ligand at 45 °C for different intervals of time (monomer concentration = 1.5 M)

Entry	M : In : Cu(I) : Cu(II) : L	t/h	Yield/%	$M_{n,theo}/g\ mol^{-1}$	$M_n(GPC)/g\ mol^{-1}$	PDI	Cloud points in PBS/ <sup>a</sup> C <sup>a</sup>	
							Cooling	Heating
1	50 : 1 : 1 : 1 : 2	0.33	36	2405	2740	1.18	n.d. <sup>b</sup>	n.d.
2		0.5	45	2988	3580	1.19	n.d.	n.d.
3		0.67	52	3403	4080	1.20	n.d.	n.d.
4		1	55	3604	4260	1.21	n.d.	n.d.
5		2	63	4133	4570	1.25	n.d.	n.d.
6		4	71	4599	4770	1.26	n.d.	n.d.
7		22	80	5211	4580	1.32	n.d.	n.d.
8	200 : 1 : 1 : 1 : 2	0.17	15	3964	4920	1.22	n.d.	n.d.
9		0.5	29	7522	7730	1.32	8.0	23.4
10		1	38	9911	9600	1.39	7.3	22.5
11		2	41	10756	11280	1.47	7.0	22.0
12		3	43	11186	12280	1.51	7.2	22.1
13		4	45	11823	11700	1.59	7.1	22.1
14		23	49	12563	12000	1.57	7.5	22.1
15	500 : 1 : 1 : 1 : 2	0.5	32	20869	18900	1.48	7.0	21.4
16		1	41	26265	24200	1.40	7.4	21.4
17		2	52	33620	29700	1.49	8.1	22.0
18		3	55	35350	29000	1.65	7.0	21.3
19		4	61	39030	32500	1.66	7.2	22.5
20		23	80	51329	29000	1.95	7.1	22.1

<sup>a</sup> Polymer concentration was 0.2 wt%. <sup>b</sup> Cloud point not determined due to very broad transition.

indicate a constant concentration of polymer chains in the first hour, after which the reaction slowed down (Fig. 4).

The plots for  $M_n$  vs. conversion were fairly linear and the polydispersity was 1.2–1.6. (Fig. 5 and 6) Number average molar masses ( $M_n$ ) agreed with the theoretical molar masses  $M_{n,theo}$  for M : In ratios up to 200 : 1. For higher M : In ratios (for example 500 : 1) although an increase in conversion and molar mass with time was observed, the difference between theoretical and observed molar masses became more at higher conversions with increased polydispersity.

Two different methods of chain extensions were carried out: a two-step method or an *in situ* chain extension procedure. Fig. 7a shows the GPC traces of the two-step approach. In this method, the poly(NAGA) with  $M_n = 4730\ g\ mol^{-1}$  (PDI = 1.20)

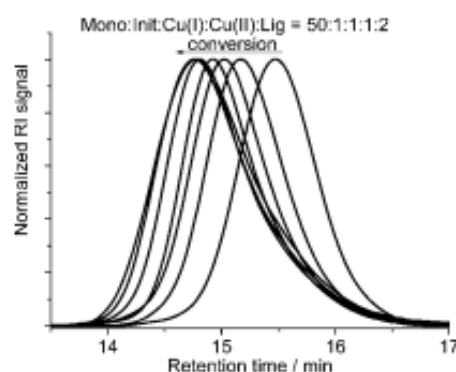


**Fig. 5** GPC elograms of poly(NAGA) synthesized by ATRP using M : In : Cu(I) : Cu(II) : Me<sub>6</sub>TREN in the ratio 50 : 1 : 1 : 1 : 2. Conversion from right to left: 36, 45, 52, 55, 63, 71, and 80%.

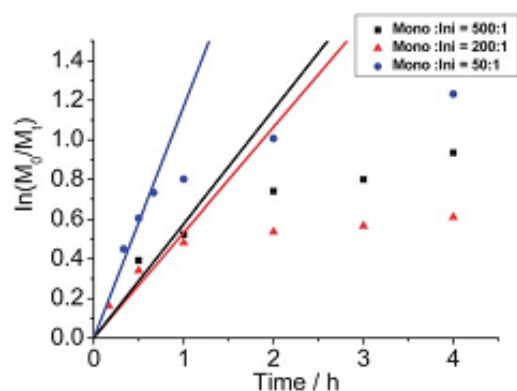


**Fig. 4** First-order kinetic plots of the ATRP of NAGA in DMSO at 45 °C with different M : In ratios. CPA/CuCl/CuCl<sub>2</sub>/Me<sub>6</sub>TREN was chosen as a catalyst system. The monomer concentration was kept constant (1.5 M).

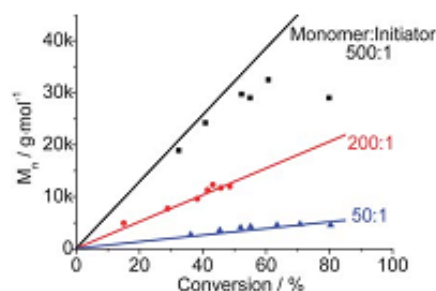


**Fig. 6** Molar masses determined by GPC as a function of conversion for different M : In ratios. CPA/CuCl/CuCl<sub>2</sub>/Me<sub>6</sub>TREN was chosen as a catalyst system. Lines =  $M_{n,theo}$ ; triangles =  $M_n$  (GPC).

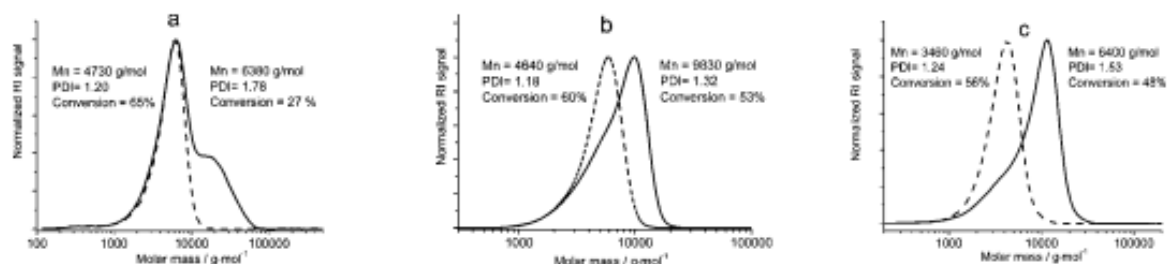


**Fig. 7** GPC traces illustrating the successful chain extension of poly(NAGA) synthesized by ATRP. Dotted line: polymer before chain extension; solid line: polymer after chain extension. (a) Two-step method; (b) *in situ* method, CuCl/CuCl<sub>2</sub> as a catalyst in the second batch; (c) *in situ* method, CuBr and CuBr<sub>2</sub> as a catalyst in the second batch.

was used as a macroinitiator for the polymerization of a second batch of NAGA. The bimodal GPC trace of the extended polymer clearly indicated that the most portion of the macroinitiator poly(NAGA) could not be reinitiated. Similar results were also found in the two-step chain extension experiment of ATRP of acrylamide in aqueous media.<sup>17</sup>

Therefore, an *in situ* method was tried. In this method, a portion of polymerizing NAGA in DMSO using CPA : CuCl : CuCl<sub>2</sub> : Me<sub>6</sub>TREN at 45 °C after 1 h was precipitated in methanol (showed  $M_n = 4640 \text{ g mol}^{-1}$ ; PDI = 1.18) and to the rest of the polymerizing system a second batch of NAGA monomer catalyst and ligand was added. The system was further polymerized for another 1 h. The polymers were precipitated in methanol and dried in a vacuum for further characterization. The polymer obtained after the addition of the second batch of NAGA showed chain extension with  $M_n = 9830 \text{ g mol}^{-1}$  (PDI = 1.32) (Fig. 7b). The extended polymer showed a unimodal but asymmetric GPC trace with a very small shoulder in the low molar mass region. The halogen exchange technique was widely used to improve the macroinitiator efficiency.<sup>25–27</sup> Therefore it was also tried for the poly(NAGA), although we have shown that ATRP of NAGA with a CuBr/CuBr<sub>2</sub> catalyst system in DMSO was slow. Fig. 7c displays the GPC trace of chain extension with an *in situ* method using CuBr and CuBr<sub>2</sub> as a catalyst in the second batch. The very small shoulder in the low molar mass region indicates that part of the polymer could not be extended and results were comparable with that of CPA : CuCl : CuCl<sub>2</sub> : Me<sub>6</sub>TREN. Although we cannot say with certainty, probable reasons could be as reported in the literature for acrylamide like inactivation of the catalyst by complexation of copper by the forming polymer and displacement of the terminal halogen atom by the amide group.<sup>11</sup>

#### Molar mass and end-group dependence of the cloud points of poly(NAGA)

As mentioned in the introduction section, the choice of polymerization conditions for NAGA is highly critical for retaining UCST-type transitions. The poly(NAGA) prepared in this work by ATRP retained this important property in water and PBS buffer. For instance, the sample with  $M_n = 12\,000 \text{ g mol}^{-1}$  (entry 14; Table 3) displayed cloud points in pure water of 12.8 °C upon cooling and 30.3 °C upon heating, respectively. In PBS the cloud

points were 7.5 °C upon cooling and 22.1 °C upon heating. All polymers showed an excellent reversibility of phase transition as shown in Fig. 8 for a sample with  $M_n = 9600 \text{ g mol}^{-1}$ ,  $D = 1.39$  (entry 10; Table 3). The effect of molar mass on cloud points as measured by turbidimetry is shown in Fig. 9. The cloud points were independent of molar mass and polydispersity even in the low molar mass range and were around 7.5 °C upon cooling and 22 °C upon heating. The poly(NAGA)

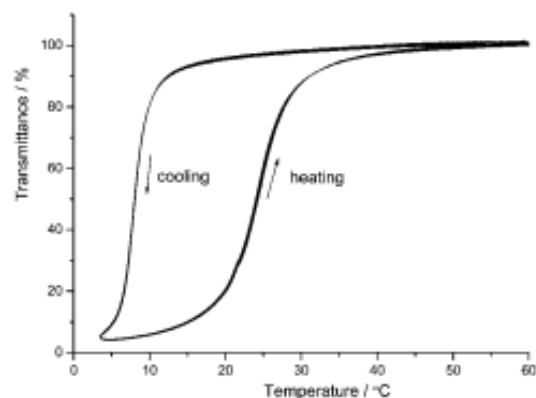


**Fig. 8** Nine consecutive turbidity measurements of poly(NAGA) synthesized by ATRP with a molar mass of  $M_n = 9600 \text{ g mol}^{-1}$ . The concentration was 0.2 wt% in PBS. The heating rate was  $1.0 \text{ °C min}^{-1}$ .

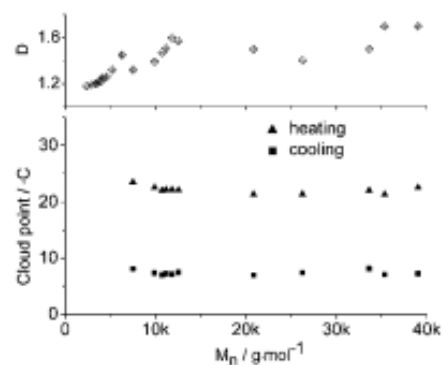


**Fig. 9** Cloud points of poly(NAGA) synthesized by ATRP in DMSO using CPA : CuCl : CuCl<sub>2</sub> : Me<sub>6</sub>TREN as a catalyst system at 45 °C as a function of molar mass.

prepared by RAFT with a hydrophobic dodecyl end-group, however, showed a continuous increase of cloud point when the molar mass was below  $M_n = 15\,000\text{ g mol}^{-1}$ .<sup>9</sup> This proved our hypothesis that the structural similarity between the chain end and the monomer repeat unit is essential to avoid the change of cloud point with the molar mass. For poly(NAGA) oligomers with molar mass below  $5000\text{ g mol}^{-1}$  the broadening of turbidity curves was observed as the polydispersity effect could be more significant for low molar mass chains. Therefore, cloud points could not be determined using a turbidity meter with any accuracy. The efficiency and sharpness of the phase transition were discussed in detail in our previous review article.<sup>2</sup> All polymer chains in solution should have the same phase transition temperature for a sharp cloud point. The increased proportion of chain-ends for low molar mass polymers would provide large dispersity in the phase transition temperature of different chains and hence broadness of turbidity curves (Fig. 10).

Fig. 11 displays the cloud points as a function of ionic strength. Low concentration of sodium chloride or sodium sulfate until 10 mM did not influence the cloud point. Above 10 mM a steady decrease of the cloud point occurred until it vanished at around 500 mM NaCl. In sodium sulfate poly(NAGA) showed a local minimum of the cloud points at around 100 mM  $\text{Na}_2\text{SO}_4$ . Beyond this concentration the cloud point

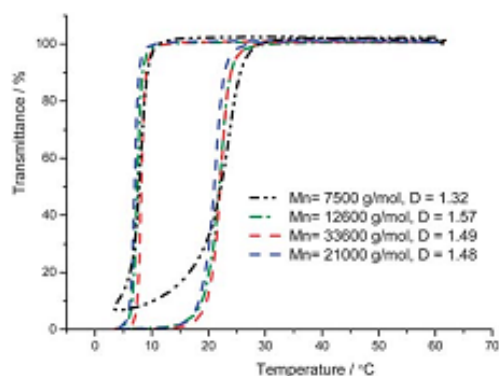


Fig. 10 Influence of the molar mass on the turbidity curve of poly(NAGA).

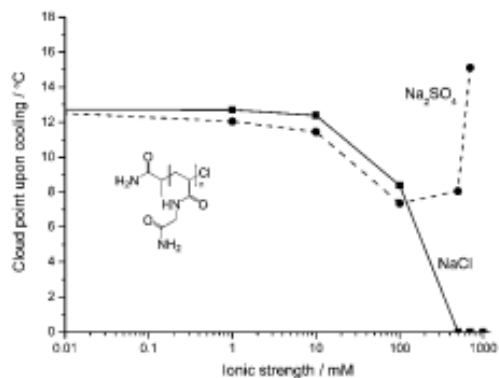


Fig. 11 Cloud points of poly(NAGA) synthesized by ATRP as a function of ionic strength. Here, a cloud point of zero means the polymer was water soluble at 0 °C.

steadily increased. This increase was in agreement with the Hofmeister series of ions.<sup>28</sup> The data presented here showed poly(NAGA) made by ATRP to be a promising candidate for use in biological fluids also. Although the UCST behavior in a real biological system is hard to predict considering the presence of a complex mixture of chaotropic and kosmotropic salts, our previous work showed that the poly(NAGA) prepared by free radical polymerization displays thermosensitivity in human blood serum.<sup>4</sup>

## Conclusions

The aim of making poly(*N*-acryloylglycinamide) (poly(NAGA)) with UCST-type phase transitions in water or electrolytes independent of the molar mass or polydispersity was achieved successfully for the molar masses above  $5000\text{ g mol}^{-1}$ . The molar mass dependence of the cloud point is dominated by the hydrophilicity/hydrophobicity of the polymer end-groups. Choosing monomer-like end-groups (primary amide groups which were introduced by choosing an appropriate initiator for ATRP) provided molar mass independence of the cloud points. Cloud points were retained even in the presence of large amounts of salts like NaCl and  $\text{Na}_2\text{SO}_4$ .

## Notes and references

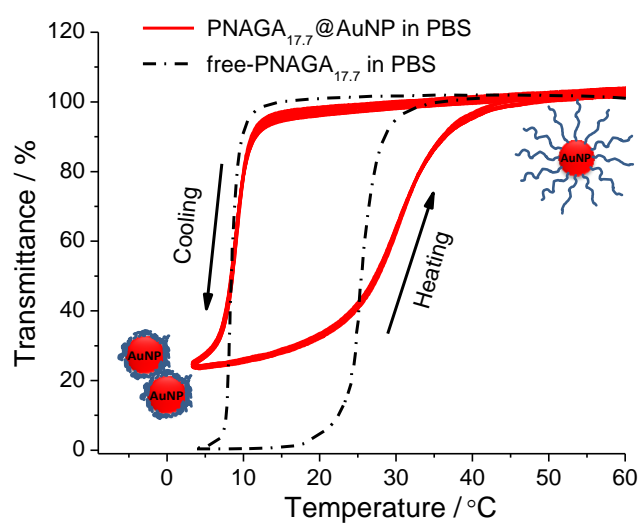
- J. Seuring and S. Agarwal, *Macromol. Chem. Phys.*, 2010, **211**, 2109.
- J. Seuring and S. Agarwal, *Macromol. Rapid Commun.*, 2012, **33**, 1898.
- H. C. Haas and N. W. Schuler, *J. Polym. Sci. Part B: Polym. Lett.*, 1964, **2**, 1095.
- J. Seuring, F. M. Frank, K. Huber and S. Agarwal, *Macromolecules*, 2012, **45**, 374.
- H. G. Schild and D. A. Tirrell, *J. Phys. Chem.*, 1990, **94**, 4353.
- P. S. Mumick and C. L. Mc Cormick, *Polym. Eng. Sci.*, 1994, **34**, 1419.
- Y. Ding, X. Ye and G. Zhang, *Macromolecules*, 2005, **38**, 904.
- S. Glatzel, N. Badi, M. Päch, A. Laschewsky and J. Lutz, *Chem. Commun.*, 2010, **46**, 4517.
- F. Liu, J. Seuring and S. Agarwal, *J. Polym. Sci., Part A: Polym. Chem.*, 2012, **50**, 4920.
- J. Ye and R. Narain, *J. Phys. Chem. B*, 2009, **113**, 676.
- K. Matyjaszewski and J. Xia, *Chem. Rev.*, 2001, **101**, 2921.
- S. K. Jewrajka and B. M. Mandal, *Macromolecules*, 2003, **36**, 311.
- S. K. Jewrajka and B. M. Mandal, *J. Polym. Sci., Part A: Polym. Chem.*, 2004, **42**, 2483.
- J. Jiang, X. Li and Y. Lu, *Polymer*, 2008, **49**, 1770.
- Y. Tan, Q. Yang, D. Sheng, X. Su, K. Xu, C. Song and P. Wang, *e-Polymers*, 2008, 025.
- H. An and C. Song, *Shiyu Huagong Gaodeng Xuexiao Xuebao*, 2011, **24**, 26.
- D. A. Z. Wever, P. Raffa, F. Picchioni and A. A. Broekhuis, *Macromolecules*, 2012, **45**, 4040.
- M. Ciampolini and N. Nardi, *Inorg. Chem.*, 1966, **5**, 41.

- 19 K. Matyjaszewski, Y. Nakagawa and C. B. Jasieczek, *Macromolecules*, 1998, **31**, 1535.
- 20 K. Matyjaszewski, T. E. Patten and J. Xia, *J. Am. Chem. Soc.*, 1997, **119**, 674.
- 21 A. Valdebenito and M. V. Encinas, *Polymer Int.*, 2010, **59**, 1246.
- 22 M. L. Coote, T. P. Davis, B. Klumperman and M. J. Monteiro, *Polym. Rev.*, 1998, **38**, 567.
- 23 S. Beuermann and M. Buback, *Prog. Polym. Sci.*, 2002, **27**, 191.
- 24 B. D. Sterck, R. Vaneerdeweg, F. D. Prez, M. Waroquier and V. V. Speybroeck, *Macromolecules*, 2010, **43**, 827.
- 25 K. Matyjaszewski, D. A. Shipp, J. L. Wang, T. Grimaud and T. E. Patten, *Macromolecules*, 1998, **31**, 6836.
- 26 S. Karanam, H. Goossens, B. Klumperman and P. Lemstra, *Macromolecules*, 2003, **36**, 3051.
- 27 N. K. Singha, S. Rimmer and B. Klumperman, *Eur. Polym. J.*, 2004, **41**, 159.
- 28 F. Hofmeister, *Arch. Exp. Pathol. Pharmacol.*, 1888, **24**, 247.

**Publication 3: Thermoresponsive gold nanoparticles with positive UCST-type thermoresponsivity**

Fangyao Liu and Seema Agarwal\*, Thermoresponsive gold nanoparticles with positive UCST-type thermoresponsivity, *Macromolecular Chemistry and Physics* **2015**, 216, 460-465.

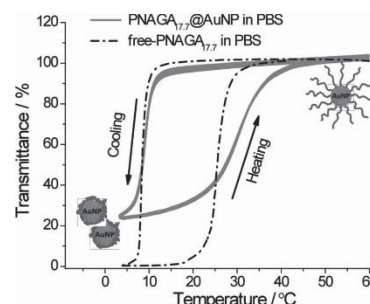
Reprinted with permission; Copyright 2014 John Wiley and Sons



# Thermoresponsive Gold Nanoparticles with Positive UCST-Type Thermoresponsivity

Fangyao Liu, Seema Agarwal\*

Trithiocarbonate end-functionalized poly(*N*-acryloylglycinamide) (PNAGA), synthesized via reversible addition–fragmentation transfer (RAFT) polymerization of different molecular weights, is grafted onto gold nanoparticles (AuNPs) by ligand exchange in phosphate-buffered saline. The PNAGA-grafted AuNPs display upper critical solution temperature (UCST)-type transitions: stable colloidal distribution and aggregation above and below the cloud points, respectively. Cloud points of PNAGA are not affected by the grafting procedure, and PNAGA@AuNPs show similar cloud points as that of the trithiocarbonate end-functionalized free-PNAGAs used for grafting. The UCST-type phase transition is reversible for many cycles. The reversible control of the phase transition is proved by turbidity measurements and UV–vis spectroscopy, as well as by transmission electron microscopy (TEM).



## 1. Introduction

Thermoresponsive polymers have been a topic of intensive research during the past decades due to reversible and fast phase separation from solution by controlling the temperature.<sup>[1–3]</sup> One of the most appealing systems studied intensively is polymers displaying a lower critical solution temperature (LCST)-type phase separation on heating due to change in conformation from coil to the globule. Such polymers are well studied with respect to their synthesis and properties not only as homopolymers but also as copolymers, different macromolecular architectures like star, block grafts, additives, surface modifiers, etc. Both academic and commercial applications have also been shown for LCST polymers like membrane, cell-culture dishes, drug-release etc. making use of smart property (hydrophilicity/hydrophobicity, conformation) changes with temperature.<sup>[4,5]</sup>

The counterpart polymers showing phase separation in water and/or electrolytes on cooling (upper critical solution temperature (UCST)-type transitions) are in contrast not well studied but picking up pace slowly.<sup>[6–8]</sup> Reversible ionic interactions or hydrogen bonding with temperature are mainly responsible for exhibiting UCST-type transitions in water. The most promising are nonionic UCST-polymers based on hydrogen-bonding interactions since the phase transitions are not disturbed by electrolytes under physiological conditions.<sup>[9,10]</sup> Poly(*N*-acryloylglycinamide) (PNAGA) is one of such most studied polymers showing UCST-type phase transition in water and retains this property in electrolyte solution like phosphate-buffered saline (PBS) when synthesized using optimized conditions of proper solvent, nonionic initiator, or chain transfer agent.<sup>[6,9,11–13]</sup> Nonionic polymers showing UCST-type phase transitions are sensitive to ionic impurities introduced during monomer/polymer synthesis, hydrolysis of chain-end /repeat units during polymerization, storage or sample preparation, compositional homogeneity and therefore could lead to either decrease or disappearance of UCST behavior.<sup>[9,14]</sup> The future use of UCST polymers for different applications requires establishment of synthetic methods

F. Liu, Prof. S. Agarwal  
Universität Bayreuth, Macromolecular Chemistry II and  
Bayreuth Center for Colloids and Interfaces, Universitätsstraße  
30, D-95440 Bayreuth, Germany  
E-mail: agarwal@uni-bayreuth.de

for making different macromolecular architectures and grafting procedures of UCST polymers on various surfaces without disturbing the phase-transition temperatures.

Gold nanoparticles (AuNPs) have gained much interest as they exhibit significantly different physical and chemical properties from the bulk solid.<sup>[15]</sup> The optical properties of AuNPs are dependent not only on the size and shape of the nanoparticles but also on the type of polymer grafted on the surface.<sup>[16]</sup> Thermoresponsive polymers of LCST-type have been grafted on AuNPs without losing thermoresponsivity of the corresponding polymers.<sup>[17–22]</sup> The present work reports thermoresponsive AuNPs with positive thermoresponsivity of UCST-type made by grafting-to procedure. Trithiocarbonate chain-end-functionalized PNAGA homopolymers of different molar masses (7000–30 000 g mol<sup>-1</sup>) were grafted onto AuNPs by ligand-exchange reaction without sacrificing the UCST-type phase transitions of the corresponding free-PNAGA. The colloidal stability of AuNPs could be reversibly controlled by temperature providing thermophilic behavior, i.e., stable colloidal solution and aggregation above and below cloud points, respectively. Homogeneously distributed densely packed nanoparticles were observed below cloud point. The concept can be easily transferred to other nonionic UCST polymers and could be highly useful for applications like cellular uptake, separation of nanoparticles by temperature control, transport across membranes, coatings, etc. It is worth mentioning that copolymers of biotin monomer *N*-(3-biotinamide-propyl)-methacrylamide (NBPMA) with *N*-acryloylglycinamide have been utilized by Kondo and co-workers<sup>[23]</sup> for making thermoresponsive magnetic nanoparticles.

## 2. Results and Discussion

Trithiocarbonate end-functionalized PNAGA of different molar masses was utilized for grafting on AuNPs. PNAGA (number-average molar mass ( $M_n$ ) 7100 g mol<sup>-1</sup> (PNAGA<sub>7.1</sub>) and 34 000 g mol<sup>-1</sup> (PNAGA<sub>34.3</sub>)) prepared in our previous work<sup>[12]</sup> were used for ligand-exchange reaction with citrate-stabilized AuNPs in this study. Trithiocarbonate end-functionalized PNAGA with molar mass 17 700 g mol<sup>-1</sup> (PNAGA<sub>17.7</sub>) and PDI of 1.2 was additionally prepared using same literature procedure.<sup>[12]</sup>

All three trithiocarbonate end-functionalized PNAGA samples showed UCST-type phase transitions at physiological pH in PBS electrolyte solution. The cloud points as measured by inflection point of % transmittance versus temperature curves for 0.2 wt% solution were 13.6, 8.1, 9.8 °C, respectively. A slight increase in cloud point of PNAGA with decrease in molar mass was due to the hydrophobic chain-end effect as already described in details in literature.<sup>[12]</sup>

Furthermore, trithiocarbonate chain ends were utilized directly for ligand-exchange reaction with citrate ligands on AuNPs (diameter around 12 nm; please see Figure S1–S3, Supporting Information) in PBS buffer for making PNAGA@AuNPs by grafting-to method as described in the experimental section. Trithiocarbonate is a well-known ligand for AuNPs.<sup>[24–27]</sup> The PNAGA-grafted AuNPs showed UCST-type temperature-dependent reversible colloidal stability at physiological pH in PBS. The temperature-dependent colloidal stability of PNAGA@AuNPs was monitored by measuring % transmittance versus temperature. The cloud points of PNAGA were not affected by grafting procedure and PNAGA@AuNPs showed similar cloud points as that of trithiocarbonate end-functionalized free-PNAGA used for grafting (14.0, 8.3, and 9.0 for PNAGA<sub>7.1</sub>@AuNP, PNAGA<sub>17.7</sub>@AuNP and PNAGA<sub>34.3</sub>@AuNP, respectively, while cooling; Figure 1 and Figure S4 and S5, Supporting

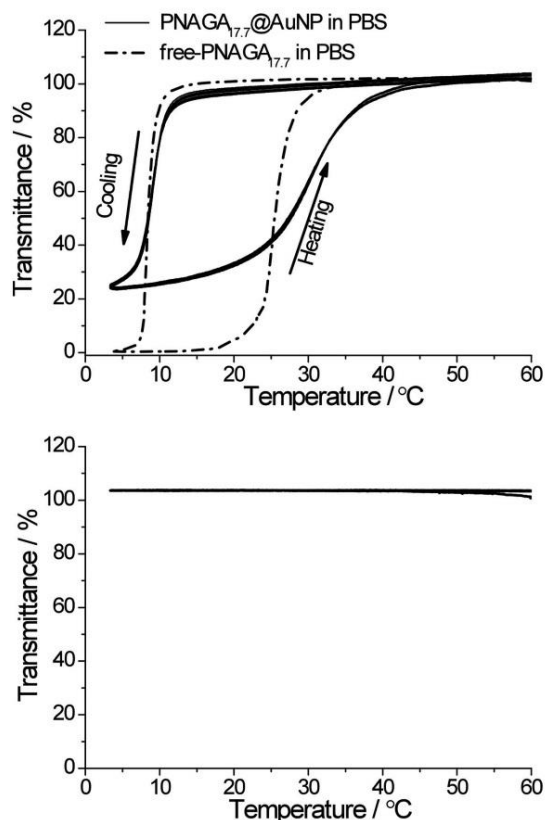


Figure 1. Phase transition behavior of 0.2 wt% solution of PNAGA<sub>17.7</sub>@AuNPs (solid curves) and free-PNAGA<sub>17.7</sub> (dash curves) in PBS buffer. PNAGA<sub>17.7</sub>@AuNPs showed repeated reversible phase transitions at least for nine consecutive times. The supernatant obtained after centrifugation of PNAGA<sub>17.7</sub>@AuNPs for 15 min at 8000 rpm at 45 °C did not show any phase transition behavior confirming absence of free-PNAGA (bottom figure).



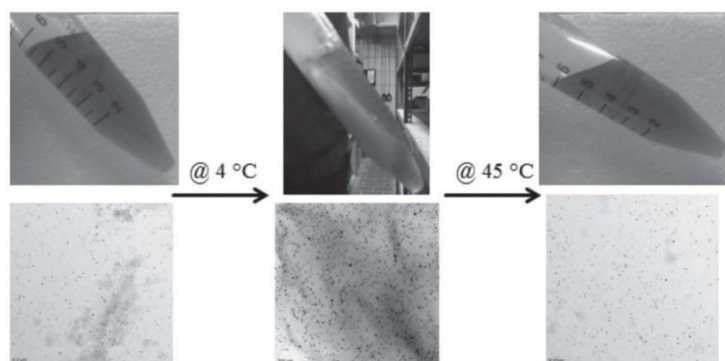


Figure 2. Visual (top row) and TEM pictures (bottom row) of a homogeneous suspension (red) of  $\text{PNAGA}_{7,7}$ @AuNPs and their distribution as seen by TEM above cloud point (left); the precipitated colloidal suspension and densely packed  $\text{PNAGA}_{7,7}$ @AuNPs at 4 °C (below cloud point) (middle); reversibility of phenomenon showing resuspension of precipitated  $\text{PNAGA}_{7,7}$ @AuNPs on heating above cloud point (right).

Information). It is worth noting that only PNAGA grafted on AuNPs was responsible for thermoresponsive behavior. To confirm this point, change of transmittance as a function of temperature for the supernatant from  $\text{PNAGA}$ @AuNP solutions after centrifugation at 45 °C was monitored. It did not show any change in transmittance with temperature thereby confirming the absence of free PNAGA in the sample (Figure 1, bottom).

The  $\text{PNAGA}$ @AuNPs reversibly aggregated and redispersed below and above the cloud points, respectively, as proved by running at least nine heating–cooling cycles during turbidity measurements. The transmission electron microscopy (TEM) images showed no aggregation of  $\text{PNAGA}$ @AuNPs below cloud point (Figure 2). A temperature-dependent packing of AuNPs was observed. Homogeneous distribution of AuNPs was seen both below and above cloud points but with varying interparticle

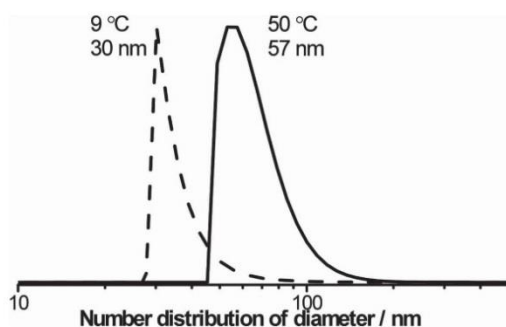


Figure 3. DLS measurement of RAFT  $\text{PNAGA}_{7,7}$ @AuNP in BPS at different temperatures. Number distribution at 9 °C and 50 °C indicated an increase in hydrodynamic radius of AuNPs with increase in temperature. Measurements were carried out after incubation for 5 min at each temperature.

distances. The AuNPs were densely packed below cloud points.

The thermoresponsive behavior of UCST type was also obvious from DLS measurements in which a significant increase in hydrodynamic radius was seen with increase in temperature of  $\text{PNAGA}$ @AuNPs. Above cloud point, the grafted polymer chains in PBS were in extended conformation thereby showing an increased particle size. (Figure 3)

Further, UV–vis characterization of  $\text{PNAGA}$ @AuNPs at room temperature (around 25 °C) showed the surface plasmon resonance peak of AuNPs at 522 nm (Figure 4). The absorption of trithiocarbonate group could be detected at 310 nm only

for  $\text{PNAGA}_{7,1}$ @AuNPs with the smallest molar mass of PNAGA used in the present work. The slight shift of absorption peak of trithiocarbonate can be due to its absorption on the AuNPs.<sup>[28]</sup> The thermoresponsivity of  $\text{PNAGA}$ @AuNPs was also shown by tracing the change in UV–vis spectrum of  $\text{PNAGA}_{17,7}$ @AuNPs in PBS at different temperatures. The surface plasmon band of AuNPs was observed at 522 nm in UV–vis spectrum on cooling a clear solution of  $\text{PNAGA}$ @AuNP from 30 to 9 °C (Figure 5A, B). Further cooling to 3 °C (i.e., a temperature below the cloud point; the cloud point of free  $\text{PNAGA}_{17,7}$ , which was used for grafting was 8.3 °C) led to a shift to a longer-wave length (525.5 nm) of the AuNP absorption peak. The shift of plasmon resonance between 522 and 525.5 nm was reversible with temperature (Figure 5C).

Amine groups are also well-known ligands for AuNPs.<sup>[29–31]</sup> Since PNAGA has amine groups in each repeat unit, a question arises regarding the use of

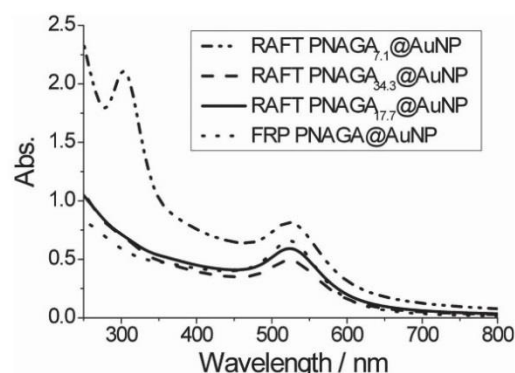


Figure 4. UV–vis spectra of  $\text{PNAGA}$ @AuNPs in PBS.

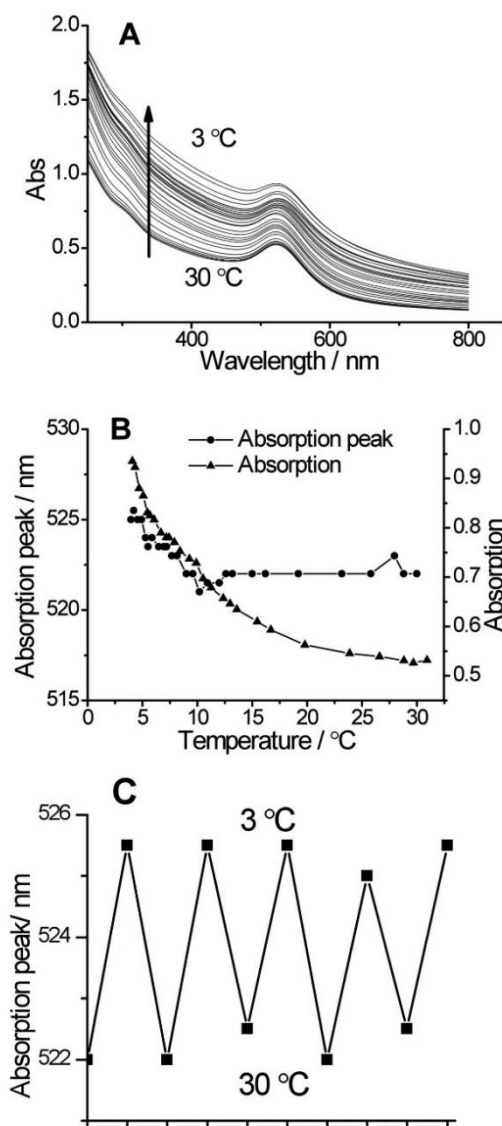


Figure 5. A) UV-vis spectra of  $\text{PNAGA}_{17.7}\text{@AuNPs}$  in PBS at different temperatures; B) Change in the position and intensity of the surface plasmon resonance peak of AuNPs in  $\text{PNAGA}_{17.7}\text{@AuNPs}$  with temperature; C) reversible shift in the position of surface plasmon resonance peak of AuNPs above and below cloud point.

trithiocarbonate end-functionalization for grafting purposes onto AuNPs. To answer this question, an extra experiment was carried out to check the possibility of making  $\text{PNAGA@AuNPs}$  by simply using free radically polymerized PNAGA of molar mass =  $30\,000\text{ g mol}^{-1}$  (designated as  $\text{FRP-PNAGA@AuNP}$ ) instead of

trithiocarbonate functionalized PNAGA. The resulting  $\text{FRP-PNAGA@AuNP}$  system also showed a change in transmittance as a function of temperature as shown in Figure 6. But the centrifugation of the sample ( $\text{FRP-PNAGA@AuNP}$ ) at  $45\text{ }^\circ\text{C}$  led to release of anchored PNAGA as supernatant showed transmittance change with temperature due to the presence of free-PNAGA. In contrast  $\text{PNAGA@AuNP}$  made by trithiocarbonate end-functionalized PNAGA provided highly stable system (Figure 1, right) most probably by having anchoring through both amide and the chain-end groups. This is also evident from cryo-TEM pictures. Grafting-to via only chain-end groups would have provided core (AuNP)-shell (PNAGA) nanoparticles. The cryo-TEM showed a three-dimensional network of polymer anchored to AuNPs with few additional core-shell structures for trithiocarbonate-end-functionalized  $\text{PNAGA@AuNPs}$  (Figure 7).

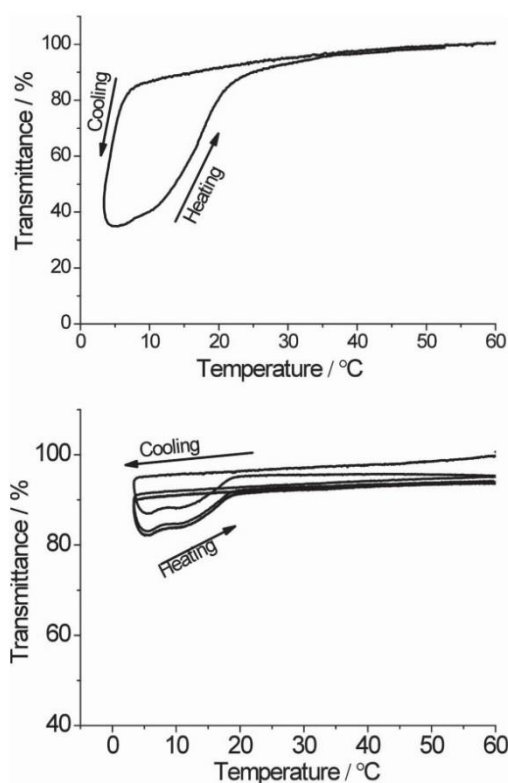


Figure 6. Phase transition behavior of 0.2 wt% solution of  $\text{FRP-PNAGA}_{30.0}\text{@AuNPs}$  in PBS buffer (top). The supernatant obtained after centrifugation of  $\text{PNAGA}_{30.0}\text{@AuNPs}$  for 15 min at 8000 rpm at  $45\text{ }^\circ\text{C}$  showed change in transmittance with temperature showing presence of free-PNAGA and the transition was reversible (bottom).

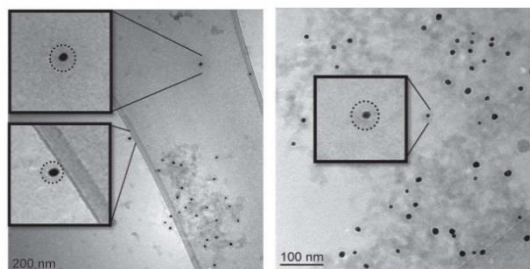


Figure 7. Cryo-TEM of aqueous solution of PNAGA<sub>17,7</sub>@AuNPs.

### 3. Conclusion

We present a simple strategy of preparing thermoresponsive AuNPs showing positive thermoresponsivity of UCST type at physiological pH. The trithiocarbonate chain-end-functionalized UCST-polymer (PNAGA) was used for grafting purposes onto AuNPs. The grafting process had no negative effect on the cloud points and PNAGA@AuNPs showed similar cloud points as that of the corresponding free-NAGA samples used for grafting purposes. The UCST behavior was reversible with temperature for at least nine cycles.

## 4. Experimental Section

### 4.1. Materials

*N*-Acryloylglycinamide (NAGA) was prepared as described in our previous work.<sup>[9]</sup> Hydrogen tetrachloroaurate (III) trihydrate (ACS, 99.99%; Alfa Aesar), tri-sodium citrate dihydrate (p.a., >99.0%; Merck) were used as received. All solvents were distilled before use. Precalibrated tablets from Aldrich were used for making PBS and water was obtained from a MilliQ PLUS (Millipore) apparatus.

### 4.2. Analytical Techniques

Thermoresponsivity was studied by measuring% relative transmittance as a function of temperature (turbidity measurement) using Tepper turbidity photometer TP1-D (wavelength 670 nm, cell path length 10 mm) while stirring the solution. For turbidity measurements, the samples were cooled from 60 to 3.5 °C at a constant rate of 1.0 °C min<sup>-1</sup> followed by reheating to the starting temperature with the same rate. The inflection point of the transmittance curve was considered as the cloud point. It was graphically determined by the maximum of the first derivative of the heating or cooling curve, respectively. UV-vis spectroscopic measurements were performed on JASCO V-630 UV-vis-Spectrophotometer with ETCS-761, a water-cooled peltier-thermostatted cell holder with stirrer.

Molar masses were determined using gel permeation chromatography (GPC) with refractive index (RI) detector. Dimethyl sulfoxide (DMSO) was used as eluent. One PSS PolarSil PSA080505

(particle size 5 μm, 8.0 mm × 50 mm<sup>2</sup>) as precolumn and two PSS PolarSil linear S (particle size 5 μm, 8.0 mm × 300 mm) columns calibrated with narrow Pullulan standards were employed. The flow rate was 0.7 mL min<sup>-1</sup> at a temperature of 75 °C. The software PSS WinGPC Unity, Build 1321 was used for analyzing the spectra.

Dynamic light scattering (DLS) measurements were performed at a scattering angle of 90° on an ALV DLS/SLS-SP 5022F equipment consisting of an ALV-SP 125 laser goniometer, an ALV 5000/E correlator, and an He-Ne laser operating at a wavelength of λ = 632.8 nm. Data processing was performed using the ALV/Static and Dynamic FIT and PLOT 4.23 software.

TEM imaging was performed on a JEM-2100 transmission electron microscope (JEOL, Tokyo, Japan) operated at 80 kV. Images were recorded using a 4000 × 4000 charge-coupled device camera (Ultra Scan 4000; Gatan, Pleasanton, CA) and Gatan Digital Micrograph software (version 1.70.16).

For cryo-TEM, a sample droplet of 2 μL was placed on a lacey carbon-film copper grid (Science Services, München), which was glow discharge for 30 s prior to use. After removing liquid, the grid was shock vitrified by rapid immersion into liquid ethane in a temperature-controlled freezing unit (Zeiss Cryobox, Zeiss NTS GmbH, Oberkochen, Germany). The frozen sample was inserted in a Zeiss EM 922 OMEGA EF-TEM using a cryo-transfer holder at 90 K. Zero-loss filtered images (ΔE = 0 eV) were taken under reduced dose conditions (100–1000 e nm<sup>-2</sup>). Images were registered digitally by a bottom-mounted CCD camera system (Ultrascan 1000, Gatan, München, Germany) combined and processed by Gatan Digital Micrograph 3.10.

### 4.3. General Polymerization Procedure

Free radical and RAFT polymerization of NAGA was performed according to the procedure reported in our previous work using nonionic initiator 2,2'-azobis(4-methoxy-2,4-dimethyl valeronitrile) (V-70) and chain-transfer agent cyanomethyl dodecyl trithiocarbonate (CMDT).<sup>[12]</sup> For a typical RAFT polymerization, 502 mg NAGA (200 eq.) was dissolved in 5.1 mL DMSO containing 0.1 M KSCN, in which 0.5 mL of a chain-transfer agent stock solution containing 6.2 mg CMDT (1 eq.) was added. A V-70 stock solution was prepared separately in the same solvent. Both solutions were degassed three times using freeze and thaw method. Under nitrogen atmosphere, 1 mL of the V-70 stock solution containing 0.5 mg of V-70 (0.08 eq.) was quickly added to the monomer solution. The solution was polymerized for 4 h at 45 °C. The reaction mixture was cooled in ice bath to stop the polymerization. After that the polymer was precipitated from 120 mL methanol. It was purified by three cycles of centrifugation-wash process with methanol. The polymers were structurally characterized using <sup>1</sup>H NMR in DMSO-d<sub>6</sub> at 100 °C. The molar mass was determined using GPC in DMSO and found to be 17 700 g mol<sup>-1</sup> (polydispersity index = 1.2). The <sup>1</sup>H NMR and GPC trace are given in Supporting Information. (Please see Figure S6 and S7, Supporting Information).

<sup>1</sup>H NMR (300 MHz, DMSO-d<sub>6</sub>, T = 100 °C, the DMSO peak was calibrated to δ = 2.50 ppm) 0.9 (alkyl-CH<sub>3</sub>), 1.3 (alkyl), 1.3–1.8 (polymer backbone, -CH<sub>2</sub>-), 1.9–2.3 (polymer backbone, -CH-), 2.3–2.4 (S-CH<sub>2</sub>-alkyl), 3.4 (S-CH<sub>2</sub>-CN) 3.4–4.0 (NH-CH<sub>2</sub>-CONH<sub>2</sub>), 6.5–7.3 (CONH<sub>2</sub>), 7.3–7.4 (CONH-).

Different molecular weight PNAGA samples (7100 and 34 300 g mol<sup>-1</sup>) were also made using similar procedure by changing monomer: CMDT ratio and polymerization time.

#### 4.4. Synthesis of Gold Nanoparticles

The AuNPs were synthesized according to the literature procedure.<sup>[32]</sup> In a typical reaction, 4 mL HAuCl<sub>4</sub> in water (10 × 10<sup>-3</sup> M) solution was diluted with 26 mL water in a 100 mL Erlenmeyer flask and boiled while stirring at 400 rpm. 4.7 mL of 1% trisodium citrate in water was then added to the gold solution. The color of the solution changed in 5 min from light golden yellow to colorless to violet and at the end to red. After that the solution was further heated for additional 10 min and then slowly cooled down. The particles were characterized for shape and size by TEM. The diameter of AuNPs as determined by TEM centered around 12 nm (Figures S1–S3, Supporting Information).

#### 4.5. Synthesis of PNAGA@AuNP via Ligand Exchange

AuNPs were grafted with PNAGA (PNAGA@AuNP) using a ligand-exchange procedure (grafting-to) in PBS electrolyte solution. 1 mL suspension of AuNPs prepared above in water was directly added to 5 mL PNAGA in PBS (2 mg mL<sup>-1</sup>). It was stirred at 45 °C overnight. 45 °C was chosen for overnight stirring as it is well above the cloud point of PNAGA providing access to chain ends for grafting-to reactions. Thereafter, it was centrifuged at 45 °C for 50 min with 8000 rpm. The supernatant was separated and the red sediments (PNAGA@AuNP) were dispersed in 5 mL PBS at 45 °C. This centrifugation-redispersion process was repeated three times for removing ungrafted PNAGA.

### Supporting Information

Supporting Information is available from the Wiley Online Library or from the author.

Acknowledgements: Authors would like to thank Deutsche Forschungsgemeinschaft (DFG) for their financial support.

Received: September 24, 2014; Revised: November 11, 2014;  
Published online: December 18, 2014; DOI: 10.1002/macp.201400497

Keywords: gold nanoparticles; ligand exchange; reversible addition-fragmentation transfer polymerization; upper critical solution temperature

- [1] M. A. C. Stuart, W. T. S. Huck, J. Genzer, M. Müller, C. Ober, M. Stamm, G. B. Sukhorukov, I. Szleifer, V. V. Tsukruk, M. Urban, F. Winnik, S. Zauscher, I. Luzinov, S. Minko, *Nat. Mater.* **2010**, *9*, 101.
- [2] D. Roy, W. L. Brooks, B. S. Sumerlin, *Chem. Soc. Rev.* **2013**, *42*, 7214.
- [3] V. Aseyev, H. Tenhu, F. M. Winnik, *Adv. Polym. Sci.* **2011**, *242*, 29.
- [4] J. Kobayashi, T. Okano, *Sci. Technol. Adv. Mater.* **2010**, *11*, 014111.
- [5] Z. M. O. Rzaev, S. Dinçer, E. Pişkin, *Prog. Polym. Sci.* **2007**, *32*, 534.
- [6] J. Seuring, S. Agarwal, *ACS Macro Lett.* **2013**, *2*, 597.
- [7] H. Zhang, X. Tong, Y. Zhao, *Langmuir* **2014**, *30*, 11433.
- [8] J. Seuring, S. Agarwal, *Macromol. Rapid Commun.* **2012**, *33*, 1898.
- [9] J. Seuring, F. M. Bayer, K. Huber, S. Agarwal, *Macromolecules* **2012**, *45*, 374.
- [10] G. Meiswinkel, H. Ritter, *Macromol. Rapid Commun.* **2013**, *34*, 1026.
- [11] J. Seuring, S. Agarwal, *Macromol. Chem. Phys.* **2010**, *211*, 2109.
- [12] F. Liu, J. Seuring, S. Agarwal, *J. Polym. Sci., Part A: Polym. Chem.* **2012**, *50*, 4920.
- [13] F. Liu, J. Seuring, S. Agarwal, *Polym. Chem.* **2013**, *4*, 3123.
- [14] B. A. Pineda-Contreras, F. Liu, S. Agarwal, *J. Polym. Sci., Part A: Polym. Chem.* **2014**, *52*, 1878.
- [15] M. C. Daniel, D. Astruc, *Chem. Rev.* **2004**, *104*, 293.
- [16] L. Liz-Marzán, *Langmuir* **2006**, *22*, 32.
- [17] M. Q. Zhu, L. Q. Wang, G. J. Exarhos, A. D. Q. Li, *J. Am. Chem. Soc.* **2004**, *126*, 2656.
- [18] C. Boyer, M. R. Whittaker, M. Luzon, T. P. Davis, *Macromolecules* **2009**, *42*, 6917.
- [19] A. Housni, Y. Zhao, *Langmuir* **2010**, *26*, 12933.
- [20] O. J. Cayre, N. Chagneux, S. Biggs, *Soft Matter* **2011**, *7*, 2211.
- [21] S. Salmaso, P. Caliceti, V. Amendola, M. Meneghetti, J. P. Magnusson, G. Pasparakis, C. Alexander, *J. Mater. Chem.* **2009**, *19*, 1608.
- [22] J. Shan, Y. Zhao, N. Granqvist, H. Tenhu, *Macromolecules* **2009**, *42*, 2696.
- [23] N. Ohnishi, H. Furukawa, H. Hideyuki, J.-M. Wang, C.-I. An, E. Fukusaki, K. Kataoka, K. Ueno, A. Kondo, *NanoBiotechnology* **2006**, *2*, 43.
- [24] A. Duwez, P. Guillet, C. Colard, J.-F. Gohy, C.-A. Fustin, *Macromolecules* **2006**, *39*, 2729.
- [25] C.-A. Fustin, C. Colard, M. Filali, P. Guillet, A. Duwez, M. A. R. Meier, U. S. Schubert, J.-F. Gohy, *Langmuir* **2006**, *22*, 6690.
- [26] M. Liang, I. C. Lin, M. R. Whittaker, R. F. Minchin, M. J. Monteiro, I. Toth, *ACS Nano* **2010**, *4*, 403.
- [27] I.-C. Lin, M. Liang, T.-Y. Liu, Z. M. Ziora, M. J. Monteiro, I. Toth, *Biomacromolecules* **2011**, *12*, 1339.
- [28] M. R. Whittaker, M. J. Monteiro, *Langmuir* **2006**, *22*, 9746.
- [29] M. Aslam, L. Fu, M. Su, K. Vijayamohan, V. P. Dravid, *J. Mater. Chem.* **2004**, *14*, 1795.
- [30] Y. Song, Z. Li, L. Wang, Y. Yao, C. Chen, K. Cui, *Microsc. Res. Technol.* **2008**, *71*, 409.
- [31] R. R. Bhat, J. Genzer, *Surf. Sci.* **2005**, *596*, 187.
- [32] A. D. McFarland, C. L. Haynes, C. A. Mirkin, R. P. Van Duyne, H. A. Godwin, S. Road, *J. Chem. Educ.* **2004**, *81*, 544.

Copyright WILEY-VCH Verlag GmbH & Co. KGaA, 69469 Weinheim, Germany, 2014.



## Supporting Information

for *Macromol. Chem. Phys.*, DOI: 10.1002/macp. 201400497

### **Thermoresponsive Gold Nanoparticles with Positive UCST-Type Thermoresponsivity**

Fangyao Liu , Seema Agarwal\*

## Supporting Information

### Thermoresponsive Gold Nanoparticles with Positive Thermoresponsivity of UCST-type

Fangyao Liu and Seema Agarwal \*

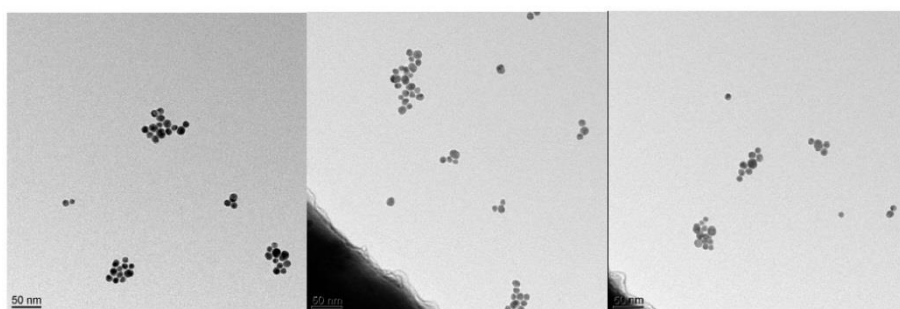


Figure S1. TEM images showing a homogeneous distribution of AuNPs in water.

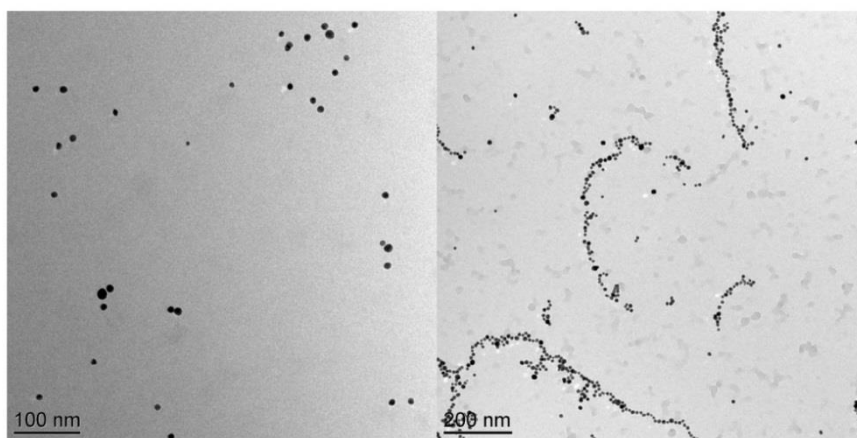


Figure S2 Cryo-TEM of aqueous solution of AuNPs stabilized by citrate ligand.

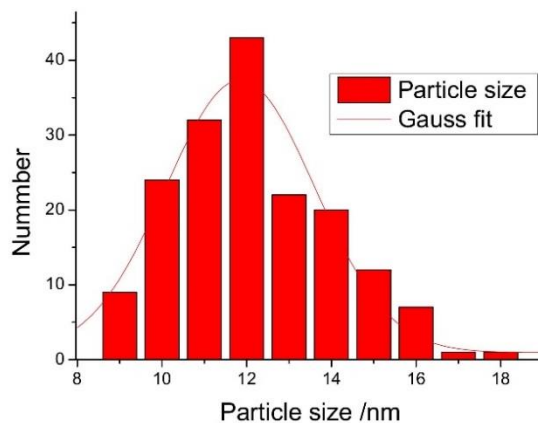


Figure S3. The average AuNP size was about 12 nm and a Gaussian size distribution was seen.

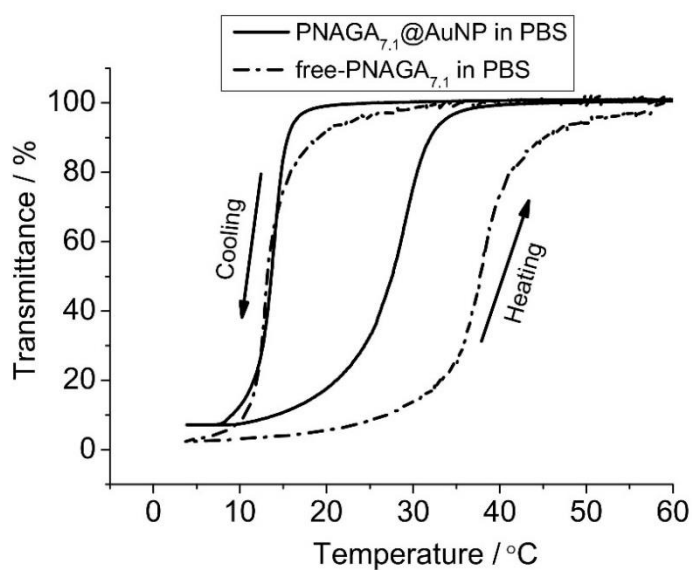


Figure S4. Phase transition behaviour of 0.2 wt% solution of PNAGA<sub>7.1</sub>@AuNPs (solid curves) and free-PNAGA<sub>7.1</sub> (dash curves) in PBS buffer.

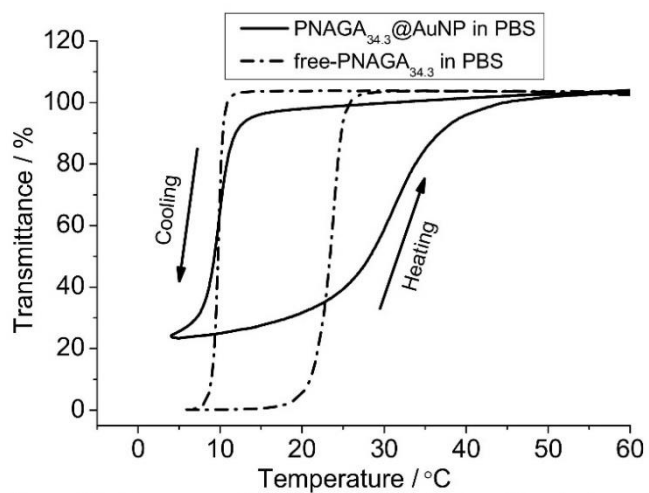


Figure S5. Phase transition behaviour of 0.2 wt% solution of PNAGA<sub>34.3</sub>@AuNPs (solid curves) and free-PNAGA<sub>34.3</sub> (dash curves) in PBS buffer.

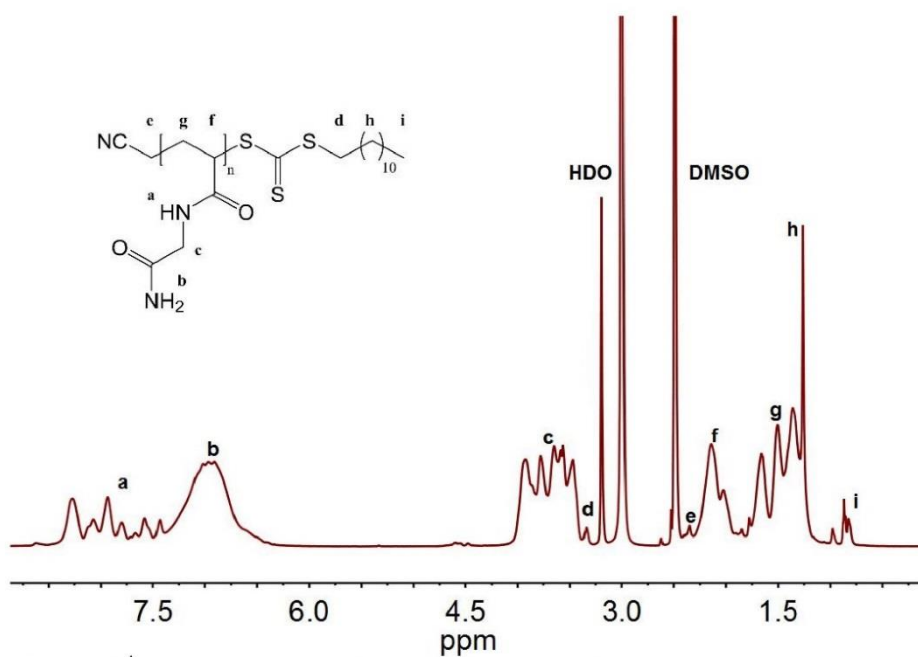


Figure S6. <sup>1</sup>H NMR spectrum of RAFT-PNAGA<sub>17.7</sub>. The spectrum were measured in DMSO-*d*<sub>6</sub> at 100 °C.



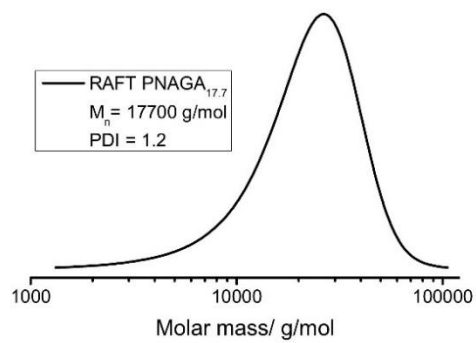
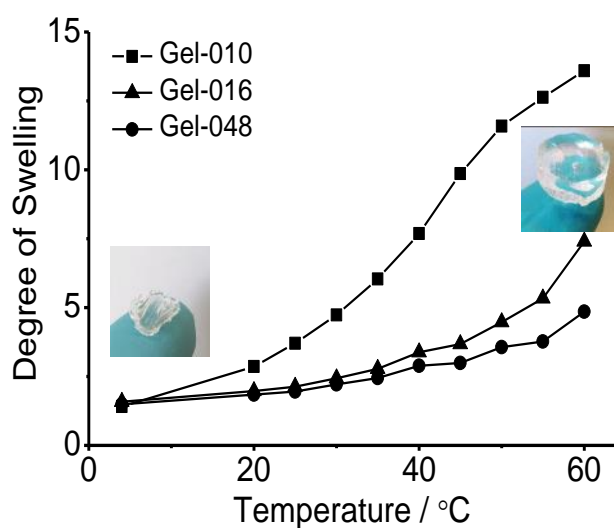


Figure S7. DMSO GPC trace of RAFT-PNAGA<sub>17.7</sub>.

**Publication 4: A non-ionic thermophilic hydrogel with positive thermosensitivity in water and electrolyte solution**

Fangyao Liu, Jan Seuring and Seema Agarwal\*, A non-ionic thermophilic hydrogel with positive thermosensitivity in water and electrolyte solution, *Macromolecular Chemistry and Physics* **2014**, 215, 1466-1472.

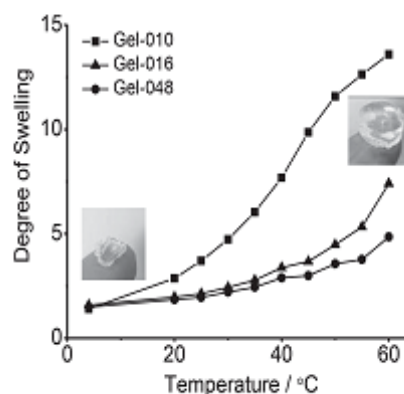
Reprinted with permission; Copyright 2014 John Wiley and Sons



# A Non-ionic Thermophilic Hydrogel with Positive Thermosensitivity in Water and Electrolyte Solution

Fangyao Liu, Jan Seuring, Seema Agarwal\*

The first example of a chemically crosslinked synthetic non-ionic hydrogel showing reversible positive swelling behavior in pure water as well as electrolyte solution is highlighted. Homopolymeric hydrogels are synthesized from *N*-acryloylglycinamide with *N,N'*-methylenebis(acrylamide) as a chemical crosslinker via free radical polymerization in dimethyl sulfoxide (DMSO). The swelling-ratio dependency of the hydrogels upon temperature as well as on the amounts of crosslinker from 1 to 4.8 mol% is studied. With 1 mol% crosslinker, the hydrogel is able to take up over three times water of its weight at 37 °C in pure water and phosphate-buffered saline. All the samples show almost 100% of reversibility for at least 6 d up to 37 °C irrespective of the amount of the crosslinker, making them promising candidates for biomedical applications. The sample with a higher amount of crosslinker, i.e., 4.8 mol% is even stable for over 6 d at 70 °C.



## 1. Introduction

Hydrogels are 3D networks of hydrophilic materials. They are capable of taking up large amounts of water and usually show excellent biocompatibility, which makes them perfect candidates for biochemical and medical applications.<sup>[1–3]</sup> Stimuli-responsive hydrogels have been well investigated as they exhibit volume transitions depending on different external stimuli such as temperature, pH, electric field, or ionic strength.<sup>[4–9]</sup> Among them,

thermoresponsive hydrogels are promising candidates for the on–off release of molecules in biomedical field besides many other applications.<sup>[10]</sup>

The most studied thermoresponsive hydrogels are based on polymers that show a lower critical solution temperature (LCST) in water. Hydrogels made of polymers with an LCST show a negative volume phase transition, i.e., swell below a volume-phase-transition temperature (VPTT) and shrink when this temperature is exceeded. They are also called “thermophobic” hydrogels.<sup>[11]</sup> In contrast, a positive volume phase transition or “thermophilic” hydrogel will swell upon heating, increasing its volume. In this case, the phenomenon is related to the upper critical solution temperature (UCST) of the polymer. This behavior in water is not very common for synthetic polymeric materials, i.e., the examples of such polymers showing UCST in water under practical relevant conditions (0–100 °C) are rare.<sup>[12]</sup> Thermophilic gels are not very well researched and often underrepresented even in review articles dealing with thermoresponsive

F. Liu, Prof. S. Agarwal  
University of Bayreuth, Faculty of Biology, Chemistry and Earth Sciences, Macromolecular Chemistry II and Bayreuth Center for Colloids and Interfaces, Universitätstrasse 30, D-95440 Bayreuth, Germany  
E-mail: agarwal@uni-bayreuth.de  
Dr. J. Seuring  
Böcklerstrasse 8, D-38102 Braunschweig, Germany

hydrogels.<sup>[13,14]</sup> One of the examples of thermophilic hydrogels is based on polysulfobetaines like poly(*N*-(2-methacryloyloxyethyl)-*N,N*-dimethyl-*N*-(3-sulfopropyl)-ammonium betaine) (PDMAAPS) showing reversible positive volume phase transition with temperature as studied by Georgiev et al.<sup>[15]</sup> Ning et al.<sup>[16]</sup> showed very recently a UCST-type transition of chemically crosslinked hydrogels based on zwitterionic sulfobetaine acrylamide.

Acrylamide (AAM)–acrylic acid (AAc)-based systems containing both hydrogen bond donors and acceptors are the most studied examples showing UCST properties/positive volume transition with temperature.<sup>[17–19]</sup> Interpolymer complexation in interpenetrating polymer networks (IPNs) of AAM and AAc led to shrunken state at lower temperatures and swollen state at higher temperatures due to complex dissociation providing a sigmoidal behavior to temperature versus transmittance. Gels made up of random copolymers of PAAc and PAAM, showed monotonical swelling, which increased with increasing temperature. The presence of hydrophobic butyl methacrylate (BMA) was necessary in IPNs for reversible swelling changes as irreversible swelling was observed for IPNs of AAM and AAc.

Nanoparticles and microgels of IPN and random polymers of AAM and AAc made by inverse emulsion polymerization are also studied as thermophilic hydrogels.<sup>[18,20]</sup> Xiao et al.<sup>[21]</sup> showed a temperature-induced volume-phase-transition behavior of the microspheres with PAAM/PAAc IPN shells and poly(AAM-co-St) cores.

IPN composed of poly(*N*-acryloylglycinamide) (PNAGA) and PAAc was also reported in order to modulate the volume-phase-transition temperature.<sup>[22]</sup> PNAGA is an interesting polymer, which has first been synthesized by Haas and Schuler in 1964 by radical polymerization and showed its thermoreversible gelling behavior in concentrated aqueous solutions.<sup>[23]</sup> Very recently, Boustta et al.<sup>[24]</sup> showed the effect of molar mass and concentration on the temperature of the gel–sol transition of PNAGA synthesized by radical polymerization in aqueous medium. The thermoreversible gelation of concentrated PNAGA solutions involves no phase separation since the gel is only one phase with homogeneous properties. UCST-type phase transition of the PNAGA homopolymer for solutions from 0.03 to 5.4 wt% was reported by us for the first time in 2010 followed by studies showing the effect of end-groups and molar mass on UCST-type transitions.<sup>[25–27]</sup>

The present work provides a non-ionic chemically crosslinked gel with positive thermosensitivity made by crosslinking of NAGA with *N,N*-methylenebis(acrylamide) (MBAAM). The volume transitions of the hydrogels were studied in pure water and electrolyte solutions. The effect of equilibration time and the hydrogel size on the volume transition as well as the reversibility

of the volume transition were studied by measuring the swelling ratio. The hydrogels showed almost 100% of reversibility at 37 °C for at least 6 d irrespective of the amount of the crosslinker. The mechanical properties of the hydrogel were characterized by rheological measurements.

## 2. Experimental Section

### 2.1. Materials

Azobisisobutyronitrile (Fluka) was recrystallized from ethanol. *N,N*-methylenebis(acrylamide) (99%; Aldrich) was used as received. Acrylate-free *N*-acryloylglycinamide ( $T_m$ (DSC) = 143 °C, residual potassium <5 ppm) was synthesized according to a recently published procedure.<sup>[28]</sup> Solvents were distilled prior to use. Ultrapure water was obtained from a TKA Micro UV system model 08.1005 (conductivity = 0.06  $\mu$ S  $\text{cm}^{-1}$ , filtered through 200 nm filter, UV treated). Phosphate buffered saline was prepared using precalibrated tablets (Aldrich).

### 2.2. Synthesis of Crosslinked Poly(*N*-acryloylglycinamide) Hydrogels

Gel-016: In a glass test tube, 500 mg of NAGA (3.9 mmol, 1.0 eq) and 9.4 mg of MBAAM (0.06 mmol, 0.016 eq) were dissolved in 1.9 mL of DMSO and purged with argon for 30 min. 100  $\mu$ L of a stock solution containing 3.5 mg AIBN was added and the tube was placed into an oil bath preheated to 70 °C. After 2 h, the tube was quickly cooled to room temperature and the tube was broken to retrieve the polymer gel. The gel was purified by dialysis against deionized water (2 L water, three times exchanged, 4 d).

Gel-048 and Gel-010 were prepared using the similar procedure but using 29.1 mg (0.189 mmol, 0.048 eq) and 6 mg (0.039 mmol, 0.01 eq) of MBAAM, respectively.

For the determination of swelling degree, the gels were cut to obtain bubble free cylinders at room temperature with a diameter of 15 mm and a height of 5 mm.

### 2.3. Swelling Experiments

The gel pieces were incubated in 100 mL water or buffer solution for certain temperatures and time intervals. The degree of swelling  $\alpha$  was determined by carefully removing unbound water with a filter paper and weighing. The degree of swelling was calculated using Equation 1. The dry mass was obtained by drying in vacuum at 65 °C for 4 d.

$$\alpha = \frac{m_{\text{water}}}{m_{\text{polymer}}} = \frac{m_{\text{swollen}} - m_{\text{dry}}}{m_{\text{dry}}} \quad (1)$$

### 2.4. Rheological Measurements

For the rheological characterization, a Bohlin Gemini 200 HR Nano rheometer was utilized. The hydrogel samples were placed

between the parallel plates of the rheometer at controlled temperature. The upper plate (diameter 40 mm) was set at a distance of 1000  $\mu\text{m}$ . A frequency of 1 Hz and a deformation amplitude  $\gamma_0 = 0.2\%$  were selected to ensure that the oscillatory deformation is within the linear regime.

### 3. Results and Discussion

#### 3.1. Thermoresponsive Behavior of Hydrogels

Three types of PNAGA hydrogels were synthesized crosslinked with 0.01 eq (Gel-010), 0.016 eq (Gel-016), and 0.048 eq (Gel-048) MBAAm. The initial experiments were carried out to determine the stability and the equilibration time of gels in water at different temperatures and time intervals (Figure 1). Tests were conducted in pure water at 4, 25, 37, 50, and 70 °C using bubble-free cylindrical samples of 15 mm diameter and 5 mm height.

Most of the samples reached equilibrium swelling after 1 d and were stable over at least 5 d except Gel-016 at 70 °C and Gel-010 at 50 °C, which continuously gained weight. After the temperature treatment, the gels were equilibrated at room temperature (RT) again.

Gel-048 showed excellent stability in the temperature range of 4–70 °C. All samples regained their initial size and weight after stored for 6 d in water. The gels with low cross-link density, i.e., Gel-016 and Gel-010 showed temperature-dependent recovery. The Gel-016 stored at 70 °C and Gel-010 stored at 50 °C showed only partial recovery and puts a limitation to the use temperature (<70 °C for Gel-016 and <50 °C for Gel-010). This could be due to the hydrolysis of amide bonds during equilibration, which is temperature and time dependent. The crucial role of the hydrolysis on the swelling of AAm-based hydrogels is well studied.<sup>[29]</sup>

The swelling ratio of gels was dependent upon temperature and crosslink density (Figure 1). For the same crosslink density, the swelling increased with temperature. The effect of crosslinker on swelling was temperature dependent. At 4 °C, the swelling was almost similar irrespective of the amount of crosslinker but at 37 °C and above (above critical temperature) the gel with the least amount of the crosslinker (gel-010) showed slightly higher swelling. For example, Gel-048 had a degree of swelling of 2.6 at 37 °C, while Gel-010 showed degree of swelling over 3.3, which was almost similar to the water uptake capacity of Gel-048 at 50 °C. Below critical temperature, i.e., at 4 °C, the polymer–polymer interactions are stronger than polymer–solvent interactions leading to almost no change in degree of swelling. Similar results regarding effect of temperature and crosslink density on swelling were observed for dry hydrogels. Before starting measurements, the gels after

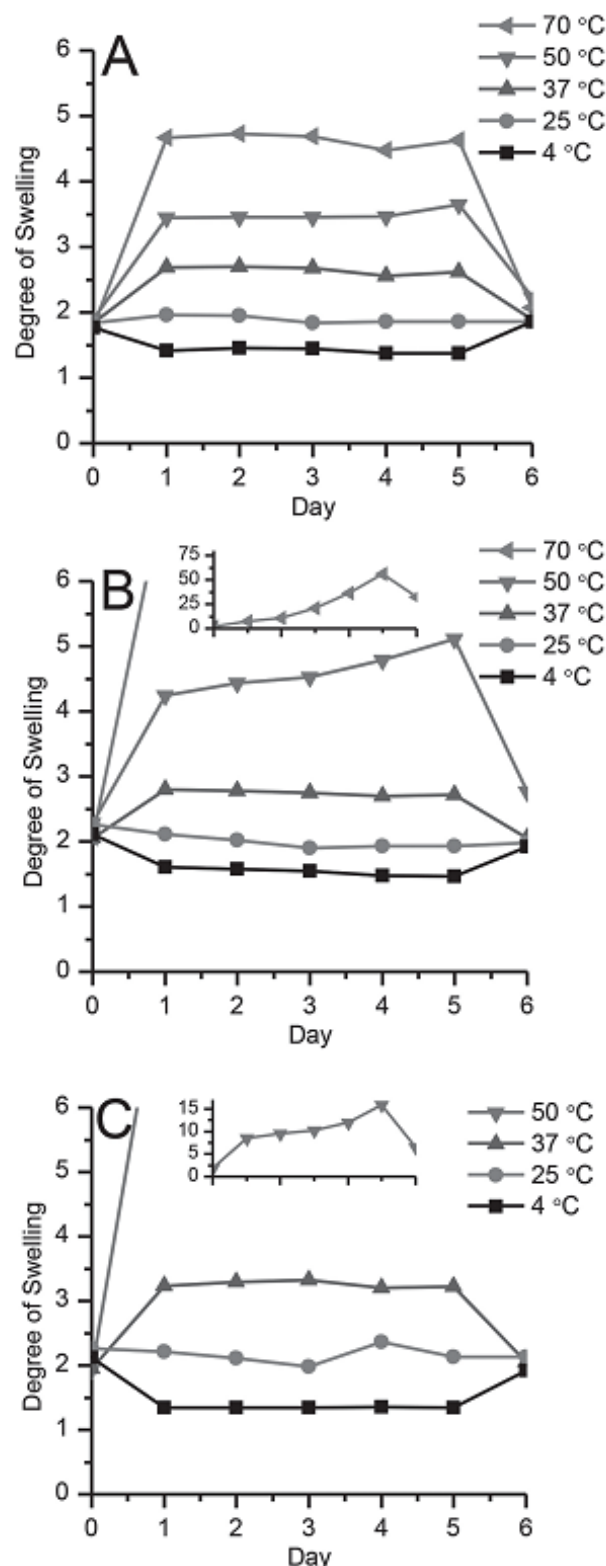


Figure 1. Stability of the PNAGA hydrogels at different temperatures. The initial weight (day zero) and weight after temperature treatment for 6 d was recorded at RT for all gels. A) Gel-048, B) Gel-016, C) Gel-010.

synthesis and purification by dialysis (as described in the experimental part) were dried at 65 °C for 3 d. The gels showed equilibration in 1 d and swelling increased with increase in temperature. The effect of crosslink density on swelling was also marginal and temperature dependent (Figure 2).

### 3.2. Reversibility of the Swelling/Deswelling Process in Water and BPS

The reversibility of the swelling/deswelling process was tested for Gel-048 and Gel-016 by alternate heating and cooling for 1 d at 37 and 4 °C or 70 and 4 °C in pure water. The results over three heating/cooling cycles are shown in Figure 3. When heating was limited to 37 °C, the volume change showed a very good reversibility. When heating up to 70 °C, the process was reversible for 4 d, after which the gels started decomposing in form slowly. Figure 4 presents the swelling/deswelling process of Gel-010. All the samples showed a good reversibility and reproducibility if the temperature does not exceed 40 °C. The degree of swelling at 40 °C was about 4.2 and at 5 °C about 1.5. The gel showed the same swelling/deswelling process even after stored at 5 °C for 40 d.

To see whether the volume change takes place under physiological pH, the reversibility was also analyzed in phosphate buffered saline starting from both swollen gels (Figure 5A) and dry gels (Figure 5B). Degrees of swelling were similar to those in pure water and the swelling–deswelling transitions were reversible. The present system showed obvious advantage in comparison to the polyzwitterionic gels that show irreversible temperature-stimulated swelling–shrinking.<sup>[15]</sup>

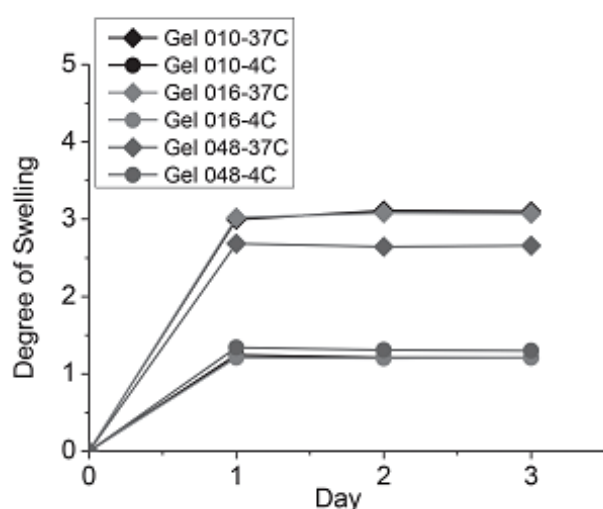


Figure 2. Effect of temperature and degree of crosslinking on swelling characteristics of dry hydrogels. The gels were dried at 65 °C for 3 d before starting the experiment.

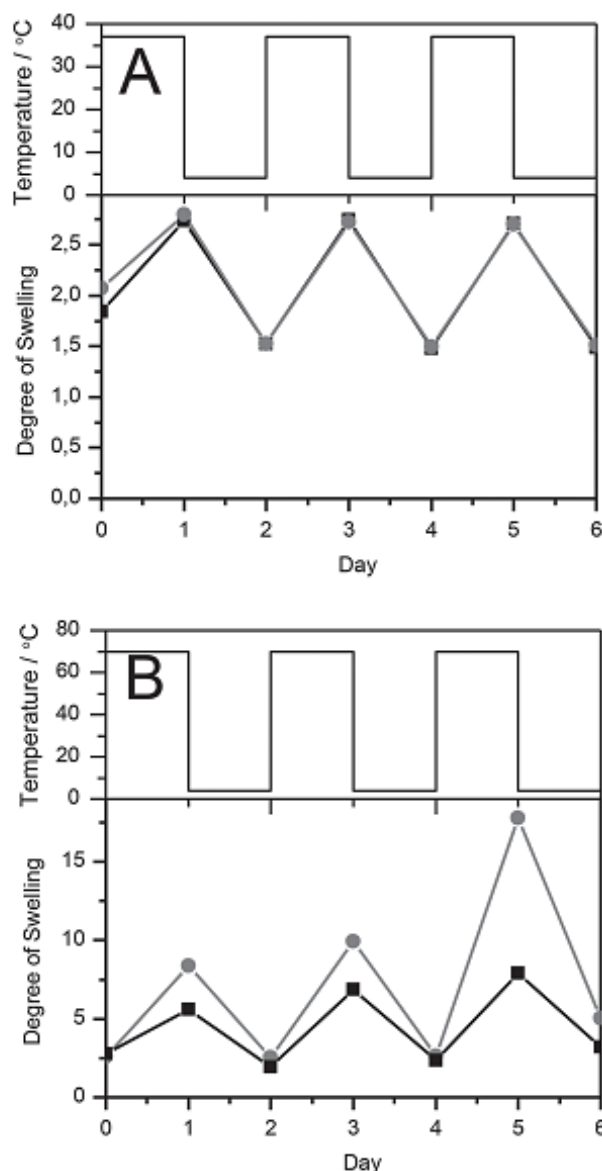


Figure 3. Reversibility of the volume change of samples in water for different temperature profiles. The initial weight (day zero) was recorded at RT for all gels. Red circles = Gel-016, black squares = Gel-048; A = temperature profile 4/37 °C, B = temperature profile 4/70 °C.

### 3.3. Temperature Dependence of Equilibrium Swelling Ratio of Gels

To get a more detailed picture of the temperature dependence of the degree of swelling, the gels were incubated at 4, 20, 25, 30, 35, 40, 45, 50, 55, and 60 °C (Figure 6) for 1 d and weighed. Up to 60 °C, all samples showed thermosensitivity with continuously increase in the degree of swelling with temperature. Similar continuous volume change depending on temperature was also shown by hydrogels of LCST-type based on PNIPAAm<sup>[30]</sup> and UCST-type copolymers

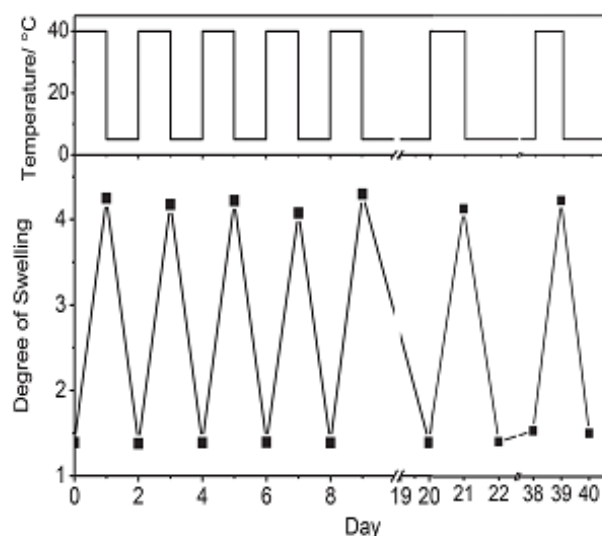


Figure 4. Reversibility of the volume change of Gel-010 sample in water. The initial weight (day zero) was recorded at 4 °C. Temperature profile: 4/40. Between 9–20 and 22–38 d, the hydrogels were placed in water at 5 °C.

and microgels based on PAAm and PAAc copolymers.<sup>[31]</sup> The degree of swelling ranged from 1.5, 1.6, and 1.4 at 4 °C to 4.9, 7.4, and 13.6 at 60 °C for Gel-048, Gel-016, and Gel-010, respectively. Gel-010 with 1 mol% chemical crosslinker showed the highest change in swelling ratio without losing its mechanical stability. The crosslinked gels did not show a sharp discontinuous change in swelling with temperature. They showed a two-phase swelling process with an initial very slow swelling followed by a relatively fast swelling phase. Non-crosslinked PNAGA in solution shows concentration-dependent phase separation behavior and cloud points with a narrow slow dissolution phase followed by a relatively broad fast dissolution phase.<sup>[28]</sup> The Gel-010 showed low degree of swelling till about 20 °C followed by an increase in degree of swelling at higher temperatures. Gels with increased amount of cross-linkers (Gel-016 and Gel-048) showed significant change in degree of swelling only at higher temperatures, i.e., between 40 and 45 °C and also to different extents. The covalent crosslinking of PNAGA would lead to the restricted segmental motion and crosslinked PNAGA segments of varied lengths depending upon the amount of crosslinkers. The sum of contributions of each segment with different length could lead to macroscopically broad and continuous change in swelling with temperature.

Degree of swelling as a function of temperature for hydrogels with different size was studied using gels with diameter of 15 mm and a height of ca. 2.5 mm (250 mg) or 5 mm (500 mg) (Figure 7). The gel samples were equilibrated at different temperatures for 2 d in water and swelling ratio was calculated. Hydrogel size had almost no effect on the degree of swelling and the swelling ratio

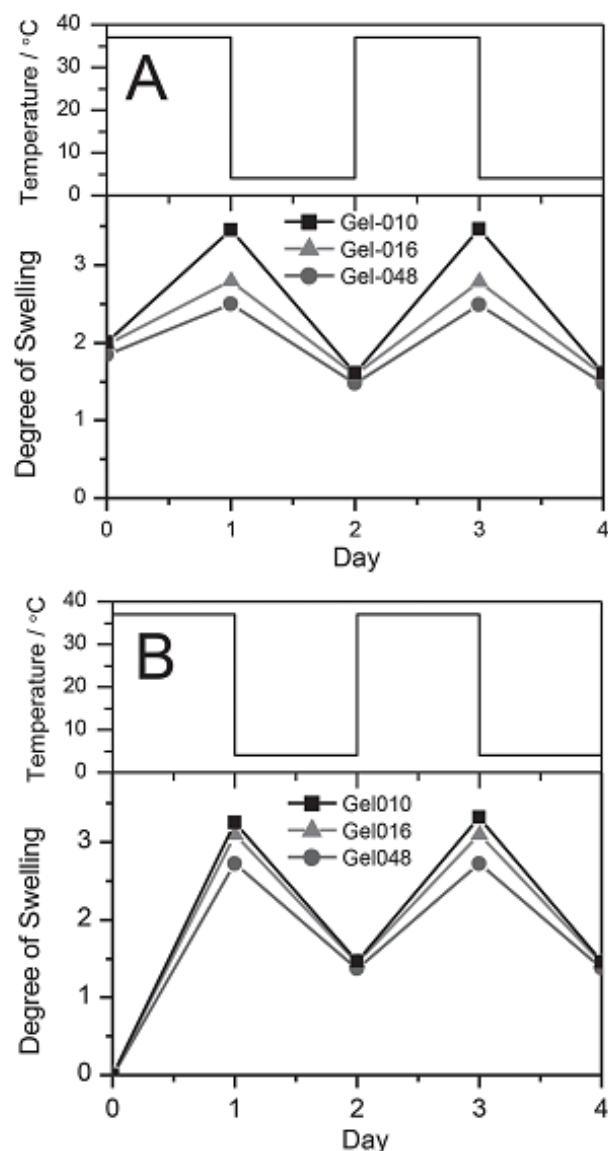


Figure 5. Reversibility of the volume change in phosphate buffered saline. Experiment started A) with already equilibrated gels B) dry gels (dried at 65 °C for 3 d). The initial weight (day zero) was recorded at RT for all gels (squares = Gel-010, triangles = Gel-016 and circles = Gel-048).

decreased from 13 to 1.3 by changing the temperature from 60 to 5 °C.

### 3.4. Rheology Measurements of Crosslinked PNAGA Hydrogels

The mechanical properties of the hydrogels were characterized by rheological analysis. Figure 8 presented the frequency sweep test of sample Gel-010 with 1 mol% crosslinker. The elastic modulus was independent of the frequency and the elastic component ( $G'$ ) was higher than

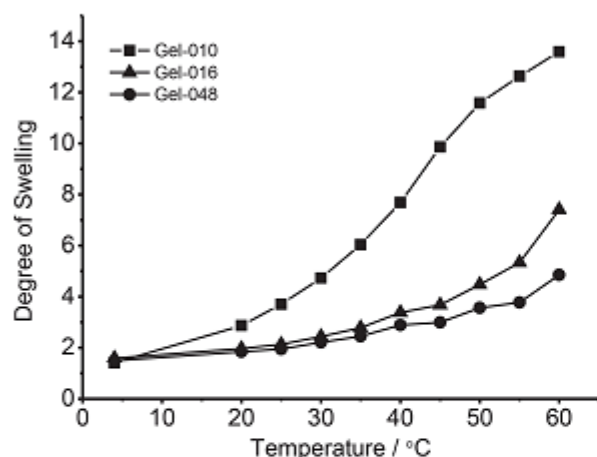


Figure 6. Degree of swelling as a function of temperature for hydrogels with different contents of chemical crosslinkers (squares = Gel-010, triangles = Gel-016, and circles = Gel-048).

the viscous component ( $G''$ ) showing characteristic gel behavior.

The strain sweep test was shown in Figure 9. It was observed that the  $G'$  and  $G''$  present a constant value up to ca. 1% strain, where  $G'$  started to decrease and  $G''$  increased giving rise to a maximum at 6% strain. The  $G'$  is higher than  $G''$  up to 6% of strain. This behavior is known as a weak-strain hardening and is directly related to the energy dissipation due to the breakage of a more complex structure.<sup>[32]</sup>

Figure 10 represented the temperature dependence of the elastic modulus  $G'$ , viscous modulus  $G''$ , and the loss factor  $\tan \delta = G''/G'$  for the sample Gel-010 containing 1 mol% MBAAm as a crosslinker.  $\tan \delta$  showed a significant change between 12 and 20 °C, which might be correlated

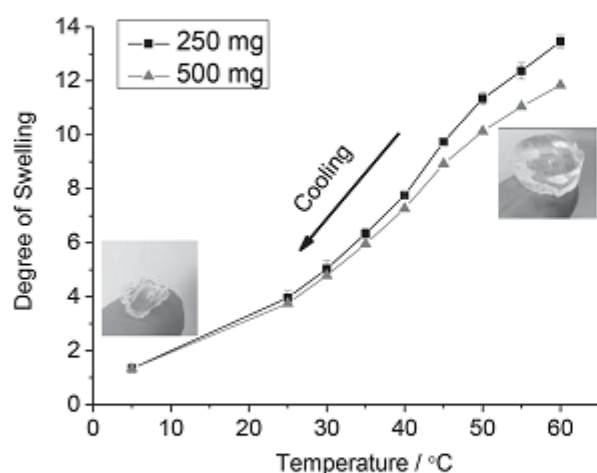


Figure 7. Degree of swelling as a function of temperature for Gel-010 with different sizes. The two samples were equilibrated at each temperature for 2 d. The two pictures of the 250 mg gel sample were taken at 5 °C (left) and at 50 °C (right).

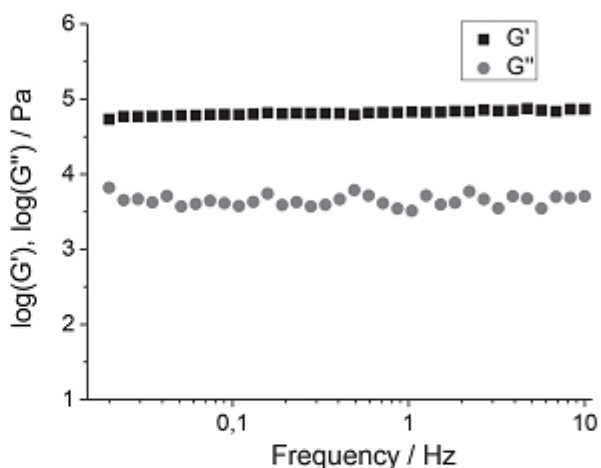


Figure 8. Elastic modulus ( $G'$ ) (squares) and viscous modulus ( $G''$ ) (circles) as a function of frequency of Gel-010 at 25 °C.

to the phase transition of crosslinked PNAGA. In a temperature range between 11 and 50 °C, the  $G' \gg G''$ ,  $\tan \delta < 1$ , indicating the gel was purely elastic.

#### 4. Conclusion

Chemically crosslinked PNAGA hydrogels showed a UCST-type thermosensitivity. At 4 °C, the degree of swelling was about 1.5 for all gels and increased up to 10 at 45 °C (1 mol% crosslinker). At temperatures below 45 °C, the volume change was reversible in pure water as well as in phosphate buffered saline. At higher temperatures, the gels were irreversibly affected by amide hydrolysis. The discontinuous/sigmoidal shape of the swelling curve that

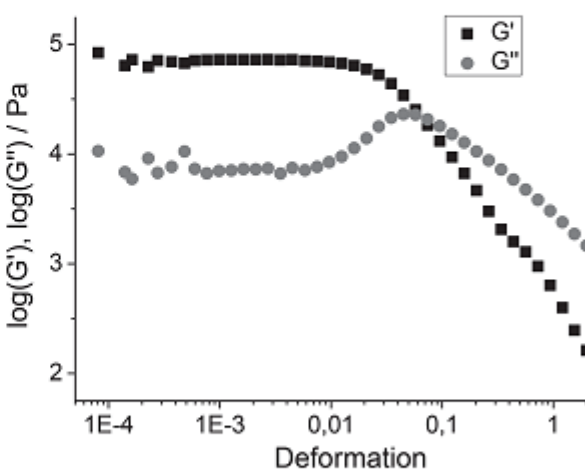


Figure 9. Elastic modulus ( $G'$ ) (squares) and viscous modulus ( $G''$ ) (circles) as a function of deformation of Gel-010 at 25 °C.



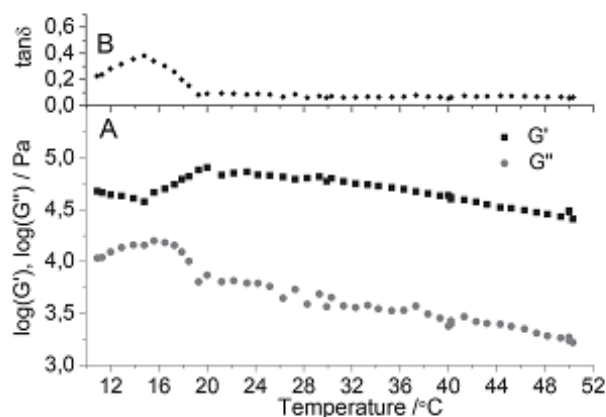


Figure 10. Temperature dependence of: A) the shear moduli  $G'$  and  $G''$  and B) loss factor  $\tan \delta$  of Gel-010 with 1 mol% MBAAm as a crosslinker.

was found for non-ionic hydrogels with LCST-type volume phase transition (e.g., poly(*N*-Isopropylacrylamide hydrogels)) was not evident for PNAGA hydrogels with higher amounts of crosslinker under the experimental conditions of this work. However, with a lower content of crosslinker (1 mol%), the volume change behavior of the gel became more similar to the phase transition of polymer chains but with broad transition. The simple molecular structure and straight forward synthesis make it an attractive candidate for different applications but requires further tuning with respect to sharp volume change with temperature.

**Acknowledgements:** The authors would like to thank Deutsche Forschungsgemeinschaft for their financial support.

Received: March 22, 2014; Revised: May 21, 2014;  
Published online: June 18, 2014; DOI: 10.1002/mcp.201400155

**Keywords:** hydrogels; *N*-acryloylglycinamide; positive volume phase transitions; upper critical solution temperature

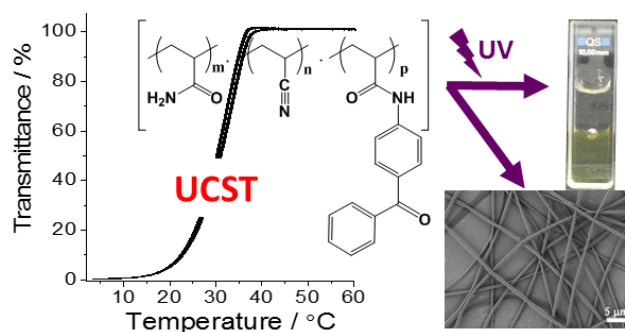
- [1] W. E. Roorda, H. E. Boddé, A. G. De Boer, H. E. Junginger, *Pharm. Weekbl., Sci. Ed.* **1986**, *8*, 165.  
[2] A. S. Hoffman, *Adv. Drug Delivery Rev.* **2002**, *43*, 3.

- [3] N. A. Peppas, J. Z. Hilt, A. Khademhosseini, R. Langer, *Adv. Mater.* **2006**, *18*, 1345.  
[4] M. Yoshida, J.-S. Yang, M. Kumakuru, M. Hagiwara, R. Katakai, *Eur. Polym. J.* **1991**, *27*, 997.  
[5] A. Gutowska, Y. H. Bae, H. Jacobs, J. Feijen, S. W. Kim, *Macromolecules* **1994**, *27*, 4167.  
[6] T. Okano, Y. H. Bae, H. Jacobs, S. W. Kim, *J. Controlled Release* **1990**, *11*, 255.  
[7] T. Okahata, T. Seki, *Macromolecules* **1984**, *17*, 1880.  
[8] S. H. Yuk, S. H. Cho, H. B. Lee, *Pharm. Res.* **1992**, *9*, 955.  
[9] R. A. Siegal, B. A. Firestone, *Macromolecules* **1988**, *21*, 3254.  
[10] L. Klouda, A. G. Mikos, *Eur. J. Pharm. Biopharm.* **2008**, *68*, 34.  
[11] E. Mah, R. Ghosh, *Processes* **2013**, *1*, 238.  
[12] J. Seuring, S. Agarwal, *Macromol. Rapid Commun.* **2012**, *33*, 1898.  
[13] N. Nath, A. Chilkoti, *Adv. Mater.* **2002**, *14*, 1243.  
[14] E. S. Gil, S. M. Hudson, *Prog. Polym. Sci.* **2004**, *29*, 1173.  
[15] G. S. Georgiev, Z. P. Mincheva, V. T. Georgieva, *Macromol. Symp.* **2001**, *164*, 301.  
[16] J. Ning, K. Kubota, G. Li, K. Haraguchi, *React. Funct. Polym.* **2013**, *73*, 969.  
[17] H. Katono, S. Kohei, N. Ogata, T. Okano, Y. Sakurai, *Polym. J.* **1991**, *23*, 1179.  
[18] P. Bouillot, B. Vincent, *Colloid Polym. Sci.* **2000**, *278*, 74.  
[19] H. Katono, A. Maruyama, K. Sanui, N. Ogata, T. Okano, Y. Sakurai, *J. Controlled Release* **1991**, *16*, 215.  
[20] D. E. Owens, Y. Jian, J. E. Fang, B. V. Slaughter, Y.-H. Chen, N. A. Peppas, *Macromolecules* **2007**, *40*, 7306.  
[21] X.-C. Xiao, L.-Y. Chu, W. Chen, J. Zhu, *Polymer* **2005**, *46*, 3199.  
[22] H. Sasase, T. Aoki, H. Katono, K. Sanui, N. Ogata, *Makromol. Chem. Rapid Commun.* **1992**, *13*, 577.  
[23] H. C. Haas, N. W. Schuler, *J. Polym. Sci., Part C: Polym. Lett.* **1964**, *2*, 1095.  
[24] M. Boustta, P.-E. Colombo, S. Lenglet, S. Poujol, M. Vert, *J. Controlled Release* **2014**, *174*, 1.  
[25] J. Seuring, S. Agarwal, *Macromol. Chem. Phys.* **2010**, *211*, 2109.  
[26] F. Liu, J. Seuring, S. Agarwal, *J. Polym. Sci., Part A: Polym. Chem.* **2012**, *50*, 4920.  
[27] F. Liu, J. Seuring, S. Agarwal, *Polym. Chem.* **2013**, *4*, 3123.  
[28] J. Seuring, F. M. Frank, K. Huber, S. Agarwal, *Macromolecules* **2012**, *45*, 374.  
[29] T. Tanaka, D. Fillmore, S. Sun, I. Nishio, G. Swislow, A. Shah, *Phys. Rev. Lett.* **1980**, *45*, 1636.  
[30] G. Kali, S. Vavra, K. László, B. Iván, *Macromolecules* **2013**, *46*, 5337.  
[31] D. Serrano-Ruiz, P. Alonso-Cristobal, M. Laurenti, B. Frick, E. López-Cabarcos, J. Rubio-Retama, *Polymer* **2013**, *54*, 4963.  
[32] C. Echeverria, N. Peppas, C. Mijangos, *Soft Matter* **2012**, *8*, 337.

**Publication 5: Thermophilic films and fibers from photo cross-linkable UCST-type polymers**

**Fangyao Liu**, Shaohua Jiang, Leonid Ionov and Seema Agarwal\*, Thermophilic films and fibers from photo cross-linkable UCST-type polymers, *Polymer Chemistry*. **2015**, DOI: 10.1039/C5PY00109A.

Published by The Royal Society of Chemistry. (Open access article, no permission required)





Cite this: DOI: 10.1039/c5py00109a

## Thermophilic films and fibers from photo cross-linkable UCST-type polymers†

Fangyao Liu,<sup>a</sup> Shaohua Jiang,<sup>a</sup> Leonid Ionov<sup>b</sup> and Seema Agarwal<sup>\*a</sup>

Photo cross-linkable thermoresponsive polymers of UCST-type based on acrylamide (AAm) and acrylonitrile (AN) useful for preparing thermophilic hydrogel films and fibers are presented. The polymers prepared *via* free radical and reversible addition fragmentation chain-transfer (RAFT) polymerization methods using *N*-(4-benzoylphenyl)acrylamide (BPAm) as photo cross-linkable comonomers provided highly stable UCST-type phase transition in water reproducible without hysteresis for many cycles. The cloud point could be manipulated by varying the acrylonitrile amount in the feed. Chemically cross-linked hydrogel films and nanofibers (average diameter 500 nm) were successfully prepared from the ter-co-polymers by solution casting and electrospinning followed by UV irradiation. These hydrogels showed a continuous positive volume transition behavior in water with increasing temperature that was utilized for the design of microactuators.

Received 26th January 2015.  
Accepted 13th February 2015  
DOI: 10.1039/c5py00109a  
www.rsc.org/polymers

### Introduction

Smart polymers are able to change their properties markedly in response to a minor change of environment, for example, magnetic field, pH, temperature, light, salt concentration *etc.* Among them, thermoresponsive polymers attract more and more attention because the temperature can be easily manipulated and the corresponding polymers are extensively applied in biological and medical areas.<sup>1–4</sup> There are two types of thermoresponsive polymers based on the type of phase transition in water. The most widely studied thermoresponsive polymers are of the type showing a lower critical solution temperature (LCST); one of the common examples is poly(*N*-isopropylacrylamide) (PNIPAM). Such polymers are soluble in water at low temperature and precipitated from the solution upon heating above a critical temperature called the cloud point. The corresponding cross-linked polymers are well-studied as thermophobic hydrogels which show a negative volume-phase transition with shrinkage above the critical temperature.<sup>5,6</sup> The other type of thermoresponsive polymer shows an upper critical solution temperature (UCST), *i.e.* it is soluble in water only above the critical temperature.<sup>7,8</sup> The cross-linked UCST-type

polymers show a positive volume-phase transition (thermophilic hydrogels).<sup>9</sup> Examples of thermophilic hydrogels are only a few and mostly based on temperature dependent ionic or hydrogen-bonding interactions in the macromolecular chains.<sup>10</sup> Examples of ionic thermophilic hydrogels are based on cross-linked zwitterionic polysulfobetaines.<sup>11,12</sup> The most studied example of non-ionic thermophilic hydrogels was the interpenetrating polymer networks (IPNs) of acrylamide (AAm) and acrylic acid (AAc).<sup>13,14</sup> Recently two more examples of non-ionic thermoresponsive hydrogels were shown. In one of the studies, Shimada *et al.* provided thermophilic hydrogels based on cross-linked poly(allylurea-*co*-allylamine) copolymers.<sup>15</sup> Poly(allylurea) based copolymers were already known to show UCST-type phase transition under physiological pH and salt conditions.<sup>16,17</sup> In our recent results, we also showed thermophilic behavior of non-ionic chemically cross-linked poly(*N*-acryloylglycinamide) poly(NAGA) with *N,N'*-methylenebis(acrylamide) (MBAAm) in pure water and electrolyte solutions.<sup>9</sup> Homopolymers of NAGA as well as copolymers of AAm and acrylonitrile (AN) prepared *via* free radical polymerization using azobisisobutyronitrile (AIBN) as a non-ionic initiator were shown to be thermoresponsive polymers of UCST-type in our previous studies.<sup>18,19</sup>

In this work we present photo cross-linkable thermoresponsive polymers of UCST-type based on copolymers of AAm and AN. The effect of the polymerization type, cross-linker structure and concentration on thermoresponsive behavior and reproducibility of thermoresponsive transitions was studied. The polymers were processed in the form of films by solution casting and nanofibers by electrospinning and subsequently cross-linked by UV light. The cross-linked films and fibers

<sup>a</sup>University of Bayreuth, Macromolecular Chemistry II and Bayreuth Center for Colloids and Interfaces, Universitätstrasse 30, D-95440 Bayreuth, Germany. E-mail: agarwal@uni-bayreuth.de; Fax: +49-921-553393; Tel: +49-921-553397

<sup>b</sup>Leibniz Institute of Polymer Research Dresden, Hohe Str. 6, D-01069 Dresden, Germany

† Electronic supplementary information (ESI) available: <sup>1</sup>H-NMR of synthesized RAFT poly(AAm-AN-BPA), UV/Vis spectroscopy of RAFT poly(AAm-AN-BPA), as well as turbidity measurements of 0.1 wt% solution of poly(AAm-AN-BPA) made by FRP using V-70 as an initiator. See DOI: 10.1039/c5py00109a



showed thermophilic hydrogel behavior with reversible swelling with change in temperature. The photo cross-linked UCST-polymer-poly(methyl methacrylate) bilayers showed thermoresponsive self-rolling behavior interesting for use in microactuators.

## Experimental part

### Materials

Acrylamide (AAM, electrophoresis grade,  $\geq 99\%$ , Sigma), acrylonitrile (AN, 99+%, Acros Organics), cyanomethyl dodecyl trithiocarbonate (CMDT, 98%, Aldrich) and 2,2'-azobis(4-methoxy-2,4-dimethyl valeronitrile) (V-70, 96%, Wako) were used as received. Azobisisobutyronitrile (AIBN, 98%, Fluka) was recrystallized from ethanol. 4-Acryloyloxybenzophenone (BPA) was synthesized according to the literature.<sup>20</sup> *N*-(4-Benzoylphenyl)acrylamide (BPAm) was prepared as described in the literature.<sup>21</sup> All solvents were distilled before use. Water was obtained from a MilliQ Plus (Millipore) apparatus.

### Analytical techniques

Thermoresponsivity was studied by measuring relative transmittance as a function of temperature (turbidity measurement) using a TP1-D Tepper turbidity photometer (wavelength 670 nm, cell path length 10 mm) while stirring the solution. For turbidity measurements the samples were cooled from 60 °C to 3.5 °C at a constant rate of 1.0 °C min<sup>-1</sup> followed by reheating to the starting temperature with the same rate. The inflection point of the transmittance curve was considered as the cloud point. It was graphically determined by the maximum of the first derivative of the heating or the cooling curve, respectively. Fiber mat transmittance measurements were performed on a JASCO V-630 UV/Vis-Spectrophotometer with ETCS-761, a water-cooled Peltier thermostatted cell holder with a stirrer. The wavelength was 670 nm. UV treatment was performed on UVAHAND 250 GS, a high-intensity ultra-violet lamp. The UV radiation spectra emitted by the UV lamp were between 320 and 390 nm (wavelength). The respective radiation intensity was about 15 mW cm<sup>-2</sup>. Molar masses and molar mass distributions of the polymers were determined by gel permeation chromatography (GPC) using dimethyl sulfoxide as the eluent. Two PSS PolarSil linear S columns (particle size 5  $\mu$ m, dimension 8 mm  $\times$  300 mm) calibrated using narrow pullulan standards and a differential refractive index detector were employed. The flow rate was 0.7 mL min<sup>-1</sup>. The molar mass distributions were calculated using the software WinGPC Unity.

A scanning electron microscope (SEM, Zeiss LEO 1530, EHT = 3 kV) was used to observe the surface morphology. The fiber diameter was measured by using Image J software. The average fiber diameter was determined statistically by measuring 100 fibers from 5 SEM photos. The samples for SEM were sputter-coated with platinum of 3.0 nm prior to scanning. The thickness and the area of the mat were observed and measured using an optical microscope (VHX 2000).

### General polymerization procedure

In a typical polymerization, 5.112 g AAM (90 eq.), 419  $\mu$ L AN (8 eq.) and 402 mg BPAm (2 eq.) were dissolved in 70 mL distilled DMSO in a 250 mL Schlenk flask. It was degassed using three freeze-pump-thaw cycles. Under nitrogen gas, 37 mg V-70 (0.15 eq.) was added to the reaction mixture. The mixture was placed in a preheated oil bath and stirred for 5.5 h at 45 °C. The reaction was stopped by cooling in liquid nitrogen and air contact. The polymers were precipitated from 800 mL methanol. It was filtered and washed with methanol. Subsequently it was dried in the vacuum oven at 70 °C for 24 h to obtain a powdery white polymer.

<sup>1</sup>H NMR (300 MHz,  $\delta$ /ppm, DMSO-*d*<sub>6</sub>, the DMSO peak was calibrated to  $\delta$  = 2.50 ppm) 1.1–1.8 (polymer backbone, -CH<sub>2</sub>-), 1.9–2.3 (polymer backbone, -CH-), 6.5–7.5 (CONH<sub>2</sub>, CONH- and aromatic H).

A similar procedure was used for making copolymers of AAM and AN with BPA *via* FRP using AIBN as an initiator and RAFT polymerization with V-70 and AIBN, where CMDT as a chain transfer agent was added together with monomers.

### Determination of swelling ratio

The 2 mm thick films were prepared by solution casting from 15 wt% solution in DMSO. The dry films were illuminated with UV light of wavelength 320–390 nm for 16 h. After UV treatment the films were cut into circles with a diameter of about 20 mm. The films were placed in water at a defined temperature for different time intervals. Thereafter, the samples were taken out and dried carefully using filter paper to remove the unbound solvent. The swelling ratio was calculated using formula (1).

$$\alpha = \frac{m_{\text{water}}}{m_{\text{polymer}}} = \frac{m_{\text{swollen}} - m_{\text{dry}}}{m_{\text{dry}}} \quad (1)$$

where  $m_{\text{swollen}}$  is the mass of the sample after immersion in water and  $m_{\text{dry}}$  is the mass of the original dry sample.

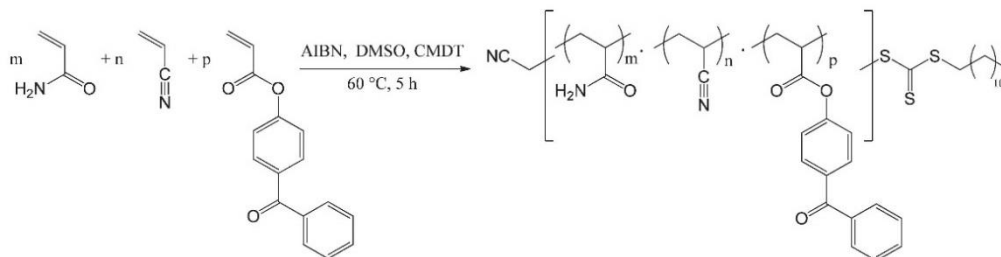
### Formation of nanofibers by electrospinning

The solution for electrospinning was prepared by dissolving 1.0 g of polymer into the mixture of solvents (1.0 g distilled water and 1.0 g of DMSO). The conventional one needle set-up was used for electrospinning and a high potential voltage of 20 kV was applied on the needle tip. The flow rate was 0.3 mL h<sup>-1</sup> and the nanofibers were collected on a collector coated with an aluminum foil with a collecting distance of 35 cm. The nanofiber mat was cross-linked by using UV light for 12 h and then dried in a vacuum oven at 60 °C for 12 h to remove the residual solvent.

## Results and discussion

Various amounts of acrylamide (AAM) and acrylonitrile (AN) were polymerized with 2 mol% of a polymerizable photo cross-linker 4-acryloyloxybenzophenone (BPA) *via* RAFT polymerization using AIBN as an initiator and cyanomethyl dodecyl





**Scheme 1** Synthetic scheme for the formation of a photo cross-linkable UCST-type polymer with 4-acryloyloxybenzophenone (BPA) as the cross-linker by the RAFT method.

**Table 1** Free radical and RAFT polymerization of AAm, AN and BPA using AIBN as an initiator and CMDT as the chain transfer agent

Entry	Type of polymerization <sup>a</sup>	AAm : AN : BPA in feed (mol%)	Conversion (%)	$M_n^b$ (kDa)	PDI <sup>b</sup>	Cloud point by cooling <sup>c</sup> (°C)
1	FRP	92 : 6 : 2	62	25	1.8	Insoluble
2	FRP	94 : 4 : 2	68	26.1	2.0	Insoluble
3	FRP	96 : 2 : 2	75	26	1.6	Insoluble
4	FRP	98 : 0 : 2	78	31.2	1.7	Soluble
5	RAFT	83 : 15 : 2	52	17.8	1.2	48
6	RAFT	88 : 10 : 2	63	21.4	1.1	38
7	RAFT	92 : 6 : 2	75	22.8	1.2	20
8	RAFT	98 : 0 : 2	88	23.1	1.1	Soluble

<sup>a</sup> For free radical polymerization, monomer:AIBN molar ratio was 100:0.5 and for RAFT polymerization monomer:AIBN:CMDT was 100:0.15:0.5. <sup>b</sup> Determined by DMSO GPC using pullulan as the calibration standard. <sup>c</sup> Turbidity measurements were carried out in water with the sample concentration of 0.2 wt%.

trithiocarbonate (CMDT) as the chain transfer agent (Scheme 1; Table 1).

CMDT was chosen as the RAFT reagent as it was demonstrated to be the most suitable agent in previous studies in terms of control over molar mass, fast rate of reaction and high polymer conversions for polymerization of monomers with primary amide side groups such as *N*-acryloylglycinamide (NAGA) and acrylamide.<sup>22,23</sup> High molar mass polymers (18 000–23 000 Da) with low molar mass dispersity (1.1–1.2) could be prepared by RAFT polymerization (Table 1). Structural characterization was done using <sup>1</sup>H NMR and UV/Vis spectroscopy (Fig. S1 and S2†). The protons from amide and BPA overlapped at 6.5–7.5 ppm in <sup>1</sup>H NMR. The existence of benzophenone in the polymer could be proved by UV/Vis spectroscopy by showing the absorption peak of benzophenone at 310 nm in DMSO.

For turbidity measurements 0.2 wt% aqueous solutions were used. The cloud points were determined by means of the first derivative of the turbidity curves. Copolymers synthesized by RAFT within a suitable composition range showed UCST-type sharp phase separation in water. Copolymers with different cloud points ranging from 20 to 48 °C could be prepared by changing the molar ratio of AAm and AN in the feed (Table 1). The results were similar to the tuning of cloud points of poly(AAm-co-AN) prepared by free radical polymerization (FRP) with a change in the amount of AN in the feed as shown by us previously.<sup>23</sup> It is worth mentioning that none of

the copolymers prepared by conventional FRP using the AIBN initiator at 60 °C provided thermoresponsive polymers. They were either soluble or insoluble in water at temperatures between 0 and 100 °C (Table 1). A similar behavior was also observed for AAm copolymers with styrene in which polymers prepared by RAFT were thermoresponsive in comparison with the polymers prepared by free-radical polymerization due to compositional homogeneity.<sup>23</sup>

Further turbidity measurements were performed for different polymer concentrations between 0.05 and 2.0 wt% (Fig. 1). It was found that in this concentration range the polymer showed a typical UCST-type cloud point dependence on concentration. The cloud point increased with an increase in solution concentration with almost no hysteresis.

The reproducibility of thermoresponsive behavior was checked by carrying out turbidity measurements for many cycles. A shift in the cloud point to a lower temperature with each new cycle was observed as shown in Fig. 2A. Nine consecutive turbidity measurements for a sample (Table 1, entry 6, AAm:AN:BPA = 88:10:2) in water with the concentration of 0.2 wt% are shown. The decrease in the cloud point with every new heating-cooling cycle was also observed for copolymers of NAGA and butyl acrylate in our previous study. In contrast, copolymers of AAm and AN (poly(AAm-co-AN)) showed highly stable UCST-type thermoresponsive behaviour for at least 9 cycles without change in cloud points as shown by us previously.<sup>19</sup> One of the pre-



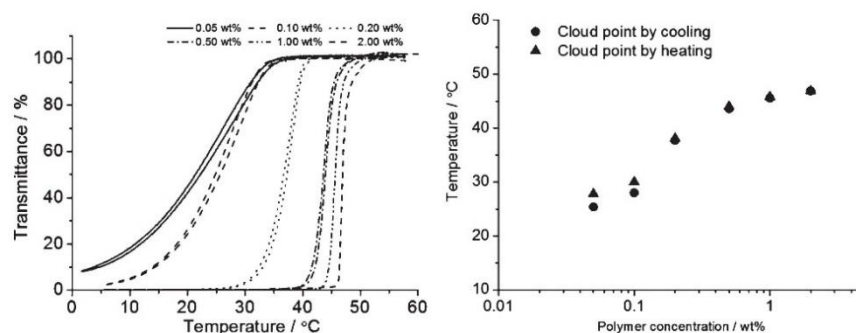


**Fig. 1** Turbidity measurements were carried out for different polymer concentrations between 0.05 and 2.0 wt% (Table 1, entry 6, AAm : AN : BPA = 88 : 10 : 2,  $M_n = 21.4$  kDa). The depicted plots show that the temperature of the phase transition is dependent on the solution concentration and varies between 20 and 50 °C for the investigated concentration range. Furthermore, it can be seen that the hysteresis is very small and vanishes at higher concentrations.

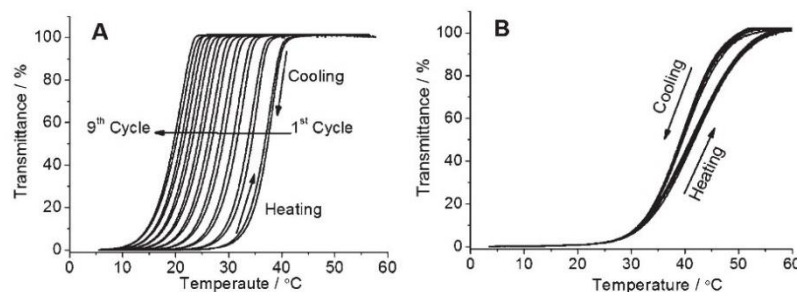


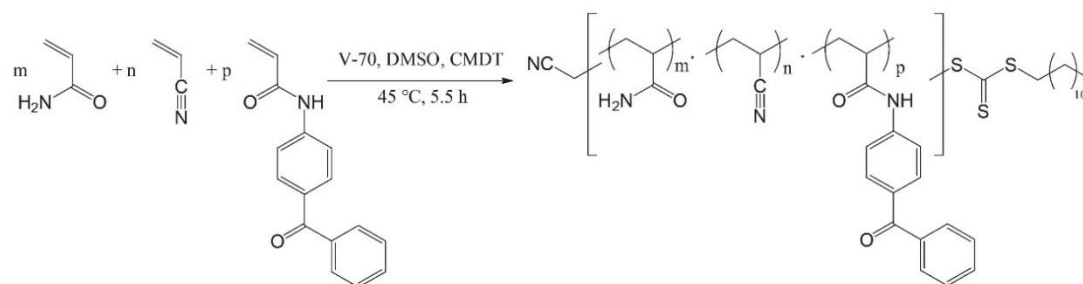
**Fig. 2** (A) Nine consecutive turbidity measurements of 0.2 wt% solution of poly(AAm-AN-BPA) in water (Table 1 entry 6, AAm : AN : BPA = 88 : 10 : 2,  $M_n = 21.6$  kDa, PDI = 1.1). (B) Turbidity measurement of the sample poly(AAm-AN) in water with a concentration of 0.5 wt% ( $M_n = 21$  kDa, PDI = 1.6, AN in polymer = 13 mol%). The nine times consecutive measurement overlap, indicating that the polymer is stable against hydrolysis.

vious data was reproduced by making a copolymer of AAm and AN (poly(AAm-co-AN),  $M_n = 21$  kDa, PDI = 1.6, AN in polymer = 13 mol%) and measuring cloud points for 9 heating-cooling cycles as shown in Fig. 2B. The different consecutive measurements overlapped, indicating a stable thermoresponsive behavior and hydrolytic stability of AAm and AN. Therefore, the decrease in the cloud point with each new heating-cooling cycle for the ter-copolymers of AAm, AN and BPA was probably due to the hydrolysis of the photo cross-linker BPA.

To avoid the possible hydrolysis during polymerization and sample preparation, 2,2'-azobis(4-methoxy-2,4-dimethyl valeronitrile) (V-70) as an initiator with low thermal decomposition temperature and *N*-(4-benzoylphenyl)acrylamide (BPAm) as the hydrolytically stable photo cross-linkable monomer were used (Scheme 2). V-70 is a DMSO soluble azo initiator and allows polymerizations at lower temperatures.<sup>24,25</sup> The terpolymers of AAm, AN and BPAm (AAm : AN : BPAm 88 : 10 : 2;  $M_n = 18\,000$  g mol<sup>-1</sup>) prepared by RAFT polymerization using V-70 an initiator showed highly reproducible UCST-type transition in water (Table 2, Fig. 3A). The cloud point did not change for at least 9 cycles thereby implying a highly stable system. Even

terpolymers prepared by FRP using V-70 as an initiator at 45 °C and AIBN at 60 °C also showed thermoresponsive behavior of UCST-type reproducible for many cycles (Table 2; Fig. S3†). This also confirmed the appropriate use of amide based BPAm as the photo cross-linkable monomer in comparison with easily hydrolysable ester based BPA. The photo cross-linkable polymers with UCST-type thermoresponsivity could also be prepared with different cloud points by just changing the amount of AN in the feed (Table 2, entries 2, 4 and 5). The cloud point of 0.1 wt% polymer solutions increased with a higher amount of AN in the feed: from 30 °C (8% AN) via 40 °C (10% AN) to 52 °C (12% AN). This result agreed with our previous contribution regarding FRP of AAm and AN that polymers with higher hydrophobicity showed a higher cloud point.<sup>19</sup> The cloud point increased with concentration as shown in Fig. 3B for a terpolymer with AAm:AN:BPAm 90 : 8 : 2 (Table 2, entry 4). The cloud point for highly concentrated solution (10 wt%) was much higher (85 °C as observed visually). The measurement of % transmittance vs. temperature was not possible for this sample (10 wt%) with a high cloud point using an available turbidity meter or UV/Vis photometer in our laboratory.





**Scheme 2** Synthetic scheme for the formation of a photo cross-linkable UCST-type polymer with *N*-(4-benzoylphenyl)acrylamide (BPAm) as the cross-linker by the RAFT method.

**Table 2** Characterization of terpolymers prepared by FRP and RAFT polymerization of AAm, AN and BPAm in DMSO

Entry	Type of polymerization <sup>a</sup>	Initiator	AAm : AN : BPAm in feed (mol%)	Time (h)	Conversion (%)	$M_n^b$ (kDa)	PDI <sup>b</sup>	Cloud point by cooling <sup>c</sup> (°C)	
								0.1 wt%	0.5 wt%
1	RAFT	V-70	88 : 10 : 2	7	60	18	1.2	33	42
2	FRP	V-70	88 : 10 : 2	5.5	81	60	1.5	52	67
3	FRP	AIBN	88 : 10 : 2	20	88	33	1.6	23	30
4	FRP	V-70	90 : 8 : 2	5.5	69	59	1.5	40	60
5	FRP	V-70	92 : 6 : 2	5.5	85	58	1.5	30	48

<sup>a</sup> For free radical polymerization, monomer : initiator molar ratio was 100 : 0.5 and for RAFT polymerization monomer : initiator : CMDT was 100 : 0.15 : 0.5. <sup>b</sup> Determined by DMSO GPC using pullulan as the calibration standard. <sup>c</sup> Turbidity measurements were carried out in water.

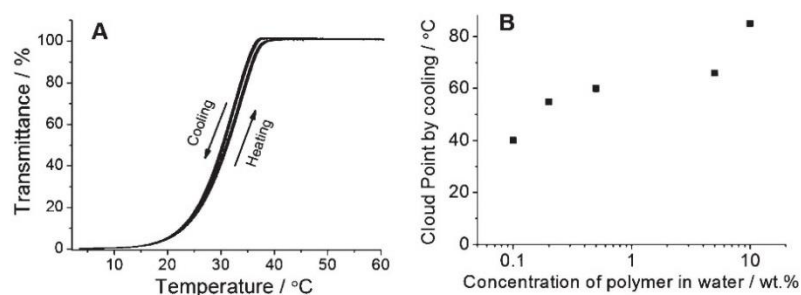


**Fig. 3** (A) Nine consecutive measurements of 0.1 wt% solution of poly(AAm-AN-BPAm) prepared by RAFT (Table 2, entry 1) using V-70 as an initiator. The copolymer showed excellent hydrolytic stability and reproducible cloud points with very negligible hysteresis (cloud point on cooling: 32.8 °C; cloud point on heating: 33.5 °C). (B) Cloud point dependence on the concentration of poly(AAm-AN-BPAm) in water by cooling (Table 2, entry 4, AAm : AN : BPAm = 90 : 8 : 2). The cloud point for 10 wt% was observed visually.

The terpolymer films prepared from DMSO solution were cross-linked by illumination with UV light for 16 h. The illuminated cross-linked films were not soluble in water but showed temperature dependent swelling with a fast equilibration in about 30 minutes. The swelling ratio increased continuously with an increase in temperature showing thermophilic behavior (Fig. 4A). The temperature dependent swelling was reversible with temperature for at least 5 cycles tested in this work (Fig. 4B).

Poly(AAm-AN-BPAm) terpolymers were also used to show the possibility of preparing thermophilic hydrogel fibrous membranes. Such membranes could be highly promising for

wound healing and drug release applications in the future. Poly(AAm-AN-BPAm) (AAm : AN : BPAm = 90 : 8 : 2) with the molecular weight of 59 kDa and polydispersity of 1.5 was chosen for preparing nanofiber mat *via* solution electrospinning. The electrospinning solution was prepared by dissolving the polymer in a mixture of water and DMSO (1 : 1 wt%) and provided fibers with the diameter  $480 \pm 78$  nm. The fibrous mat also showed thermophilic behavior with the change in swelling as observed from changed dimensions of mat with temperature (Fig. 5). The diameter of dry nanofibers also changed from  $480 \pm 78$  nm to  $880 \pm 91$  nm after placing in water at 20 °C for 1 h retaining their fibrous structure (Fig. 6).



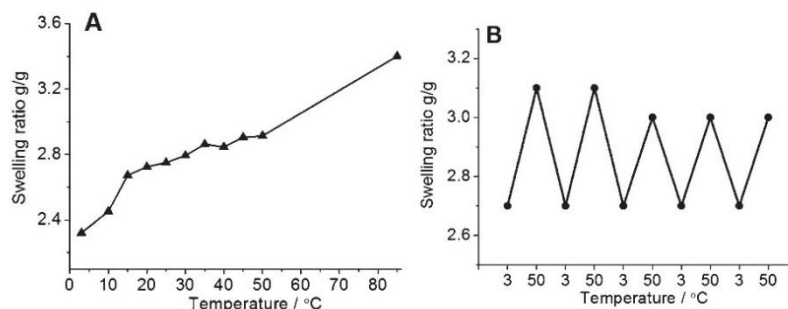


**Fig. 4** (A) Temperature dependence of swelling ratio of hydrogels in water prepared by using UV irradiation from the terpolymer DMSO solution (Table 2, entry 4, AAm : AN : BPAm = 90 : 8 : 2). The measurements were performed starting from 50 °C followed by cooling to 3 °C. The swelling ratio data at 85 °C were obtained by testing an extra sample to avoid the effect of possible hydrolysis of the hydrogel. At each temperature the samples were equilibrated for 30 min. (B) Reversibility of the volume transition of hydrogel in water.

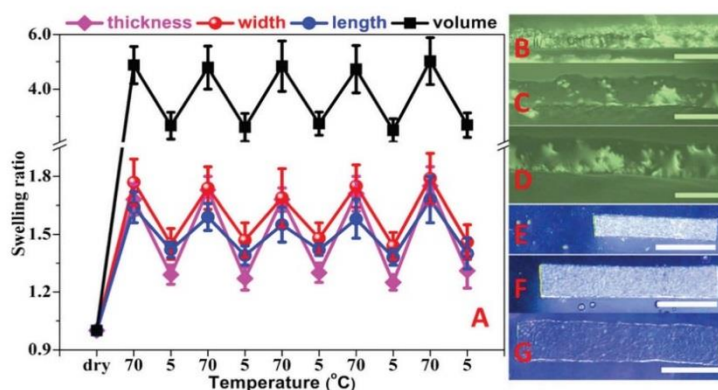


**Fig. 5** (A) Temperature dependent swelling behavior (thickness, width, length and volume changes) of electrospun fibrous mat; (B–D) microscopy photos of thickness change of the nanofiber mat in the dry state, the wet state at 5 °C and 70 °C respectively; (E–G) microscopy photos of a small piece of nanofiber mat in the dry state, the wet state at 5 °C and 70 °C. Scale bar of (B–D) = 100  $\mu$ m and scale bar of (E–G) = 500  $\mu$ m.

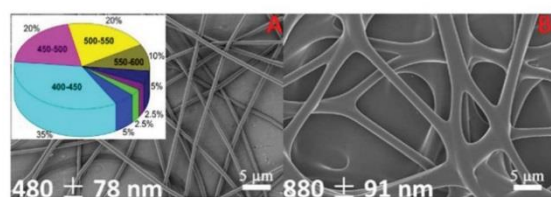


**Fig. 6** SEM images of polymer nanofibers in the (A) dried and (B) wet state. Insert: pie chart of the fiber diameter distribution.

The fibrous mat also displayed a temperature dependent reversible change in transparency as shown in Fig. 7.

Finally we demonstrated the fabrication of thermoresponsive self-rolled polymer films with UCST behavior using synthesized polymers. In order to approach this goal, we first explored the possibilities of fabricating microstructures formed by poly(AAm-AN-BPAm) (Table 2, entry 4, AAm : AN : BPAm =

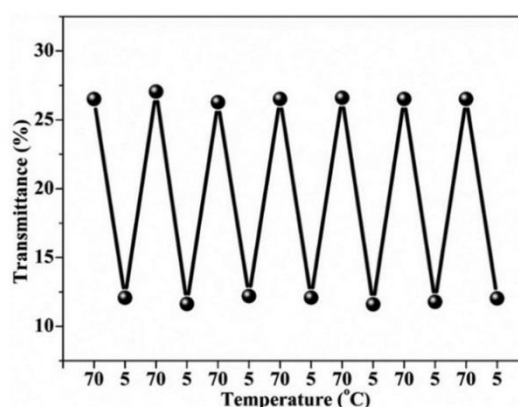


**Fig. 7** Temperature dependent transmittance of the polymer fibrous mat in cold water (5 °C) and hot water (70 °C). The thickness of the mat in the dry state is about 40  $\mu$ m.





## Polymer Chemistry

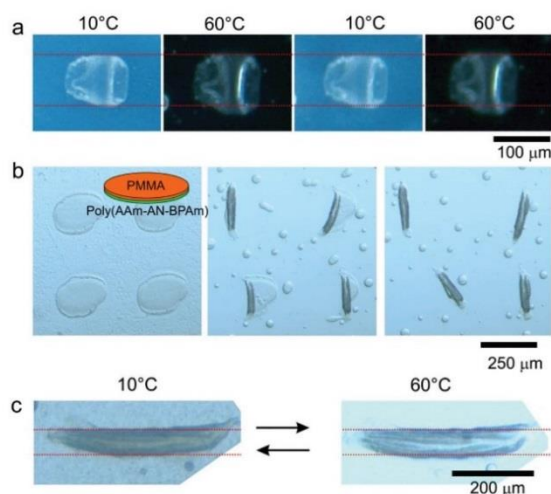


**Fig. 8** Actuation behavior of poly(AAm-AN-BPAm)-based photocross-linked films. (a) Swelling/deswelling of the crosslinked poly(AAm-AN-BPAm) film at different temperatures; (b) rolling of a poly(AAm-AN-BPAm)/poly(methyl methacrylate) bilayer; (c) actuation behavior of self-rolled poly(AAm-AN-BPAm)/poly(methyl methacrylate) tubes at different temperatures.

90:8:2) only. The polymer was positioned on the silicon wafer by dip-coating from its 6% DMSO solution. The dried film was irradiated through the photomask by using 254 nm UV light. The formed film was immersed in water and its actuation behavior was investigated by optical microscopy (Fig. 8a). We observed that the non-cross-linked polymer dissolves when the temperature increases above 60 °C. The patches of the crosslinked polymer remain intact on the surface of the wafer. We observed that the size of cross-linked pieces of polymer changes with temperature *i.e.* size reduces at a low temperature ( $T = 10$  °C) and reversibly increases at an elevated temperature ( $T = 60$  °C). The change in the size was completely reversible and can be repeated many times. We found that the increase in width and length of the samples is *ca.* 12–14%. Considering that the hydrogel is isotropic one can assume that the change in the thickness must also be in this range. Thus, the increase in the volume of hydrogel because of swelling can be estimated as 50% that is larger than in the case of macroscopic pieces (Fig. 4, change in the volume is *ca.* 15%). This could be due to a difference in the cross-linking density.

Next we investigated rolling of poly(AAm-AN-BPAm)-poly(methyl methacrylate) bilayers. The bilayers were prepared as described earlier.<sup>26</sup> The bilayers are flat and undeformed at low temperature (Fig. 8b, left) because the thermoresponsive polymer is not swollen. Increase in temperature results in swelling of poly(AAm-AN-BPAm) and rolling of the bilayer. As a result poly(AAm-AN-BPAm)-poly(methyl methacrylate) bilayer tubes are formed (Fig. 8b, central and right images). The formed tubes are unable to unroll upon cooling that is commonly observed when the tubes are formed by multiple

rolling. On the other hand, cooling results in a slight decrease in the diameter of the tubes (Fig. 8c). The decrease and increase in the diameter of the tubes upon cooling and heating are completely reversible processes and can be repeated many times.

## Conclusions

Photo cross-linkable thermoresponsive polymers showing phase transition of UCST-type in water could be successfully prepared by copolymerization of AAm, AN and BPAm with almost no hysteresis during heating and cooling cycles. The UCST-behavior was highly stable and reproducible for at least 9 cycles tested in the present work. The cloud point could be easily tuned by changing the feed composition. The polymers could be easily processed to films and fibers. The UV cross-linking provided the corresponding thermophilic hydrogels in the form of film and fibrous membranes showing temperature dependent positive volume transitions that was unitized for the design of microactuators. The hydrogels could be highly promising in future for use in wound dressing, drug release applications, microactuators and biofabrication.

## Acknowledgements

Deutsche Forschungsgemeinschaft (DFG) is kindly acknowledged for the financial support.

## Notes and references

- J. P. Chen and A. S. Huffman, *Biomaterials*, 1990, **11**, 631.
- A. Kondo, H. Kamura and K. Higashitani, *Biotechnol. Bioeng.*, 1994, **44**, 1.
- Y. Oni and W. O. Soboyejo, *Mater. Sci. Eng., C*, 2012, **32**, 24.
- W. L. J. Hinrichs, N. M. E. Schuurmans-Nieuwenbroek, P. van de Wetering and W. E. Hennink, *J. Controlled Release*, 1999, **60**, 249.
- N. Nath and A. Chilkoti, *Adv. Mater.*, 2002, **14**, 1243.
- E. Gil and S. Hudson, *Prog. Polym. Sci.*, 2004, **29**, 1173.
- J. Seuring and S. Agarwal, *Macromol. Rapid Commun.*, 2012, **33**, 1898.
- J. Seuring and S. Agarwal, *ACS Macro Lett.*, 2013, **2**, 597.
- F. Liu, J. Seuring and S. Agarwal, *Macromol. Chem. Phys.*, 2014, **215**, 1466.
- E. Mah and R. Ghosh, *Processes*, 2013, **1**, 238.
- G. S. Georgiev, Z. P. Mincheva and V. T. Georgieva, *Macromol. Symp.*, 2001, **164**, 301.
- J. Ning, K. Kubota, G. Li and K. Haraguchi, *React. Funct. Polym.*, 2013, **73**, 969.
- E. A. Bekturov and L. A. Bimend, in *Adv. Polym. Sci.*, Springer, Berlin, Heidelberg, 1980, vol. 41, pp. 99–147.
- H. Katono, A. Maruyama, K. Sanui, N. Ogata, T. Okano and Y. Sakurai, *J. Controlled Release*, 1991, **16**, 215.



- 15 N. Shimada, S. Kidoaki and A. Maruyama, *RSC Adv.*, 2014, **4**, 52346.
- 16 N. Shimada, H. Ino, K. Maie, M. Nakayama, A. Kano and A. Maruyama, *Biomacromolecules*, 2011, **12**, 3418.
- 17 N. Shimada, M. Nakayama, A. Kano and A. Maruyama, *Biomacromolecules*, 2013, **14**, 1452.
- 18 J. Seuring, F. M. Bayer, K. Huber and S. Agarwal, *Macromolecules*, 2012, **45**, 374.
- 19 J. Seuring and S. Agarwal, *Macromolecules*, 2012, **45**, 3910.
- 20 G. Stoychev, N. Pureskiy and L. Ionov, *Soft Matter*, 2011, **7**, 3277.
- 21 J.-D. Cho, S.-G. Kim and J.-W. Hong, *J. Appl. Polym. Sci.*, 2006, **99**, 1446.
- 22 F. Liu, J. Seuring and S. Agarwal, *J. Polym. Sci., Part A: Polym. Chem.*, 2012, **50**, 4920.
- 23 B. A. Pineda-Contreras, F. Liu and S. Agarwal, *J. Polym. Sci., Part A: Polym. Chem.*, 2014, **52**, 1878.
- 24 J. Brandrup, E. H. Immergut and E. A. Grulke, *Polymer Handbook*, John Wiley, New York, 1998.
- 25 R. Bryaskova, C. Detrembleur, A. Debuigne and R. Jérôme, *Macromolecules*, 2006, **39**, 8263.
- 26 S. Zakharchenko, N. Pureskiy, G. Stoychev, M. Stamm and L. Ionov, *Soft Matter*, 2010, **6**, 2633.



Supporting information for

**Thermophilic films and fibers from photo cross-linkable UCST-type polymers**Fangyao Liu<sup>a</sup>, Shaohua Jiang<sup>a</sup>, Leonid Ionov<sup>b</sup>, Seema Agarwal<sup>a\*</sup><sup>a</sup>: University of Bayreuth, Macromolecular Chemistry II and Bayreuth Center for

Colloids and Interfaces, Universitätstrasse 30, D-95440 Bayreuth, Germany

<sup>b</sup>: Leibniz Institute of Polymer Research Dresden, Hohe Str.6, D-01069 Dresden,

Germany

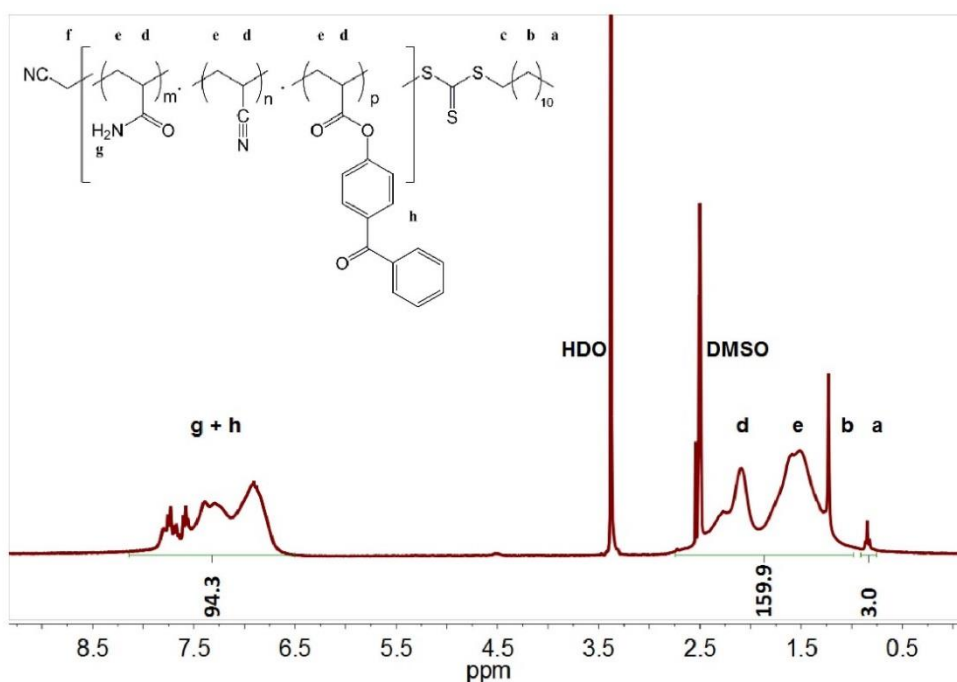


Figure S1. <sup>1</sup>H NMR spectra of RAFT poly(AAm-AN-BPA) (table 1, entry 7, monomer in feed= 92:6:2). The spectra were measured in DMSO-*d*<sub>6</sub> at 60 °C. Protons from amide and BPA overlap at 6.5 -7.5 ppm making it not possible to determine the polymer composition.

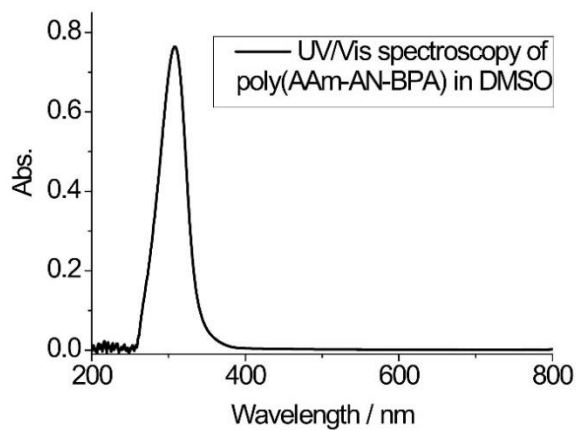


Figure S2. UV/Vis spectroscopy of RAFT poly(AAm-AN-BPA) (table 1, entry 7, monomer in feed= 92:6:2) in DMSO.

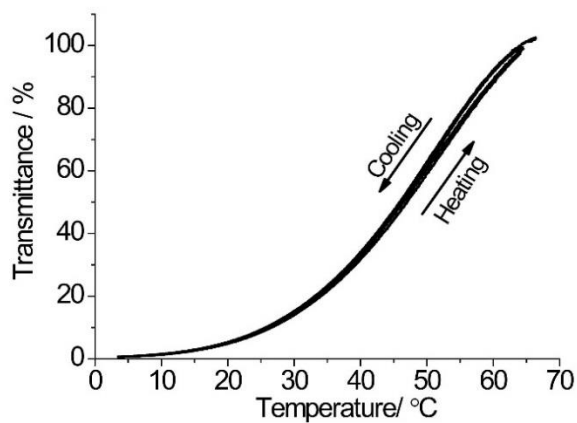


Figure S3. Turbidity measurements of 0.1 wt.% solution of poly(AAm-AN-BPAm) made by FRP using V-70 as initiator. (Table 2 entry 2, AAm : AN : BPAm = 88 : 10 : 2,  $M_n$  = 60 kDa, PDI = 1.5).

## 4 Outlook

Polymers with UCST-type thermoresponsive behavior have attracted increasingly attention due to their unique properties: dissolve at high temperature and separate out upon cooling. In this thesis, polymers with linear and cross-linked structure have been synthesized and their UCST-type thermoresponsivity was studied by turbidity measurement with different polymer end-groups, molar mass and salt concentration etc., while hydrogels were measured by the degree of swelling.

For further understanding of polymer with UCST-type thermoresponsivity based on hydrogen bonding, more hydrolytic stable polymers are required. So far nonionic UCST-type polymers are focusing on polymers containing amide group, other hydrophilic polymers with suitable content of hydrogen bonding units could theoretically display UCST property. One promising approach is to introduce strong hydrogen bonding in conventional hydrophilic polymers *via* post-modification. This may enlarge the UCST-type polymer family greatly.

The non-ionic hydrogels with positive thermoresponsivity could be used as drug loading/release system and their applications in biomedicine areas are also promising.

Nevertheless, the terpolymer system with UV cross-linkable comonomer makes it possible to produce cross-linked UCST polymers from linear polymers. Materials with different forms could be prepared as demanded simply by irradiation of UV light. Promising application areas are for example lithography, microactuators and self-rolling systems etc..

**5 List of publications**

- 08/2012      **Fangyao Liu**, Jan Seuring, Seema Agarwal  
Controlled Radical Polymerization of *N*-Acryloylglycinamide and UCST-Type Phase Transition of the Polymers  
*J. Polym. Sci., Part A: Polym. Chem.* **2012**, *50*, 4920-4928
- 03/2013      **Fangyao Liu**, Jan Seuring, Seema Agarwal  
Atom transfer radical polymerization as a tool for making poly(*N*-acryloylglycinamide) with molar mass independent UCST-type transitions in water and electrolytes  
*Polym. Chem.* **2013**, *4*, 3123-3131
- 04/2014      Beatriz A. Pineda-Contreras, **Fangyao Liu**, Seema Agarwal  
Importance of compositional homogeneity of macromolecular chains for UCST-type transitions in water: Controlled versus conventional radical polymerization  
*J. Polym. Sci., Part A: Polym. Chem.* **2014**, *52*, 1878-1884
- 06/2014      **Fangyao Liu**, Jan Seuring, Seema Agarwal  
A Non-ionic Thermophilic Hydrogel with Positive Thermosensitivity in Water and Electrolyte Solution  
*Macromol. Chem. Phys.* **2014**, *215*, 1466-1472
- 02/2015      **Fangyao Liu**, Seema Agarwal  
Thermoresponsive Gold Nanoparticles with Positive UCST-Type Thermoresponsivity  
*Macromol. Chem. Phys.* **2015**, *216*, 460-465
- 02/2015      **Fangyao Liu**, Shaohua Jiang, Leonid Ionov, Seema Agarwal  
Thermophilic films and fibers from photo cross-linkable UCST-type polymers  
*Polym. Chem.* **2015**, DOI: 10.1039/C5PY00109A

## 6 Conference participations

- 09/2012 Oral presentation  
**Materials Science and Engineering Conference 2012**  
in Darmstadt, Germany  
*Special water soluble polymers: Universal approach to polymers with an Upper Critical Solution Temperature in water and electrolytes*  
**Fangyao Liu**, Jan Seuring, Seema Agarwal
- 07/2013 Oral presentation  
**5<sup>th</sup> Scientific Seminar of the “Nordbavarian Biomaterials Alliance”**  
in Würzburg, Germany  
*Thermoresponsive polymers of UCST-type for biomedical applications*  
**Fangyao Liu**, Seema Agarwal
- 09/2013 Poster presentation  
**Bayreuth Polymer Symposium 2013**  
in Bayreuth, Germany  
*Thermoresponsive polymers of UCST-type for biomedical applications*  
**Fangyao Liu**, Seema Agarwal
- 10/2014 Oral presentation  
**2014 GCCCD\* Annual Conference**  
in Berlin, Germany  
*Thermoresponsive polymers of UCST-type for biomedical applications*  
**Fangyao Liu**, Seema Agarwal  
\* Gemeinschaft Chinesischer Chemiker und Chemieingenieure in Deutschland e.V. (GCCCD, VR 17428)

LIST OF PUBLICATIONS AND CONFERENCE PARTICIPATIONS

12/2014      Poster presentation  
**The 10<sup>th</sup> SPSJ International Polymer Conference**  
in Tsukuba, Japan  
*Thermoresponsive Polymers of UCST-type for Biomedical Applications*  
**Fangyao Liu, Seema Agarwal**  
**(Young Scientist Poster Award)**



## 7 Acknowledgments

First and foremost, I would like to express my special appreciation and thanks to my advisor Prof. Dr. Seema Agarwal. I would like to thank her for encouraging my research and for allowing me to grow as a research scientist. Her advice on both research as well as on my career have been priceless.

Also, I would like to thank Prof. Dr. Andreas Greiner for his very valuable and helpful suggestions.

I would like to thank Dr. Jan Seuring for his guidance since the first day I came in the lab and for generously introducing me into this wonderful research area.

I also thank Dr. Shaohua Jiang and Dr. Leonid Ionov for the fruitful cooperation, Dr. Marina Krekhova for the support in TEM measurement and Johannas Martin, Nadja Passing, Thomas Schmitt, Miriam Mauer, Max Männel, Lukas Kreuzer and Andreas Kräck for their motivated assistance during their research training.

I am grateful to all MC II chair members at University of Bayreuth. Your unhesitant support and the wonderful atmosphere have made every moment enjoyable. I thank Peter Ohlendorf, Melissa Koehn, Tobias Moss, Dr. Roland Dersch, Matthias Burgard, Markus Langner, Amanda Pineda and Paul Pineda for helping me with the correcting. By the way, Peter is also an ideal travel partner.

Special thank I would give to my UCST-teammate Amanda Pineda and her soulmate Paul Pineda, who gave me the warmest embrace and help me through many hard times. This work would not have been possible without their support.

I thank my love Yiru for her selfless support and letting me find the beauty of life.

Finally, I thank my family for their unconditional support through all these years.



## **(Eidesstattliche) Versicherungen und Erklärungen**

(§ 8 S. 2 Nr. 6 PromO)

*Hiermit erkläre ich mich damit einverstanden, dass die elektronische Fassung meiner Dissertation unter Wahrung meiner Urheberrechte und des Datenschutzes einer gesonderten Überprüfung hinsichtlich der eigenständigen Anfertigung der Dissertation unterzogen werden kann.*

(§ 8 S. 2 Nr. 8 PromO)

*Hiermit erkläre ich eidesstattlich, dass ich die Dissertation selbständig verfasst und keine anderen als die von mir angegebenen Quellen und Hilfsmittel benutzt habe.*

(§ 8 S. 2 Nr. 9 PromO)

*Ich habe die Dissertation nicht bereits zur Erlangung eines akademischen Grades anderweitig eingereicht und habe auch nicht bereits diese oder eine gleichartige Doktorprüfung endgültig nicht bestanden.*

(§ 8 S. 2 Nr. 10 PromO)

*Hiermit erkläre ich, dass ich keine Hilfe von gewerblichen Promotionsberatern bzw. -vermittlern in Anspruch genommen habe und auch künftig nicht nehmen werde.*

Hofheim, 02.08.15

.....

Ort, Datum, Unterschrift